

# *CP* violation studies at Super Tau-Charm Facility

Hai-Yang Cheng<sup>a</sup>, Zhi-Hui Guo<sup>b</sup>, Xiao-Gang He<sup>c</sup>, Yingrui Hou<sup>d</sup>,  
 Xian-Wei Kang<sup>e</sup>, Andrzej Kupsc<sup>f,g</sup>, Ying-Ying Li<sup>h,p</sup>, Liang Liu<sup>h</sup>, Xiao-Rui Lyu<sup>d</sup>,  
 Jian-Ping Ma<sup>i,j</sup>, Stephen Lars Olsen<sup>k,l</sup>, Haiping Peng<sup>h</sup>, Qin Qin<sup>m</sup>, Pablo Roig<sup>n,o</sup>,  
 Zhi-Zhong Xing<sup>p</sup>, Fu-Sheng Yu<sup>q</sup>, Yu Zhang<sup>f</sup>, Jianyu Zhang<sup>d</sup>, Xiaorong Zhou<sup>h</sup>

<sup>a</sup>*Institute of Physics, Academia Sinica, Taipei, 11529, China*

<sup>b</sup>*Hebei Normal University, Shijiazhuang, 050024, China*

<sup>c</sup>*Tsung-Dao Lee Institute and School of Physics and Astronomy, Shanghai Jiao Tong University, Shanghai, 200240, China*

<sup>d</sup>*University of Chinese Academy of Sciences, Beijing, 100049, China*

<sup>e</sup>*Beijing Normal University, Beijing, 100875, China*

<sup>f</sup>*National Centre for Nuclear Research, Warsaw, 02-093, Poland*

<sup>g</sup>*Uppsala University, Uppsala, SE-75120, Sweden*

<sup>h</sup>*University of Science and Technology of China, Address One, 230026, China*

<sup>i</sup>*Henan Normal University, Xinxiang, 453007, China*

<sup>j</sup>*Institute of Theoretical Physics, Chinese Academy of Sciences, Beijing, 100190, China*

<sup>k</sup>*High Energy Physics Center, Chung-Ang University, Seoul, 06974, Korea*

<sup>l</sup>*Particle and Nuclear Physics Institute, Institute for Basic Science, Daejeon, 34126, Korea*

<sup>m</sup>*Huazhong University of Science and Technology, Wuhan, 430074, China*

<sup>n</sup>*Departamento de Física, Centro de Investigación y de Estudios Avanzados del Instituto Politécnico Nacional, Mexico City, AP 14740, CP 07000, Mexico*

<sup>o</sup>*IFIC, Universitat de València – CSIC, Paterna, E-46980, Spain*

<sup>p</sup>*Institute of High Energy Physics, Chinese Academy of Sciences, Beijing, 100049, China*

<sup>q</sup>*Lanzhou University, Lanzhou, 730000, China*

<sup>r</sup>*University of South China, Hengyang, 421001, China*

---

## Abstract

Charge-parity (*CP*) violation in the tau-charm energy region is a promising area for sensitive tests of Standard Model (SM) predictions and searches for new, beyond the SM physics. A future Tau-Charm Facility that operates at center-of-mass energies between 2.0 and 7.0 GeV, with a peak luminosity of  $0.5 \times 10^{35} \text{ cm}^{-2}\text{s}^{-1}$ , would provide huge numbers of hadrons and tau ( $\tau$ ) leptons that are produced in low-background environments and with well understood kinematic properties. In this report, prospects for unique studies of *CP* violation in the decay of charmed hadrons, and in the production and decay of hyperons and  $\tau$  leptons at a next-generation tau-charm facility are discussed. In addition,

opportunities for improved tests of  $CPT$  invariance test in  $K^0 - \bar{K}^0$  mixing are presented.

---

## Contents

<b>1</b>	<b>Introduction</b>	<b>5</b>
<b>2</b>	<b><i>CP</i> violation in hyperon sector</b>	<b>10</b>
2.1	Direct <i>CP</i> violation in strange quark systems . . . . .	10
2.2	Hyperon two-body hadronic weak decays . . . . .	11
2.3	Spin entangled baryon–antibaryon systems . . . . .	17
2.4	Radiative and semileptonic decays . . . . .	22
2.5	<i>CP</i> violation in production via EDM . . . . .	26
2.6	Prospect of hyperon <i>CP</i> violation study at STCF . . . . .	30
<b>3</b>	<b><i>CP</i> violation in <math>\tau</math> sector</b>	<b>36</b>
3.1	Hadronic form factors in semileptonic $\tau$ decays . . . . .	36
3.2	Structure functions in $\tau$ decays with hadronic final states . . . . .	39
3.3	<i>CP</i> violation observables in hadronic $\tau$ decays . . . . .	40
3.4	<i>CP</i> violation in $\tau \rightarrow K_S^0 \pi \nu_\tau$ decays: the BaBar anomaly and the Belle measurement . . . . .	42
3.5	<i>CP</i> violation proposed via EDM . . . . .	45
3.6	Prospect of $\tau$ <i>CP</i> violation study at STCF . . . . .	46
<b>4</b>	<b><i>CP</i> violation in charm sector</b>	<b>50</b>
4.1	CKM unitarity triangle in the charm sector . . . . .	50
4.2	<i>CP</i> violation in the direct decays . . . . .	51
4.3	<i>CP</i> violation associated with $D^0$ - $\bar{D}^0$ mixing . . . . .	57
4.4	<i>CP</i> violation from the interplay between decay and mixing . . . . .	66
4.5	<i>CP</i> violation due to the final-state $K^0$ - $\bar{K}^0$ mixing . . . . .	67
4.6	<i>CP</i> violation due to $D^0 - \bar{D}^0$ and $K^0 - \bar{K}^0$ oscillating interference . . . . .	68
4.7	Prospects of charm <i>CP</i> violation studies at STCF . . . . .	70
<b>5</b>	<b>Tests of the <i>CPT</i> invariance with <math>J/\psi</math> decays</b>	<b>75</b>
5.1	<i>CPT</i> and the Theory of Everything . . . . .	76
5.2	Neutral $K$ mesons and tests of the <i>CPT</i> theorem . . . . .	77
5.3	The neutral kaon mass eigenstates with no <i>CPT</i> -invariance related restrictions . . . . .	78
5.4	Interference measurements of the $\phi_{+-}$ and $\phi_{00}$ phases . . . . .	80
5.5	Comment on the Bell-Steinberger relation . . . . .	82
5.6	Prospects of kaon <i>CPT</i> study at STCF . . . . .	85

5.7 Further comments . . . . .	88
<b>6 Summary</b>	<b>90</b>
<b>Acknowledgements</b>	<b>92</b>

## 1. Introduction

The future Super Tau-Charm Facility (STCF) will operate at center-of-mass energies between 2.0 and 7.0 GeV with a peak luminosity of  $0.5 \times 10^{35} \text{ cm}^{-2}\text{s}^{-1}$ , and produce huge numbers of hadrons and tau ( $\tau$ ) leptons with experimentally favorable kinematic conditions and low-backgrounds in a state-of-the-art  $4\pi$ -solid-angle particle detector. It will support a rich physics program that addresses issues involving non-perturbative Quantum Chromodynamics (QCD) and exotic hadron spectroscopy, precision measurements of electroweak interactions, as well as searches for the new, beyond the Standard Model physics (NP) [1]. In this report, we review the prospects for using the large STCF data samples for studies of  $CP$  violations in charmed particle decays, searches for  $CP$  violations in the production and decays of hyperons and  $\tau$  leptons, and tests of  $CPT$  invariance with large samples of strangeness-tagged neutral kaon decays.

The study of  $CP$  violations is a subject of central importance to particle physics and cosmology. The universe is predominantly composed of matter, with trace amounts of anti-matter particles that have only fleeting existences. The Standard Model (SM) has no explanation for this famous Baryon Asymmetry of the Universe (BAU), and whatever the (still unknown) new physics processes that are responsible for this asymmetry might be, they must violate the  $CP$  symmetry.

In the SM of elementary particles [2], the source of  $CP$ -violation is an irreducible complex phase in the Cabibbo [3] Kobayashi-Maskawa [4] quark-flavor mixing matrix,  $V_{CKM}$ , that modifies the coupling of  $W$ -bosons to the three-generation quark currents, the so-called Kobayashi-Maskawa (KM) mechanism. In this scheme, the interaction Lagrangian is given by

$$\mathcal{L} = -\frac{g}{\sqrt{2}}\bar{U}\gamma^\mu W_\mu^+ V_{CKM}D + h.c., \quad (1)$$

where  $U = (u, c, t)$  and  $D = (d, s, b)$  represent the known quarks.  $V_{CKM}$  is a  $3 \times 3$  unitary matrix that has three mixing angles  $\theta_{12}, \theta_{23}, \theta_{13}$  and a complex phase  $\delta$  and is usually parameterized as

$$\begin{aligned} V_{KM} &= \begin{pmatrix} V_{ud} & V_{us} & V_{ub} \\ V_{cd} & V_{cs} & V_{cb} \\ V_{td} & V_{ts} & V_{tb} \end{pmatrix} \\ &= \begin{pmatrix} c_{12}c_{13} & s_{12}c_{13} & s_{13}e^{-i\delta} \\ -s_{12}c_{23} - c_{12}s_{23}s_{13}e^{i\delta} & c_{12}c_{23} - s_{12}s_{23}s_{13}e^{i\delta} & s_{23}c_{13} \\ s_{12}s_{23} - c_{12}c_{23}s_{13}e^{i\delta} & -c_{12}s_{23} - s_{12}c_{23}s_{13}e^{i\delta} & c_{23}c_{13} \end{pmatrix}, \quad (2) \end{aligned}$$

where  $s_{ij} = \sin \theta_{ij}$  and  $c_{ij} = \cos \theta_{ij}$ . The phase  $\delta$  is the source of  $CP$ -violation.

$CP$  violation in the neutral  $K$  meson system was discovered in particle-physics experiments prior to the emergence of SM and the KM mechanism. Since then,  $CP$  violations have also been observed in the  $B$ - and  $D$ -meson systems. Unlike violations of  $P$ , or  $C$ , which are maximal,  $CP$  violations in the  $K$  and  $D$  meson systems are small effects, but they can still be consistently explained by the KM phase in SM. All of the elements in the  $V_{CKM}$  matrix, including the  $CP$  phase  $\delta$  have been experimental measured with reasonably good precision, and are summarized in the following widely used Wolfenstein parameterization [5],

$$V_{CKM} = \begin{pmatrix} 1 - \lambda^2/2 & \lambda & A\lambda^3(\rho - i\eta) \\ -\lambda & 1 - \lambda^2/2 & A\lambda^2 \\ A\lambda^3(1 - \rho - i\eta) & -A\lambda^2 & 1 \end{pmatrix} + \mathcal{O}(\lambda^4), \quad (3)$$

where  $\lambda = 0.22501 \pm 0.00068$ ,  $A = 0.826_{-0.015}^{+0.016}$ ,  $\bar{\rho} = \rho(1 - \lambda^2/2) = 0.1591 \pm 0.0094$  and  $\bar{\eta} = \eta(1 - \lambda^2/2) = 0.3523_{-0.0071}^{+0.0073}$ . In terms of the quark mixing angles and  $CP$  phase, the parametrization of Eq. (2) translates to numerical values of  $s_{12} = 0.22501 \pm 0.00068$ ,  $s_{13} = 0.003732_{-0.000085}^{+0.000090}$ ,  $s_{23} = 0.04183_{-0.00069}^{+0.00079}$  and  $\delta = 1.147 \pm 0.026$  [6].

In the SM, the single complex phase  $\delta$  accounts for all of the  $CP$ -violating phenomena that have been observed in laboratory-based experiments, but it cannot explain the baryon asymmetry in the universe. This is characterized by the ratio of the baryon and photon densities in the universe, which is measured with about 10% precision to be  $\eta \approx 6 \times 10^{-10}$ . However, calculations of  $\eta$  that are based on the phase  $\delta$  in the CKM matrix, find values of  $\eta$  that are nine orders of magnitude smaller than its measured value. This large discrepancy strongly motivates experimental searches for  $CP$  violations in laboratory experiments that cannot be explained by the SM's KM mechanism and is, therefore, evidence for new, non-SM physics interactions.

Although all observations of  $CP$  violations in  $K$ -,  $D$ -, and  $B$ -meson systems that have been reported to date can be explained by the SM's  $\delta$  phase, there is still a need to establish that the KM-mechanism is correct in a broader scope of interactions. The nonzero phase in the mixing matrix originates from the mass matrix that couples quarks to the scalar sector of the SM that involves the Higgs field and Electro-weak spontaneous symmetry breaking. Unlike the other sectors of the SM, the Higgs sector is still poorly understood. It is not clear why there are three generations of quarks with the observed inter-generation mixing pattern between generations that produces the  $CP$  violation that is observed. Although

the SM has been very successful, there are both observational and theoretical reasons that indicate that NP beyond SM should exist. On the observational side, in addition to the BAU problem mentioned above, there are no SM explanations for the non-vanishing neutrino masses that have been established by the discovery of neutrino oscillations, QCD's strong  $CP$  problem, or for the universe's dark matter and dark energy. Among the theoretical arguments that call for NP are the many free parameters in the SM, the poorly understood Higgs sector physics, and its related hierarchy problem. In this review, we focus on possible NP sources of  $CP$  violation. Most proposed NP scenarios have additional  $CP$ -violating phases. If a  $CP$  violation is found in a process for which the SM prediction is zero or unmeasurably small, it will be an unquestionable evidence for NP. Therefore, searches for  $CP$  violation will play an important role for a better understanding of the SM as well as in the quest for NP.

Table 1: Some typical event numbers expected per year at STCF.

c.m. energy (GeV)	Lumi $\text{ab}^{-1}$	Samples	$\sigma$ (nb)	Numbers of Events
3.097	1	$J/\psi$	3400	$3.4 \times 10^{12}$
		$J/\psi \rightarrow \Lambda\bar{\Lambda}$		$7.0 \times 10^9$
		$J/\psi \rightarrow \Xi\bar{\Xi}$		$2.3 \times 10^9$
		$J/\psi \rightarrow K^\mp\pi^\pm K^0/\bar{K}^0$		$3.4 \times 10^9$
3.670	1	$\tau^+\tau^-$	2.4	$2.4 \times 10^9$
3.686	1	$\tau^+\tau^-$	2.5	$2.5 \times 10^9$
		$\psi(3686) \rightarrow \tau^+\tau^-$		$2.0 \times 10^9$
3.770	1	$\psi(3770) \rightarrow D^0\bar{D}^0$	3.6	$3.6 \times 10^9$
		$\psi(3770) \rightarrow D^+D^-$	2.8	$2.8 \times 10^9$
		$\psi(3770) \rightarrow \tau^+\tau^-$	2.9	$2.9 \times 10^9$
4.040	1	$\psi(4040) \rightarrow D_s^+D_s^-$	0.20	$2.0 \times 10^8$
		$\psi(4040) \rightarrow \tau^+\tau^-$	3.5	$3.5 \times 10^9$
4.630	1	$\psi(4630) \rightarrow \Lambda_c\bar{\Lambda}_c$	0.20	$2.0 \times 10^8$
		$\psi(4630) \rightarrow \tau^+\tau^-$	3.4	$3.4 \times 10^9$

Since the observational effects of  $CP$  violation are, in general, expected to be small, tests of  $CP$  symmetry and searches for new examples of  $CP$ -violating processes will require large statistical samples of high quality data that would be available at the proposed STCF [1]. In the energy range covered by the STCF,

a number of  $J^{PC} = 1^{--}$  charmonium states can be copiously produced via  $s$ -channel  $e^+e^-$  annihilations at c.m. energies corresponding to the resonance peaks. The numbers of quantum-correlated  $\tau^+\tau^-$ , or meson-antimeson, or baryon-antibaryon pairs that can be produced via decays of these resonance states are shown for some example processes in Table 1. (More detailed compilations of expected event numbers can be found in Ref. [1].) To the extent that  $CP$  is conserved in the  $e^+e^-$  annihilation and charmonium decay processes, these particle-antiparticle pairs will be produced in a pure  $CP$ -odd eigenstate. These conditions, *i.e.* the particle-antiparticle quantum correlations and their pure  $CP$  quantum number, make charmonium  $\rightarrow$  particle-antiparticle pairs unique, and very powerful reactions for  $CP$  violation studies. Quantum correlations are essential for tests of  $CP$  symmetry in hyperon systems.

Improved searches for  $CP$  violations in non-leptonic decays of strange hyperon, especially  $\Lambda \rightarrow N\pi$  and  $\Xi \rightarrow \Lambda\pi$ , are of particular interest because the level of SM-induced  $CP$  violations in these decays [7] are two orders of magnitude below the current levels of experimental sensitivity. The effectiveness of using the  $J/\psi \rightarrow$  hyperon antihyperon reaction for  $CP$  studies has been demonstrated by the BESIII experiment that has reported the world's best limits on NP  $CP$  violating processes in strange hyperon decays using 3.2 M  $J/\psi \rightarrow \Lambda\bar{\Lambda}$  and 0.9 M  $J/\psi \rightarrow \Xi\bar{\Xi}$  events [8–10]. These measurements have  $\mathcal{O}(1\%)$  backgrounds and small  $\mathcal{O}(0.2\%)$  systematic errors. At the STCF, the  $J/\psi \rightarrow \Lambda\bar{\Lambda}$  and  $\Xi\bar{\Xi}$  event samples would be more than three orders of magnitude larger than the existing BESIII data samples, and could support searches for NP  $CP$  violations with a factor of  $\sim 40$  higher sensitivities, which would nearly reach the SM-model-predicted levels.

Included in Table 1 is a projection of 3.4 B detected strangeness-tagged  $K^0$  and  $\bar{K}^0$  events produced via  $J/\psi \rightarrow K^\mp\pi^\pm K^0(\bar{K}^0)$  decays that can be used to improve the precision of the magnitude and phases of the  $\eta_{+-}$  and  $\eta_{00}$   $CP$ -violating parameters of the neutral kaon system, and extend the sensitivity of tests of  $CPT$  invariance in  $K^0$ - $\bar{K}^0$  mixing. The current state of the art sensitivities for neutral kaon  $CP$  parameter measurements and  $CPT$  tests are thirty year old CPLEAR measurements that are based on  $\sim 70$  M strangeness-tagged neutral kaon decays [11, 12]. With fifty times more strangeness-tagged decays in a more sophisticated detector and a cleaner event environment, STCF would provide an order of magnitude improved sensitivity.

In addition to studies of  $CP$  violation in the decays of the above-mentioned particles, searches for  $CP$  violation in the charmonium decay processes or in their production via the  $e^+e^-$  annihilation at non-resonant energy points that could be

performed are discussed below. This can provide additional information about  $CP$  symmetry.

Since hyperon-antihyperon,  $\tau^+\tau^-$  and charmed-anticharmed hadron pair data samples at STCF will be especially large, this review is mainly focus on  $CP$  tests with these systems. In addition we include a study of the possibility of an improved test of the combined  $C$ ,  $P$  and time reversal  $T$  symmetries, *i.e.*  $CPT$  invariance.  $CPT$  invariance is expected to be exact from our current understanding of space-time and interactions, at last in the framework of local quantum field theory, but its validity has to be experimentally tested. In Chaps. 2, 3 and 4, we discuss current theoretical and experimental progress, as well as the prospected potential at STCF, on relevant processes for hyperon-antihyperon,  $\tau^+\tau^-$  and charmed-anticharmed hadron systems, respectively. In Chap. 5, we discuss how  $CPT$  invariance could be tested with the large data sample of strangeness-tagged neutral  $K$ -mesons that will be produced at STCF. In Chap. 6, we provide our summaries.

## 2. $CP$ violation in hyperon sector

### 2.1. Direct $CP$ violation in strange quark systems

Direct  $CP$  violation requires that amplitudes for a given process and its  $CP$ -transformed process to have different complex phases. For example, if the amplitude for a particle decay is  $\mathcal{A} = |\mathcal{A}| \exp(i\xi + i\delta)$ , then the amplitude for the  $CP$ -transformed process is  $\bar{\mathcal{A}} = |\mathcal{A}| \exp(-i\xi + i\delta)$ , where  $\xi$  is the  $CP$ -odd phase that changes sign after the  $CP$  transformation, while  $\delta$  is the  $CP$ -even strong phase due to final state re-scattering, that does not change sign. In order to observe an effect due to the  $CP$ -odd phases, an interference with other amplitudes contributing to the process is needed. A usually studied  $CP$  violating observable is the decay rate asymmetry,  $A_{CP}$ , defined as

$$\begin{aligned} A_{CP} &= \frac{|\mathcal{A}|^2 - |\bar{\mathcal{A}}|^2}{|\mathcal{A}|^2 + |\bar{\mathcal{A}}|^2} \\ &= -\frac{2 \sum_{j \neq k} |\mathcal{A}_j| |\mathcal{A}_k| \sin(\xi_j - \xi_k) \sin(\delta_j - \delta_k)}{\sum_j |\mathcal{A}_j|^2 + 2 \sum_{j \neq k} |\mathcal{A}_j| |\mathcal{A}_k| \cos(\xi_j - \xi_k) \cos(\delta_j - \delta_k)}. \end{aligned} \quad (4)$$

It is clear that, in order to have a non-zero  $A_{CP}$ , there must exist at least two amplitudes with different  $CP$  conserving and violating phases. That is,  $\mathcal{A} = \sum_j |\mathcal{A}_j| \exp(i\xi_j + i\delta_j)$ , with  $j$  larger than 1. Since in the SM the  $CP$ -odd phases  $\xi_i$  are small, one has  $\sin(\xi_1 - \xi_2) \approx \xi_1 - \xi_2$  for the weak transitions of the strange quarks. Therefore, a significant contribution to the  $CP$  violation might be due to a NP effect.

One process where the direct  $CP$  violation was first observed is the combined weak and strong decay of  $K^0$  meson into a pion pair  $K^0 \rightarrow \pi^+ \pi^-$ . There are two final states that have distinct properties with respect to the strong interactions by having different values of the isospin quantum number  $I = 0$  and  $I = 2$  for the two-pion system. The initial weak transitions can proceed to one of the two states and are represented by the amplitudes  $\mathcal{A}_0$  and  $\mathcal{A}_2$ . One parameterizes the decay amplitudes as

$$\begin{aligned} A(K^0 \rightarrow \pi^+ \pi^-) &= \sqrt{\frac{2}{3}} A_0 e^{i(-\xi_0 + \delta_0)} + \sqrt{\frac{1}{3}} A_2 e^{i(-\xi_2 + \delta_2)}, \\ A(K^0 \rightarrow \pi^0 \pi^0) &= \sqrt{\frac{1}{3}} A_0 e^{i(-\xi_0 + \delta_0)} - \sqrt{\frac{2}{3}} A_2 e^{i(-\xi_2 + \delta_2)}, \end{aligned} \quad (5)$$

where, experimentally,  $\mathcal{A}_2/\mathcal{A}_0 \approx 0.05$ .

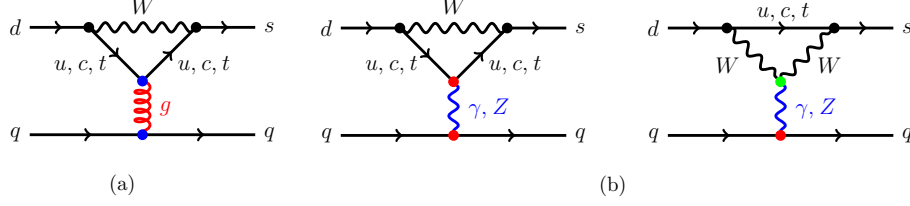


Figure 1: Quark level diagrams for the weak processes involving kaons or hyperons that contribute to the  $CP$ -odd phases in SM: (a) QCD-penguin operators and (b) electroweak penguin operators. This figure was created using a modified script from Ref. [16].

The direct  $CP$  violation observable  $A_{CP}$  is expressed as [13, 14]:

$$A(K^0 \rightarrow \pi^+\pi^-)_{CP} \approx \sqrt{2}(\xi_0 - \xi_2) \sin(\delta_0 - \delta_2) \frac{\mathcal{A}_2}{\mathcal{A}_0}. \quad (6)$$

This quantity is directly related to the well-know experimentally measured quantity  $\text{Re}(\epsilon') \approx (\xi_0 - \xi_2) \sin(\delta_0 - \delta_2) (\mathcal{A}_2/\mathcal{A}_0)$ , with

$$\text{Re}(\epsilon') = \frac{1}{3} \text{Re} \left( \frac{A(K_L \rightarrow \pi^+\pi^-)}{A(K_S \rightarrow \pi^+\pi^-)} - \frac{A(K_L \rightarrow \pi^0\pi^0)}{A(K_S \rightarrow \pi^0\pi^0)} \right) \approx (\xi_0 - \xi_2) \frac{\mathcal{A}_2}{\mathcal{A}_0}. \quad (7)$$

The measured value of  $\text{Re}(\epsilon')$  is  $(3.7 \pm 0.5) \times 10^{-6}$  [15], corresponding to the weak-phase difference  $\xi_0 - \xi_2 \approx 10^{-4}$  radian.

In the SM, the contributions to the  $CP$ -odd phases  $\xi_{0,2}$  are given by the loops that involve all three quark generations, as shown in the diagrams in Fig. 1. An order of magnitude estimate for these contributions is determined from the CKM matrix [3, 4] and can be expressed by the product of the Wolfenstein parameters [5] as  $\lambda^4 A^2 \eta \approx 6 \times 10^{-4}$  [6, 15]. Recent SM predictions for the  $CP$  violation in kaon decays that include hadronic effects are given in the framework of the low-energy effective field theory [16] and the lattice QCD [17, 18]. The agreement with the  $\text{Re}(\epsilon')$  parameter measurement is satisfactory but -due to the large uncertainties- there is room for a NP contribution.

## 2.2. Hyperon two-body hadronic weak decays

The direct  $CP$  violation is also possible in the main decays of the ground-state baryons with one or more strange quarks — hyperons. The spin of a baryon provides an additional degree of freedom that can be used to construct independent

$CP$  tests that can be very sensitive. A quantum state of a spin-1/2 baryon  $B$  is described by Pauli matrices:

$$|B\rangle = \sigma_0 + \mathbf{P}_B \cdot \boldsymbol{\sigma} , \quad (8)$$

where  $\sigma_0$  is the  $2 \times 2$  unit matrix and  $\boldsymbol{\sigma} := (\sigma_1, \sigma_2, \sigma_3)$  represents spin  $x, y, z$  projections in the baryon rest frame. The polarization vector  $\mathbf{P}_B$  describes the preferred spin direction for an ensemble of the  $B$ -baryons. Consider the  $B \rightarrow b\pi$  transition between two spin-1/2 baryons with positive internal parities where a negative parity pion is emitted. Examples of such processes are the decays  $\Xi^- \rightarrow \Lambda\pi^-$  or  $\Lambda \rightarrow p\pi^-$ . The baryon  $b$  can have the same or opposite direction of spin as the baryon  $B$ , and the angular momentum conservation requires  $s$ - or  $p$ -wave for the  $b$ - $\pi$  system. The parity of the final state is negative for the  $s$ -wave and positive for the  $p$ -wave. Both are allowed, since parity is not conserved in weak decays. The decay amplitude is given by the transition operator

$$\mathcal{A}(B \rightarrow b\pi) \propto \mathcal{S}\sigma_0 + \mathcal{P}\boldsymbol{\sigma} \cdot \hat{\mathbf{n}} , \quad (9)$$

where  $\hat{\mathbf{n}}$  is the direction of the  $b$ -baryon in the  $B$ -baryon rest frame. The complex parameters  $\mathcal{S}$  and  $\mathcal{P}$  can be represented as  $\mathcal{S} = |\mathcal{S}| \exp(i\xi_S + i\delta_S)$  and  $\mathcal{P} = |\mathcal{P}| \exp(i\xi_P + i\delta_P)$ . The strong interaction of the  $b$ - $\pi$  system is given by the  $\delta_P$  and  $\delta_S$  phases and the  $CP$ -odd phases of weak interaction are  $\xi_P$  and  $\xi_S$ . The amplitude ratios  $|\mathcal{P}/\mathcal{S}|$  for  $\Lambda \rightarrow p\pi^-$  and  $\Xi^- \rightarrow \Lambda\pi^-$  are 0.442(4) and 0.188(2), respectively [19]. Since only the angular distributions will be discussed, the probability of the decay  $\Gamma \propto |\mathcal{S}|^2 + |\mathcal{P}|^2$  is set to  $|\mathcal{S}|^2 + |\mathcal{P}|^2 = 1$ . The real and imaginary parts of the amplitude interference term are

$$\alpha = 2\text{Re}(\mathcal{S}^*\mathcal{P}) \propto 2|\mathcal{S}||\mathcal{P}| \cos(\xi_P + \delta_P - \xi_S - \delta_S), \quad (10)$$

$$\beta = 2\text{Im}(\mathcal{S}^*\mathcal{P}) \propto 2|\mathcal{S}||\mathcal{P}| \sin(\xi_P + \delta_P - \xi_S - \delta_S). \quad (11)$$

The real part, given by the  $\alpha$  parameter, can be determined from the angular distribution of the baryon  $b$  when the baryon  $B$  has known non-zero polarization, or by measuring the polarization of the daughter baryon. For example, the proton angular distribution in the  $\Lambda(\Lambda \rightarrow p\pi^-)$  decay is given as

$$\frac{1}{\Gamma} \frac{d\Gamma}{d\Omega} = \frac{1}{4\pi} (1 + \alpha_\Lambda \mathbf{P}_\Lambda \cdot \hat{\mathbf{n}}) , \quad (12)$$

where  $\hat{\mathbf{n}}$  is the proton momentum direction and  $\mathbf{P}_\Lambda$  is the  $\Lambda$  polarization vector.

The imaginary part of the interference term given by the parameter  $\beta$  is a  $T$ -odd variable. Measurement of  $\beta$  requires that the polarization of both baryon  $B$  and the daughter baryon is determined. For the decay  $\Xi^- \rightarrow \Lambda \pi^-$ , where the cascade is polarized, the  $\beta_\Xi$  parameter can be determined using the subsequent  $\Lambda \rightarrow p \pi^-$  decay that acts as  $\Lambda$  polarimeter. The polarization  $\mathbf{P}_\Lambda$  of the final baryon  $\Lambda$  is given by the Lee–Yang formula [20]

$$\mathbf{P}_\Lambda = \frac{(\alpha_\Xi + \mathbf{P}_\Xi \cdot \hat{\mathbf{n}})\hat{\mathbf{n}} + \beta_\Xi \mathbf{P}_\Xi \times \hat{\mathbf{n}} + \gamma_\Xi \hat{\mathbf{n}} \times (\mathbf{P}_\Xi \times \hat{\mathbf{n}})}{1 + \alpha_\Xi \mathbf{P}_\Xi \cdot \hat{\mathbf{n}}}, \quad (13)$$

where  $\hat{\mathbf{n}}$  is, now, the  $\Lambda$  momentum direction and  $\gamma = |\mathcal{S}|^2 - |\mathcal{P}|^2$ . If the  $\hat{\mathbf{z}}$  axis in the  $\Xi^-$  rest frame is defined along the  $\hat{\mathbf{n}}$  direction, then the relation between the polarization vectors is

$$\begin{bmatrix} P_\Lambda^x \\ P_\Lambda^y \\ P_\Lambda^z \end{bmatrix} = \frac{1}{1 + \alpha_\Xi P_\Xi^z} \begin{pmatrix} \gamma_\Xi & \beta_\Xi & 0 \\ -\beta_\Xi & \gamma_\Xi & 0 \\ 0 & 0 & 1 \end{pmatrix} \begin{bmatrix} P_\Xi^x \\ P_\Xi^y \\ \alpha_\Xi + P_\Xi^z \end{bmatrix}. \quad (14)$$

This equation implies that  $\Lambda$  in the decay of unpolarized  $\Xi^-$  has the longitudinal polarization vector component  $P_\Lambda^z = \alpha_\Xi$ . Using a polar angle parameterization such that  $\beta = \sqrt{1 - \alpha^2} \sin \phi$  and  $\gamma = \sqrt{1 - \alpha^2} \cos \phi$ , the  $\phi$  parameter has the interpretation of the rotation angle between the  $\Xi$  and  $\Lambda$  polarization vectors in the transversal  $x$ - $y$  plane. It is convenient to rewrite the Eq. (14) for a general two-body decay  $D \equiv B \rightarrow b \pi$ , where  $\pi$  represents a pseudoscalar meson, in terms of a  $4 \times 4$  matrix,  $a_{\mu\nu}^D$ , describing the transformations between the Pauli matrices  $\sigma_\mu^B$  and  $\sigma_\nu^b$  defined in the  $B$  and  $b$  baryon helicity frames, respectively [21]:

$$\sigma_\mu^B \rightarrow \sum_{\nu=0}^3 a_{\mu\nu}^D \sigma_\nu^b. \quad (15)$$

The explicit form of the matrix is

$$a_{\mu\nu}^D = \begin{pmatrix} 1 & 0 & 0 & \alpha_D \\ 0 & \gamma_D & -\beta_D & 0 \\ 0 & \beta_D & \gamma_D & 0 \\ \alpha_D & 0 & 0 & 1 \end{pmatrix}. \quad (16)$$

Here  $\alpha_D$ ,  $\beta_D$  and  $\gamma_D$  correspond to the Lee-Yang polarization parameter  $-\alpha_B$ ,  $\beta_B$  and  $\gamma_B$ , respectively.

We consider the case in which the direction of the outgoing baryon  $b$  in the  $B$  rest frame is given by an arbitrary (not aligned with the  $B$  spin direction)  $\theta_b$  and  $\varphi_b$  polar and azimuth angles, respectively. The polarization transformation matrix should be multiplied by the following four-dimensional rotation matrix:

$$\mathcal{R}_{\mu\nu}^{(4)}(\Omega) = \begin{pmatrix} 1 & 0 & 0 & 0 \\ 0 & \cos\theta \cos\phi & -\sin\phi & \sin\theta \cos\phi \\ 0 & \cos\theta \sin\phi & \cos\phi & \sin\theta \sin\phi \\ 0 & -\sin\theta & 0 & \cos\theta \end{pmatrix}, \quad (17)$$

which is the 4D rotation where the spatial part  $\mathcal{R}_{jk}(\Omega)$  corresponds to the product of the following three axial rotations:

$$\begin{aligned} \mathcal{R}_{jk}(\Omega) &= R_z(\phi)R_y(\theta) \\ &= \begin{pmatrix} \cos\phi & -\sin\phi & 0 \\ \sin\phi & \cos\phi & 0 \\ 0 & 0 & 1 \end{pmatrix} \begin{pmatrix} \cos\theta & 0 & \sin\theta \\ 0 & 1 & 0 \\ -\sin\theta & 0 & \cos\theta \end{pmatrix}. \end{aligned} \quad (18)$$

We call the resulting matrix, the *decay matrix*  $a_{\mu\nu}(\theta_b, \varphi_b; \alpha_D, \beta_D)$ :

$$a_{\mu\nu} := \begin{pmatrix} 1 & 0 & 0 & 0 \\ 0 & \cos\theta_b \cos\varphi_b & -\sin\varphi_b & \sin\theta_b \cos\varphi_b \\ 0 & \cos\theta_b \sin\varphi_b & \cos\varphi_b & \sin\theta_b \sin\varphi_b \\ 0 & -\sin\theta_b & 0 & \cos\theta_b \end{pmatrix} \begin{pmatrix} 1 & 0 & 0 & \alpha_D \\ 0 & \gamma_D & -\beta_D & 0 \\ 0 & \beta_D & \gamma_D & 0 \\ \alpha_D & 0 & 0 & 1 \end{pmatrix}. \quad (19)$$

If the polarization of the final baryon  $b$  is not measured, as in the case of  $\Lambda \rightarrow p\pi^-$  decay, only  $a_{\mu 0}$  elements of the matrix contribute. Contrary, for the unpolarized baryon  $B$ , the  $b$ -baryon polarization is given by the  $a_{0\mu}$  elements. In the case of two body weak decays, this polarization is aligned along the  $b$ -momentum in  $\mathbb{R}_B$  reference frame. The remaining elements of the matrix show direction between the  $B$  and  $b$  polarization vectors.

Some of the hyperon hadronic processes are listed in Table 2, where the Particle Data Group (PDG) averages before 2018 [22] and the most recent results are reported.

Several processes can be related by isospin relations. Using the isospin decomposition, in the notation similar to Ref. [30], of the  $L = S, P$  amplitudes for

Table 2: **Properties of two-body hadronic decays of the ground-state hyperons.** The recent BESIII results, **in bold**, are compared to the world averages before 2018 (reported in PDG18 [22]). In addition BESIII [8] and [23] measured  $B_{\text{CP}} = -0.005(14)(3)$  and  $-0.003(8)(7)$  for  $\Xi^- \rightarrow \Lambda\pi^-$ ,  $B_{\text{CP}} = -0.0001(69)(9)$  for  $\Xi^0 \rightarrow \Lambda\pi^0$  [10]. Branching fractions  $\mathcal{B}$  of the decays are rounded within 0.5% accuracy.

	$\mathcal{B}$	$\langle\alpha\rangle$	$\langle\phi\rangle$	$A_{\text{CP}}$	Comment
$\Lambda \rightarrow p\pi^-$	64%	0.642(13)*	-0.113(61)*	0.006(21)	PDG18 [22]
		<b>0.754(3)(2)</b>	-	<b>-0.006(12)(7)</b>	BESIII [24]
		0.721(6)(5)*	-	-	CLAS [25]
		<b>0.760(6)(3)</b>	-	<b>-0.004(12)(9)</b>	BESIII [8]
		<b>0.7542(10)(24)</b>	-	<b>-0.0025(46)(12)</b>	BESIII [9]
$\Lambda \rightarrow n\pi^0$	36%	0.65(4)*	-	-	PDG18 [22]
		<b>-0.692(17)**</b>	-	-	BESIII [24]
		<b>0.670(9)(9)</b>	-	<b>0.001(9)(3)</b>	BESIII [23]
$\Sigma^+ \rightarrow p\pi^0$	52%	-0.980(23)*	0.628(59)*	-	PDG18 [22]
		<b>-0.994(4)(2)</b>	-	<b>-0.004(37)(1)</b>	BESIII [26]
$\Sigma^+ \rightarrow n\pi^+$	48%	0.068(13)*	2.91(35)*	-	PDG18 [22]
		<b>0.0506(26)(19)</b>	-	<b>-0.080(52)(28)</b>	BESIII [27]
$\Sigma^- \rightarrow n\pi^-$	100%	-0.068(8)*	0.174(26)*	-	PDG18 [22]
$\Xi^0 \rightarrow \Lambda\pi^0$	100%	-0.406(13)*	0.36(21)*	-	PDG18 [22]
		<b>-0.3770(24)(14)</b>	-	<b>0.0069(58)(18)</b>	BESIII [10]
		<b>-0.367(4)(3)</b>	<b>-0.013(12)(8)</b>	<b>-0.009(8)(7)</b>	BESIII [23]
$\Xi^- \rightarrow \Lambda\pi^-$	100%	-0.458(12)*, <sup>o</sup>	-0.042(16)*	-	PDG18 [22, 28]
		<b>-0.373(5)(2)</b>	<b>0.016(14)(7)</b>	<b>0.006(13)(6)</b>	BESIII [8]
		<b>-0.367(4)(3)</b>	<b>-0.013(12)(8)</b>	<b>-0.009(8)(7)</b>	BESIII [23]
$\Omega^- \rightarrow \Lambda K^-$	68%	0.0181(22)*	-	-0.02(13)	PDG18 [22]
		<b>-0.04(3)</b>	<b>1.08(51)</b>	-	BESIII [29]
$\Omega^- \rightarrow \Xi^0\pi^-$	24%	0.09(14)	-	-	PDG18 [22]
$\Omega^- \rightarrow \Xi^-\pi^0$	8%	0.05(21)	-	-	PDG18 [22]

\* – result only available for hyperons

\*\* – result only available for antihyperons

<sup>o</sup> – measured as a product with the  $\alpha_\Lambda$  value

$\Lambda \rightarrow N\pi$  into the two possible weak transitions  $\Delta I = 1/2, 3/2$ :

$$\begin{aligned}
L_{[\Lambda p]} &= -\sqrt{\frac{2}{3}}L_{1,1} \exp(i\xi_{1,1}^L + i\delta_1^L) + \sqrt{\frac{1}{3}}L_{3,3} \exp(i\xi_{3,3}^L + i\delta_3^L), \\
L_{[\Lambda n]} &= \sqrt{\frac{1}{3}}L_{1,1} \exp(i\xi_{1,1}^L + i\delta_1^L) + \sqrt{\frac{2}{3}}L_{3,3} \exp(i\xi_{3,3}^L + i\delta_3^L), \quad (20)
\end{aligned}$$

where in the  $L = P$  case  $P_{[\Lambda p]}$  and  $P_{[\Lambda n]}$  on the left-hand sides are to be replaced by  $(1 + \Delta_{[\Lambda p]})P_{[\Lambda p]}$  and  $(1 + \Delta_{[\Lambda n]})P_{[\Lambda n]}$ , respectively, as per the discussion in the previous paragraph. Analogously, for the  $\Xi \rightarrow \Lambda\pi$  channels one has

$$\begin{aligned} L_{[\Xi^-]} &= L_{1,2} \exp(i\xi_{1,2}^L + i\delta_2^L) + \frac{1}{2}L_{3,2} \exp(i\xi_{3,2}^L + i\delta_2^L), \\ L_{[\Xi^0]} &= \frac{1}{\sqrt{2}}L_{1,2} \exp(i\xi_{1,2}^L + i\delta_2^L) - \frac{1}{\sqrt{2}}L_{3,2} \exp(i\xi_{3,2}^L + i\delta_2^L). \end{aligned} \quad (21)$$

The isospin decomposition for the processes  $\Sigma \rightarrow N\pi$  is more complicated, since the initial state has  $I = 1$  and the final states with the isospins  $1/2$  and  $3/2$  can be reached by weak transitions with  $\Delta I = 1/2, 3/2$  and  $5/2$ . Each weak transition can include a weak  $CP$ -odd phase. However, the  $\Delta I = 1/2$  transitions dominate, and the  $CP$  violation experiments can be analysed neglecting other contributions.

For the charge conjugation-transformed baryon decay process  $\bar{B} \rightarrow \bar{b}\bar{\pi}$ , the amplitude is:

$$\bar{\mathcal{A}}(\bar{B} \rightarrow \bar{b}\bar{\pi}) \propto \bar{\mathcal{S}}\sigma_0 - \bar{\mathcal{P}}\boldsymbol{\sigma} \cdot \hat{\mathbf{n}}, \quad (22)$$

where the complex parameters  $\bar{\mathcal{S}}$  and  $\bar{\mathcal{P}}$  are obtained from  $\mathcal{S}$  and  $\mathcal{P}$  by reversing the sign for the weak  $CP$ -odd phases  $\xi_S$  and  $\xi_P$ . Since the product of the  $P$ -odd and  $P$ -even terms changes sign, the decay parameters are:

$$\bar{\alpha} \propto -2|\mathcal{S}||\mathcal{P}| \cos(-\xi_P + \delta_P + \xi_S - \delta_S), \quad (23)$$

$$\bar{\beta} \propto -2|\mathcal{S}||\mathcal{P}| \sin(-\xi_P + \delta_P + \xi_S - \delta_S). \quad (24)$$

The weak phase difference  $\xi_P - \xi_S$  can be determined using two independent experimental observables:

$$A_{CP} = \frac{\alpha + \bar{\alpha}}{\alpha - \bar{\alpha}} = (\xi_P - \xi_S) \tan(\delta_P - \delta_S), \quad B_{CP} = \frac{\beta + \bar{\beta}}{\alpha - \bar{\alpha}} = (\xi_P - \xi_S). \quad (25)$$

Here we have assumed  $\xi_P - \xi_S$  to be small, so that  $\sin(\xi_P - \xi_S) \approx \xi_P - \xi_S$ .

The goal of the  $CP$  tests in hadronic decays of hyperons is to determine the weak-phase differences between  $P$  and  $S$  final states for the two decays.

The BESIII results based on  $1.3 \times 10^9$  and  $10^{10}$   $J/\psi$  data for  $(\xi_P - \xi_S)^\Xi$  [8] and  $(\xi_P - \xi_S)^\Lambda$  [9], respectively, are presented in Fig. 2 by the blue rectangle. The red band represents the HyperCP experimental result on  $A_{CP}^\Lambda + A_{CP}^\Xi$  [31]. Interpretation of this measurement requires the value of  $\tan(\delta_P - \delta_S)_\Xi$ , that is poorly known. Projection for the statistical uncertainties of the analysis using full BESIII data set for  $e^+e^- \rightarrow J/\psi \rightarrow \Xi\bar{\Xi}$  is given by the brown rectangle. The

results should be compared to SM predictions of  $(\xi_P - \xi_S)^\Lambda = (-0.2 \pm 2.2) \times 10^{-4}$  and  $(\xi_P - \xi_S)^\Xi = (-2.1 \pm 1.7) \times 10^{-4}$  [32, 33].

In case of hyperon decays, the SM contribution is dominated by QCD-penguin diagrams shown in Fig. 1(a). The results on the weak phases in kaon and in the hyperon decays can be combined in order to search for NP. The present kaon data imply the limits  $|\xi_P - \xi_S|_{\text{NP}}^\Lambda \leq 5.3 \times 10^{-3}$  and  $|\xi_P - \xi_S|_{\text{NP}}^\Xi \leq 3.7 \times 10^{-3}$  [34]. Clearly, the hyperon  $CP$ -violation measurements with much improved precision will provide an independent constraint on the NP contributions in the strange quark sector. However, a lot also remains to be done on the theory side, as the present predictions suffer from considerable uncertainties. It is hoped that the lattice analyses [35] could help solve this problem in the future.

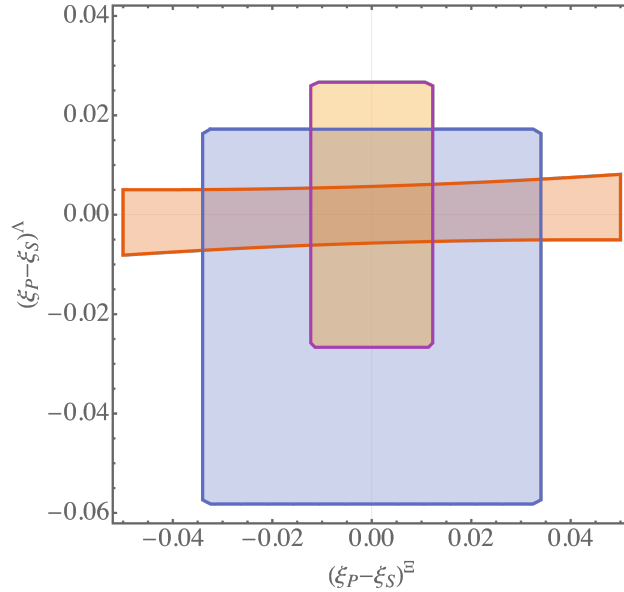


Figure 2: Summary of the results for the weak phases  $(\xi_P - \xi_S)^\Xi$  and  $(\xi_P - \xi_S)^\Lambda$ . The present BESIII results are given by the blue rectangle [8, 9]. The red horizontal band is the HyperCP result [31]. The brown rectangle is the projection of the statistical uncertainties for the complete BESIII data set.

### 2.3. Spin entangled baryon–antibaryon systems

STCF provides a novel method to search for  $CP$  violation in baryon decays using entangled baryon–antibaryon pairs. For stable spin 1/2 hyperons, copiously produced pairs from the  $J/\psi$  resonance decays can be used. In general, the spin

state of a baryon–antibaryon system can be represented as

$$|B\bar{B}\rangle = \sum_{\mu,\nu=0}^3 C_{\mu\nu}^{B\bar{B}} \sigma_{\mu}^{(B)} \otimes \sigma_{\nu}^{(\bar{B})}, \quad (26)$$

where the Pauli operators  $\sigma_{\mu}^{(B)}$  and  $\sigma_{\nu}^{(\bar{B})}$  act in the rest frames of the baryon and antibaryon, respectively. The coefficients of the spin correlation–polarization matrix,  $C_{\mu\nu}^{B\bar{B}}$ , depend on the baryon-pair production process. At STCF, the pair can be produced in a single photon annihilation process of an electron–positron pair.

The vertex function  $\Gamma_{\mu}$  for the single photon annihilation in the  $e^+e^- \rightarrow B\bar{B}$  process with a particle-antiparticle pair of spin 1/2 and mass  $m_B$  is [36]

$$\Gamma_{\mu} := F_1(q^2) \gamma_{\mu} + F_2(q^2) \frac{i\sigma_{\mu\nu}q^{\nu}}{2m_B}, \quad (27)$$

where  $q = p_1 + p_2$  denotes the momentum of the virtual photon. These form factors are related to the helicity amplitudes by

$$\begin{aligned} G_E \propto A_{+1/2,+1/2} &= 2m_B (F_1 + \tau F_2), \\ G_M \propto A_{+1/2,-1/2} &= \sqrt{2q^2} (F_1 + F_2), \end{aligned} \quad (28)$$

where  $\tau = q^2/4m_B^2$ . The expressions are formally the same for the process that proceeds via a decay of a neutral vector meson, such as  $J/\psi$  or  $\psi(2S)$ . If the meson decays via a single photon annihilation, the electromagnetic form factors  $G_E$  and  $G_M$  at the resonance are directly related to the continuum form factors via hadronic vacuum polarization. However, if *e.g.* the decay process is strong, the interpretation of the form factors is different and relates to the properties of the resonance. For example, for intermediate vector charmonia resonances, they are often called *psonic* form factors [37] to differentiate them from the electromagnetic form factors. Therefore, the single photon annihilation is fully described by two complex scalars. If we ignore the unmeasurable global phase, there are three real parameters that fully define the properties of the process. One of the parameters defines the overall normalization and the total cross section of the reaction. In the standard setting, the collider beams are unpolarized and the elements of the  $C_{\mu\nu}^{B\bar{B}}$  matrix are known functions of the baryon  $B$  production angle,  $\theta$ . The functions for a given c.m. energy depend on the two remaining parameters that need to be determined from data [21, 37]. The  $G_M$  and  $G_E$  form factors are functions of the centre-of-mass energy squared,  $s$ . The distribution of the production angle

$\theta$  is given as

$$\frac{1}{\sigma} \frac{d\sigma}{d\cos\theta} = \frac{3}{2} \frac{1 + \alpha_P \cos^2\theta}{3 + \alpha_P}, \quad (29)$$

where

$$\alpha_P = \frac{\tau|G_M|^2 - |G_E|^2}{\tau|G_M|^2 + |G_E|^2} = \frac{\tau - R^2}{\tau + R^2} \quad (30)$$

with  $R := |G_E|/|G_M|$ . In addition, if the relative complex phase between the amplitudes  $\Delta\Phi := \text{Arg}(G_E/G_M)$  is not zero, the baryons spin is polarized in the direction perpendicular to the reaction plane, given by the  $\hat{y}$  unit vector. The polarization vector component  $P_y(\theta)$  and the spin correlation terms  $C_{ij}(\theta)$ ,  $i, j = x, y, z$  are:

$$C_{\mu\nu}^{B\bar{B}} = \frac{1}{\sigma} \frac{d\sigma}{d\cos\theta} \begin{pmatrix} 1 & 0 & P_y & 0 \\ 0 & C_{xx} & 0 & C_{xz} \\ -P_y & 0 & C_{yy} & 0 \\ 0 & -C_{xz} & 0 & C_{zz} \end{pmatrix}, \quad (31)$$

where the orientations of the coordinate systems in the rest frames of  $B$  and  $\bar{B}$  are related as  $(\hat{x}, \hat{y}, \hat{z})_B = (\hat{x}, -\hat{y}, -\hat{z})_{\bar{B}}$ . The explicit expressions for the spin correlation matrix terms are:

$$\begin{aligned} P_y &= \sqrt{1 - \alpha_P^2} \sin(\Delta\Phi) \sin\theta \cos\theta := \beta_P \sin\theta \cos\theta, \\ C_{xy} &= \sqrt{1 - \alpha_P^2} \cos(\Delta\Phi) \sin\theta \cos\theta := \gamma_P \sin\theta \cos\theta, \\ C_{xx} &= \sin^2\theta, \\ C_{yy} &= \alpha_P \sin^2\theta, \\ C_{zz} &= \alpha_P + \cos^2\theta. \end{aligned}$$

The above expressions were derived for unpolarized electron and positron beams. At STCF longitudinally polarized electron beams will be available. The corresponding spin correlation matrix is given in Ref. [19].

For hyperon decay studies at STCF, reactions of special interest are  $J/\psi$  decays. This is due to the huge yield of hyperon–antihyperon pairs from strong  $J/\psi$  decays. These are manifested by the large branching fractions of 1–2 per mil. The branching ratios and the form factor parameters  $\alpha_\psi$  and  $\Delta\Phi_\psi$  for the relevant  $e^+e^- \rightarrow J/\psi \rightarrow B\bar{B}$  processes are given in Table 3. Due to the non-zero phase between the form factors, the hyperons are polarized in the direction perpendicular to the production plane in the case of unpolarized beams. This polarization changes with the production angle as shown in Fig. 3 by the solid lines. The

Table 3: Properties of the  $e^+e^- \rightarrow J/\psi \rightarrow B\bar{B}$  decays to the pairs of ground-state octet hyperons.

Final state	$\mathcal{B}(\times 10^{-4})$	$\alpha_\psi$	$\Delta\Phi_\psi(\text{rad})$	Comment
$\Lambda\bar{\Lambda}$	19.43(3)	0.4748(22)(31)	0.7521(42)(66)	[9, 24, 38]
$\Sigma^+\bar{\Sigma}^-$	15.0(24)	-0.508(7)	-0.270(15)	[26, 39]
$\Sigma^-\bar{\Sigma}^+$	— no data —			
$\Sigma^0\bar{\Sigma}^0$	11.64(4)	-0.4133(85)	-0.0828(76)	[40]
$\Xi^0\bar{\Xi}^0$	11.65(43)	0.514(6)(15)	1.168(19)(18)	[10, 41]
$\Xi^-\bar{\Xi}^+$	9.7(8)	0.611(7)(13)	1.30(3)(3)	[8, 23, 42]

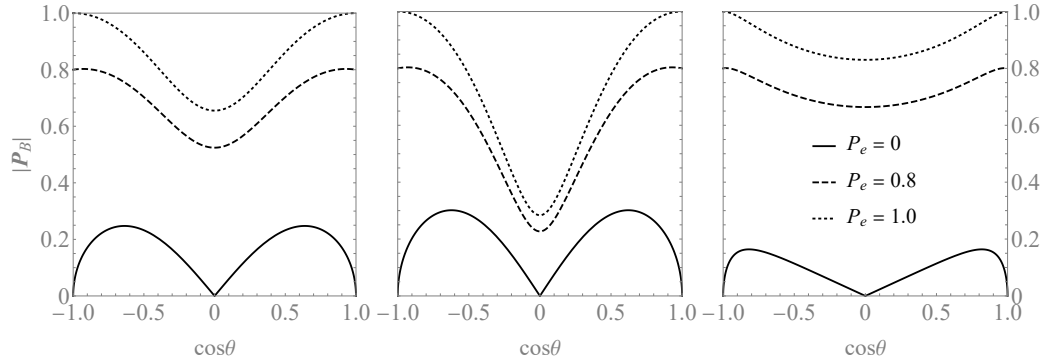


Figure 3: Magnitudes of the hyperon polarization as a function of the production angle for: (a)  $\Lambda$ , (b)  $\Xi^-$  and (c)  $\Sigma^+$  for the electron beam polarizations  $P_e = 0, 0.8, 1$  (solid, dashed and dotted lines, respectively). The  $\alpha_\psi$  and  $\Delta\Phi_\psi$  values are taken from Table 3.

impact of the electron beam polarization for the absolute value of the hyperon polarization is shown by dashed and dotted lines for the beam polarization of 80% and 100%, respectively. For the polarized beam, the direction of the hyperon polarization vector is not restricted to the direction orthogonal to the production plane.

Equation (9) implies that in the parity-violating weak decays of the hyperons, the average spin direction is reflected by the angular distributions of the decay products. For example, in the case of the  $e^+e^- \rightarrow \Lambda\bar{\Lambda}$  reaction with one-step

decays  $\Lambda(\bar{\Lambda})$  into  $p\pi^-(\bar{p}\pi^+)$  the complete five-fold angular distribution is

$$\mathcal{W}(\theta, \mathbf{n}_\Lambda, \mathbf{n}_{\bar{\Lambda}}) \propto \quad (32)$$

$$(1 + \alpha_P \cos^2 \theta) \left[ 1 + (\alpha_\Lambda n_{\Lambda,y} + \alpha_{\bar{\Lambda}} n_{\bar{\Lambda},y}) P_y + \alpha_\Lambda \alpha_{\bar{\Lambda}} \sum_{i,j=x,y,z} C_{ij}^{\Lambda\bar{\Lambda}} n_{\Lambda,i} n_{\bar{\Lambda},j} \right], \quad (33)$$

where  $n_{\Lambda,i}$  and  $n_{\bar{\Lambda},j}$  are directional cosines of the proton (antiproton) in the  $\Lambda$  and  $\bar{\Lambda}$  reference frames, respectively. It can be rewritten in the modular form as

$$\mathcal{W}(\boldsymbol{\xi}; \boldsymbol{\omega}_\Lambda) = \sum_{\mu,\nu=0}^3 C_{\mu\nu}^{\Lambda\bar{\Lambda}} a_{\mu 0}^\Lambda a_{\nu 0}^{\bar{\Lambda}}. \quad (34)$$

For multi-step processes there are more kinematic variables and the expression for the probability density function is much more complicated. They can be conveniently expressed in modular form, as derived in Ref. [21]. In addition to the  $\alpha_B$  parameter also the  $\beta_B$  can be involved. For example, in the  $e^+e^- \rightarrow \Xi\bar{\Xi}$  process with two-step decay sequence  $\Xi \rightarrow \Lambda\pi$  and  $\Lambda \rightarrow p\pi^-$ , one can determine separately  $\alpha_\Xi$ ,  $\beta_\Xi$  and  $\alpha_\Lambda$  parameters. The production and the two-step decays in the  $e^+e^- \rightarrow \Xi^-\bar{\Xi}^+$  case are described by a nine-dimensional vector  $\boldsymbol{\xi}$  of the helicity angles. The structure of the nine-dimensional angular distribution is determined by eight global parameters  $\boldsymbol{\omega}_\Xi := (\alpha_\psi, \Delta\Phi, \alpha_\Xi, \phi_\Xi, \bar{\alpha}_\Xi, \bar{\phi}_\Xi, \alpha_\Lambda, \bar{\alpha}_\Lambda)$  and in the modular form gives [21]:

$$\mathcal{W}(\boldsymbol{\xi}; \boldsymbol{\omega}_\Xi) = \sum_{\mu,\nu=0}^3 C_{\mu\nu}^{\Xi\bar{\Xi}} \sum_{\mu',\nu'=0}^3 a_{\mu\mu'}^\Xi a_{\nu\nu'}^{\bar{\Xi}} a_{\mu'0}^\Lambda a_{\nu'0}^{\bar{\Lambda}}. \quad (35)$$

The BESIII experiment has studied two reactions that provide the best sensitivity for the  $CP$  tests in hyperon decays:  $e^+e^- \rightarrow J/\psi \rightarrow \Lambda\bar{\Lambda}$  [9, 24] and  $e^+e^- \rightarrow J/\psi \rightarrow \Xi\bar{\Xi}$  [8]. At the BESIII experimental setting -that should be similar to STCF- for every million of the produced  $J/\psi$  resonances, 320 and 56 of fully reconstructed  $\Lambda\bar{\Lambda}$  and  $\Xi\bar{\Xi}$  pairs are selected, respectively.

With  $10^{10}$   $J/\psi$  mesons available at BESIII, precision measurements of the hyperon decay parameters are possible. The average baryon polarizations  $|P_y|$  in the  $e^+e^- \rightarrow J/\psi \rightarrow \Lambda\bar{\Lambda}$  and  $e^+e^- \rightarrow J/\psi \rightarrow \Xi\bar{\Xi}$  reactions are 18% and 23%, respectively. The two production reaction parameters, the decay parameters  $\alpha_\Lambda$ ,  $\alpha_\Xi$  and  $\beta_\Xi$ , as well as the  $CP$ -violating variables  $A_{CP}^\Lambda$ ,  $A_{CP}^{\bar{\Xi}}$  and  $B_{CP}^{\bar{\Xi}}$ , can

be determined using unbinned maximum likelihood fit to the measured angular distributions. The statistical uncertainty of the observable  $A_{CP}^\Lambda$  in the process  $e^+e^- \rightarrow J/\psi \rightarrow \Lambda\bar{\Lambda}$  is inversely proportional to the  $\Lambda$  polarization [19]. The weak phase difference for the  $\Xi$  baryon decay is directly given by the measurement of the  $B_{CP}^\Xi$  observable in the process  $e^+e^- \rightarrow J/\psi \rightarrow \Xi\bar{\Xi}$ . The sensitivity of such measurement depends on the average squared of the  $\Xi$  polarization and the  $\Xi\bar{\Xi}$  spin correlation terms [19].

#### 2.4. Radiative and semileptonic decays

Hyperon radiative decays  $B_1 \rightarrow B_2\gamma$  have branching fractions of the order of per mil. The angular distribution of the daughter baryon in a radiative decay of a polarized hyperon  $B_1$  has the same form as in the case of weak hadronic decays. It is described by a decay asymmetry parameter  $\alpha_\gamma$ . The branching fractions and the values of decay parameters are summarized in Table 4. However, polarization of the baryon  $B_2$  is given by the following aligned decay matrix correspond-

Table 4: Hyperon radiative decays: branching fractions,  $\mathcal{B}$ , and decay asymmetries,  $\alpha_\gamma$ .

Decay	$\mathcal{B} \times 10^3$	$\alpha_\gamma$	Comment
$\Sigma^+ \rightarrow p\gamma$	1.04(6)	-0.76(8)	[6]
$\Sigma^+ \rightarrow p\gamma$	0.996(28)	-0.652(56)	[43]
$\Lambda \rightarrow n\gamma$	0.832(66)	-0.16(11)	[6]
$\Xi^0 \rightarrow \Sigma^0\gamma$	3.33(10)	-0.69(6)	[6]
$\Xi^0 \rightarrow \Lambda\gamma$	1.17(7)	-0.70(7)	[6]
$\Xi^0 \rightarrow \Lambda\gamma$	1.347(85)	-0.741(65)	[44]
$\Xi^- \rightarrow \Sigma^-\gamma$	0.13(2)	-	[6]

ing to the situation where the radiative photon helicities are unmeasured [45]:

$$b_{\mu\nu}^\gamma \propto \begin{pmatrix} 1 & 0 & 0 & \alpha_\gamma \\ 0 & 0 & 0 & 0 \\ 0 & 0 & 0 & 0 \\ -\alpha_\gamma & 0 & 0 & -1 \end{pmatrix}. \quad (36)$$

Therefore, even if the final baryon polarization is measured, only the  $\alpha_\gamma$  parameter is accessible. The  $CP$  symmetry can be studied by comparing the branching fractions and the decay parameters for a hyperon decay to the charge conjugated process of the antihyperon. Studies with the hyperon–antihyperon pairs produced

at an electron–positron collider provide these quantities simultaneously. For example, for  $\Sigma^+ \rightarrow p\gamma$ , BESIII has determined  $\Delta_{CP} = (\mathcal{B}_+ - \mathcal{B}_-)/(\mathcal{B}_+ + \mathcal{B}_-) = 0.006(12)$  and  $A_{CP} = (\alpha_+ + \alpha_-)/(\alpha_+ - \alpha_-) = 0.095(89)$  [43].

The weak radiative processes and the hadronic weak decays are coupled channels that can mix due to parity-conserving electromagnetic interactions. For example, according to the BESIII data [46], the branching fraction for decay  $\Lambda \rightarrow n\gamma$  is completely saturated by the unitarity lower limit of  $0.85 \times 10^{-3}$  [47], where the two intermediate weak processes  $\Lambda \rightarrow p\pi^-$  and  $\Lambda \rightarrow n\pi^0$  combine with the inverse photoproduction processes  $p\pi^- \rightarrow n\gamma$  and  $n\pi^0 \rightarrow n\gamma$ . On the other hand, the amplitude of  $\Sigma^+ \rightarrow p\gamma$  requires a significant real part of the amplitude, due to short-range contributions, since the unitarity lower limit is only  $0.69 \times 10^{-5}$ , *i.e.* more than two orders of magnitude lower than the observed branching fraction. Closely related are decays where the produced radiative photon converts externally into an electron–positron pair. It is possible to define additional  $CP$  tests (similar as for semileptonic (SL) processes discussed below), however, they are suppressed by  $\alpha_{em}$ , what limits the sensitivity. An example of such process is  $\Xi^0 \rightarrow \Lambda e^+e^-$ , with branching fraction  $7.6(6) \times 10^{-6}$ , and the decay asymmetry  $\alpha_{\gamma^*} = -0.8(2)$ , measured by the NA48 collaboration [48]. Other interesting conversion decay is  $\Sigma^+ \rightarrow p\mu^+\mu^-$ , where the first observation at HyperCP [49] suggested an anomalously large branching fraction of  $(8.6_{-5.5}^{+6.6} \pm 5.5) \times 10^{-8}$ . Moreover, the  $\mu^+\mu^-$  invariant masses for the three observed events were within 1 MeV, suggesting a narrow resonance contribution. The experiment was repeated by the LHCb collaboration, determining the branching fraction  $(2.2_{-0.8-1.1}^{+0.9+1.5}) \times 10^{-8}$  [50], consistent with the SM predictions [51, 52]. It is important to mention the first attempts to calculate this decay from first principles using Lattice QCD [53].

In addition, in the electromagnetic decay  $\Sigma^0 \rightarrow \Lambda\gamma$ , flavour-diagonal  $CP$  violation can be searched for, by first determining a non-zero value for  $\alpha_\gamma$  which would indicate edm contribution and then comparing it with the  $\bar{\alpha}_\gamma$  value [54, 55].

SL decays  $B_1 \rightarrow B_2\ell\bar{\nu}_\ell$  proceed via external emission of the intermediate  $W$  boson. At STCF exclusive measurements of many SL decays can be performed using a tagging method, that allows to determine the complete kinematic information of the processes with the neutrino escaping the detector. Therefore, in principle, all decay form factors can be determined.

The amplitude for a SL decay of a  $1/2^+$  hyperon  $B_1$  into a  $1/2^+$  baryon  $B_2$  and an off-shell  $W^-$ -boson decaying to the lepton pair  $l^-\bar{\nu}_l$  with the momenta and masses denoted as  $B_1(p_1, M_1) \rightarrow B_2(p_2, M_2) + l^-(p_l, m_l) + \bar{\nu}_l(p_\nu, 0)$  due to the

Table 5: Branching fractions of semileptonic decays of hyperons [6].

Transition	$\mathcal{B}$	
	$e^- \bar{\nu}_e$	$\mu^- \bar{\nu}_\mu$
$\Lambda \rightarrow pW^-$	$8.34(14) \times 10^{-4}$	$1.51(19) \times 10^{-4}$
$\Sigma^- \rightarrow nW^-$	$1.007(34) \times 10^{-3}$	$4.5(4) \times 10^{-4}$
$\Sigma^+ \rightarrow \Lambda W^+$	$2.3(4) \times 10^{-5}$	—
$\Sigma^+ \rightarrow nW^+$	$< 5 \times 10^{-6}$	$< 3.0 \times 10^{-5}$
$\Xi^0 \rightarrow \Sigma^+ W^-$	$2.52(8) \times 10^{-4}$	$2.33(35) \times 10^{-6}$
$\Xi^0 \rightarrow \Sigma^- W^+$	$< 1.6 \times 10^{-4}$	$< 9 \times 10^{-4}$
$\Xi^0 \rightarrow pW^-$	$< 1.3 \times 10^{-3}$	$< 1.3 \times 10^{-3}$
$\Xi^- \rightarrow \Xi^0 W^-$	$< 1.9 \times 10^{-5}$	—
$\Xi^- \rightarrow \Sigma^0 W^-$	$8.7(17) \times 10^{-5}$	$< 8 \times 10^{-4}$
$\Xi^- \rightarrow \Lambda W^-$	$1.27(23) \times 10^{-4}$	$3.5(35) \times 10^{-4}$

vector  $J_\mu^V$  and axial-vector  $J_\mu^A$  currents is [56]

$$\begin{aligned}
 \langle B_2 | J_\mu^V + J_\mu^A | B_1 \rangle = & \bar{u}(p_2) \left[ \gamma_\mu (F_1^V(q^2) + F_1^A(q^2)\gamma_5) + \frac{i\sigma_{\mu\nu}q^\nu}{M_1} (F_2^V(q^2) + F_2^A(q^2)\gamma_5) \right. \\
 & \left. + \frac{q_\mu}{M_1} (F_3^V(q^2) + F_3^A(q^2)\gamma_5) \right] u(p_1), \tag{37}
 \end{aligned}$$

where  $q_\mu := (p_1 - p_2)_\mu = (p_l + p_\nu)_\mu$  is the four-momentum transfer. The four-momentum squared  $q^2$  ranges from  $m_l^2$  to  $(M_1 - M_2)^2$ . The form factors  $F_{1,2,3}^{V,A}(q^2)$  are complex functions of  $q^2$  that describe hadronic effects in the transition. Neglecting possible  $CP$ -odd weak phases, the corresponding form factors are the same for the  $(l^-, \bar{\nu}_l)$  and  $(l^+, \nu_l)$  transitions. To fully determine the hadronic part of a SL decay, the six involved form factors should be extracted as a function of  $q^2$ . The form factors are usually parameterized by the axial-vector to vector  $g_{av}^D$  coupling, the weak-magnetism  $g_w^D$  coupling and the pseudoscalar  $g_{av3}^D$  coupling. They are obtained by normalizing to  $F_1^V(0)$ :

$$g_{av}^D(q^2) = \frac{F_1^A(q^2)}{F_1^V(0)}, \quad g_w^D(q^2) = \frac{F_2^V(q^2)}{F_1^V(0)}, \quad g_{av3}^D(q^2) = \frac{F_3^A(q^2)}{F_1^V(0)}. \tag{38}$$

Since the hyperon decays have limited range of  $q^2$ , the  $q^2$ -dependence, in the first approximation, can be completely neglected by using the values at the  $q^2 = 0$  point. An improved approximation includes an effective-range parameter  $r_i$  that

represents a linear dependence on  $q^2$ :

$$F_i(q^2) = F_i(0) [1 + r_i q^2 + \dots] . \quad (39)$$

In addition, since there are no hadronic intermediate states in this limited  $q^2$  range, the form factors are real-valued functions. The couplings and the effective range parameters can be determined from the multidimensional distributions observed in experiments. The optimal approach for such parametric estimation is the maximum likelihood method using multidimensional unbinned data. The experiments do not measure spin of the leptons but if a hyperon is produced, its spin can be determined from a sub-sequential weak decay. This information about a SL decay can be summarized in terms of the following aligned decay matrix [45]:

$$b_{\mu\nu} = \begin{pmatrix} b_{00} & b_{01} & 0 & b_{03} \\ b_{10} & b_{11} & 0 & b_{13} \\ 0 & 0 & b_{22} & 0 \\ b_{30} & b_{31} & 0 & b_{33} \end{pmatrix} . \quad (40)$$

In the  $B_1$  reference frame,  $\mathbb{R}_1$ , the four-momentum vector of the off-shell  $W^-$  is  $q_\mu = (q_0, p \sin \theta_W \cos \phi_W, p \sin \theta_W \sin \phi_W, p \cos \theta_W)$ . The energy  $q_0$  and the magnitude of the three-momentum  $p$  of the off-shell  $W^-$  boson are the following functions of  $q^2$

$$q_0(q^2) = \frac{1}{2M_1} (M_1^2 - M_2^2 + q^2) \quad (41)$$

and

$$p(q^2) = |\mathbf{p}_2| = \frac{1}{2M_1} \sqrt{Q_+ Q_-}, \quad (42)$$

where

$$Q_\pm = (M_1 \pm M_2)^2 - q^2. \quad (43)$$

The decay  $W^- \rightarrow l^- \bar{\nu}_l$  is described in the  $\mathbb{R}_W$  reference frame, where the emission angles of the  $l^-$  lepton are  $\theta_l$  and  $\phi_l$ . The value of the lepton momentum in this frame is

$$|\mathbf{p}_l| = \frac{q^2 - m_l^2}{2\sqrt{q^2}} . \quad (44)$$

Contrary to the decay matrices for two body decays, each element is a function of  $q^2$  and  $\cos \theta_l$ . Moreover, the alignment of the decay plane for a three-body decay requires all three Euler angles. The differential decay rate is obtained from

$b_{00}$  by multiplying by the kinematic and spinor normalization factors that depend on  $q^2$

$$d\Gamma = \frac{G_F^2}{(2\pi)^5} |V_{us}|^2 \frac{|\mathbf{p}_l||\mathbf{p}_2|}{16M_1^2} (q^2 - m_l^2) b_{00} dq d\Omega_2 d\Omega_l \quad (45)$$

$$= G_F^2 |V_{us}|^2 V_{Ph}(q^2) (q^2 - m_l^2) b_{00} dq d\Omega_2 d\Omega_l, \quad (46)$$

where  $V_{Ph}(q^2) = (2\pi)^{-5} (4M_1)^{-2} |\mathbf{p}_l||\mathbf{p}_2|$  is the three-body phase space density factor [15]. The momenta  $|\mathbf{p}_2|$  and  $|\mathbf{p}_l|$  of the baryon  $B_2$  and the lepton are given in Eqs. (42) and (44), respectively. The virtue of hyperon SL decays is that they can be used as complementary determination of the  $|V_{us}|$  element of the CKM matrix [57]. The necessary form factors are two-point functions which might be soon accessible in Lattice QCD calculations [58, 59].

### 2.5. *CP violation in production via EDM*

$\Lambda$  hyperon is the only one in the hyperon family with a measured EDM upper limit of  $1.5 \times 10^{-16}$  e cm, at Fermilab [60]. The  $\Lambda$  EDM absolute value, indirectly estimated from the neutron EDM upper limit, is  $< 4.4 \times 10^{-26}$  e cm [61–64]. No indirect predictions exist for hyperons with two or three strange valence quarks. Challenges in direct EDM measurements for hyperons include their limited lifetimes and difficulties in preparing diverse hyperon sources for a single fixed-target experiment.

STCF can efficiently produce and reconstruct massive entangled pairs of  $\Lambda$ ,  $\Sigma$ , and  $\Xi$  hyperon-antihyperon from charmonium  $J/\psi$  decays, which allows us to study minute violations of conservation laws. The entangled production of hyperon-antihyperon pairs incorporates the electric dipole form factor in the  $P$ - and  $CP$ -violating components of the Lorentz invariant amplitude, providing a unique opportunity to indirectly extract hyperon EDM. If we assume a  $J = 1$  object in the  $s$ -channel for the annihilation of electron–positron into a baryon–antibaryon pair but without imposing  $P$  and  $C$  conservation, there are four complex form factors to describe the process [65]. To make direct link to the EDM of baryon, we write the helicity amplitude of  $J/\psi \rightarrow B\bar{B}$  decay with four complex form factors following Ref. [65] as:

$$\begin{aligned} \mathcal{M}_{\lambda_1, \lambda_2} = \epsilon_\mu (\lambda_1 - \lambda_2) \bar{u}(\lambda_1, p_1) & \left[ F_V(q^2) \gamma^\mu + \frac{i}{2m} \sigma^{\mu\nu} q_\nu H_\sigma(q^2) \right. \\ & \left. + \gamma^\mu \gamma^5 F_A(q^2) + \sigma^{\mu\nu} \gamma^5 q_\nu H_T(q^2) \right] v(\lambda_2, p_2), \end{aligned} \quad (47)$$

where  $q^2 = M_{J/\psi}^2$ ,  $m$  is  $B$  hyperon mass, and  $p_1$  and  $p_2$  are the four-momenta of hyperon  $B$  and anti-hyperon  $\bar{B}$ , respectively.

Processes involving a flavor-diagonal  $CP$ -violating vertex contribute to the electric dipole form factor  $H_T$ , connecting hyperon EDM to fundamental theories. Various extensions of the SM lead to unique contributions to these operators, impacting hyperon EDM differently. Hyperon EDM measurements offer a direct way to assess the contributions of quark EDM and quark chromoelectric dipole moment [66], as the effects of high-dimensional operators are suppressed and neutron EDM measurements constrain the QCD  $\theta$  term. NP, like supersymmetry, could significantly enhance hyperon EDM, which would indicate a special coupling between strange quarks and NP. By establishing a connection between the  $CP$  violation form factor  $H_T$  and the hyperon EDM contribution, one finds [65, 67, 68]:

$$H_T(q^2) = \frac{2e}{3M_{J/\psi}^2} g_V d_B(q^2). \quad (48)$$

The EDM form factor  $d_B(q^2)$  is typically a complex number for nonzero timelike momentum transfer, equal to the real EDM of hyperon  $B$  in the vanishing  $q^2$  limit. This form factor can effectively be treated as an EDM under the assumption that the momentum transfer dependence is negligible, by considering an unknown extension to the zero region. The contribution from the exotic form factors could be accommodated in the spin-density matrix  $C_{\mu\nu}^{B\bar{B}}$  corresponding to eq. (31) by adding the components related to the CPV contribution

$$\begin{aligned} C_{0x}^{\text{CPV}} &= m_B^2 \sin 2\theta (\tau \text{Im } a - \text{Re } b) \\ C_{x0}^{\text{CPV}} &= -m_B^2 \sin 2\theta (\tau \text{Im } a + \text{Re } b) \\ C_{0z}^{\text{CPV}} &= -\sqrt{\tau} [(\text{Re } c - 2\text{Im } d) \cos^2 \theta + \text{Re } c + 2\text{Im } d] \\ C_{0z}^{\text{CPV}} &= \sqrt{\tau} [(\text{Re } c + 2\text{Im } d) \cos^2 \theta + \text{Re } c - 2\text{Im } d] \\ C_{xy}^{\text{CPV}} &= -\sqrt{\tau} \sin^2 \theta (\text{Im } c - 2\text{Re } d) \\ C_{yx}^{\text{CPV}} &= \sqrt{\tau} \sin^2 \theta (\text{Im } c + 2\text{Re } d) \\ C_{yz}^{\text{CPV}} &= m_B^2 \sin 2\theta (\tau \text{Im } a - \text{Re } b) \\ C_{zy}^{\text{CPV}} &= -m_B^2 \sin 2\theta (\tau \text{Im } a + \text{Re } b) \end{aligned} \quad (49)$$

and the ones due to the EDM contribution

$$C_{\mu\nu}^P = -2m_B^2 d_J |G_M|^2 \frac{\tau}{1 + \alpha_P} \begin{pmatrix} 0 & \gamma_P \sin \theta & 0 & 2\tau \zeta_P \cos \theta \\ \gamma_P \sin \theta & 0 & 0 & 0 \\ 0 & 0 & 0 & \gamma_P \sin \theta \\ -2\tau \zeta_P \cos \theta & 0 & \gamma_P \sin \theta & 0 \end{pmatrix} \quad (50)$$

with

$$\zeta_P := \frac{1 + \alpha_P + \gamma_P}{1 + \alpha_P} \quad (51)$$

$$a := F_A G_M^* \quad (52)$$

$$b := \frac{1}{2m_B} H_T G_E^* \quad (53)$$

$$c := \frac{1}{m_B} F_A G_E^* \quad (54)$$

$$d := \frac{1}{m_B^2} H_T G_M^* . \quad (55)$$

The combined production matrix is then the sum  $C_{\mu\nu}^{B\bar{B}} + C_{\mu\nu}^{\text{CP}} + C_{\mu\nu}^P$  and it can be applied for a modular description of the joined angular distributions.

To evaluate the EDM measurement sensitivity for various hyperon systems at STCF, we generated 500 pseudo-data sets using a cascade decay probability density function that incorporates hyperon production and decay processes [65, 69]. Factors such as branching fractions, detection efficiencies, and the effect of a longitudinally polarized electron beam were taken into account. These pseudo-data sets were analyzed through a maximum likelihood fit, simultaneously extracting all hyperon-related parameters and estimating the expected experimental sensitivities. The results are presented in Fig 4 [69]. The sensitivity for  $\Lambda$  EDM reaches  $10^{-21}$  e cm (red full triangle), marking a significant 5-orders-of-magnitude enhancement compared to the existing measurement at Fermilab with similar statistics. Additionally, the STCF experiment maintains high sensitivities of  $10^{-20}$  e cm for the  $\Sigma^+$ ,  $\Xi^-$ , and  $\Xi^0$  hyperons [66, 69]. Hyperon EDM measurements will serve as a crucial milestone and a rigorous test for NP theories like SUSY and the left-right symmetrical model.

At  $J/\psi$  one can use hadronic vacuum polarization to increase sensitivity for the EDM effect. Contribution of the two photon processes is negligible.

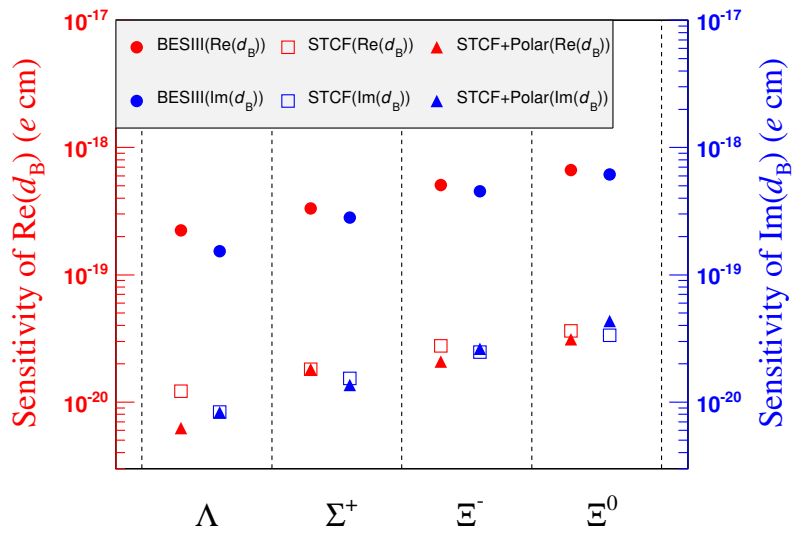


Figure 4: Sensitivity of EDM for different hyperons. The markers for hyperons  $\Lambda$ ,  $\Sigma^+$ ,  $\Xi^-$ , and  $\Xi^0$  are located within dashed regions, respectively. The red and blue markers correspond to the sensitivity of the physical quantities represented by the red title (left Y axis) and blue title (right Y axis) in the graph. The full circle, open square, and full triangle up correspond to the estimated sensitivities for the BESIII experiment, the STCF experiment with an unpolarized beam, and the STCF experiment with 80% polarized electron beam, respectively.

## 2.6. Prospect of hyperon $CP$ violation study at STCF

The advantage of studying hyperon  $CP$  violation at Tau-Charm factory is obvious. The polarization of hyperons can be disentangled, and the measured precision of the hyperon  $CP$  violation can match that of fixed target experiment with three orders of magnitude less statistics. The  $CP$  violation test of all the SU(3) hyperons can be performed with pair production from  $J/\psi$  decay. Thus more  $CP$  violation observables can be constructed. Since 2019, the BESIII experiment has shown its great potential in the search of hyperon  $CP$  violation via the decay of 10 billion  $J/\psi$  events [24]. With the large branching fraction of  $J/\psi \rightarrow B\bar{B}$  with  $B\bar{B}$  denoting hyperon pairs, ten million of hyperons and anti-hyperons can be obtained at BESIII. Moreover, the hyperons are naturally polarized transversely due to the non-zero phase of two helicity amplitudes

$$P_y = -\frac{\sqrt{1 - \alpha_\psi^2} \sin \theta \cos \theta}{1 + \alpha_\psi \cos^2 \theta} \sin \Delta\Phi_\psi, \quad (56)$$

where  $\alpha_\psi$  and  $\Delta\Phi$  are the parameters that describe  $J/\psi \rightarrow B\bar{B}$ . Moreover, by the cascade decays, the weak phase can be determined for the first time [8]. It is quite promising to discover the hyperon  $CP$  violation with more statistics at STCF. With the current designed energy spread, more than 3.4 trillion  $J/\psi$  events will be collected at STCF with  $1 \text{ ab}^{-1}$  integrated luminosity. Following the statistical sensitivity of the  $CP$  violation test will be discussed.

Charged tracks are selected based on the criteria in the fast simulation. Efficiency loss occurs due to the acceptance requirement  $|\cos \theta| < 0.93$ , where  $\theta$  is set in reference to the beam direction, and the requirements on the  $\Lambda$  mass and decay vertex. The decay process of  $J/\psi \rightarrow \Lambda\bar{\Lambda}$  can be described as follows: the  $\Lambda$  decays into a  $p$  and  $\pi^-$ , while the  $\bar{\Lambda}$  decays into a  $\bar{p}$  and  $\pi^+$ . Therefore, the candidate event must have at least four charged tracks. Charged tracks are divided into two categories, where positively charged tracks are  $p$  and  $\pi^+$ , and negatively charged tracks are  $\bar{p}$  and  $\pi^-$ . Based on the momentum of tracks, the momentum of the particle track can subsequently be identified as  $p(\bar{p})$  or  $\pi^+(\pi^-)$ . Specifically, particles with a momentum exceeding 500 MeV/ $c$  are identified as  $p(\bar{p})$ , while those with a momentum less than 500 MeV/ $c$  are classified as  $\pi^+(\pi^-)$ . For selected events, multiple charged tracks must be present for  $p$ ,  $\bar{p}$ ,  $\pi^+$  and  $\pi^-$ , respectively. A second vertex fit is performed by looping over all combinations of positively and negatively charged tracks. The selected  $p\pi^-$  ( $\bar{p}\pi^+$ ) pairs must decay from the same vertex. The invariant mass of  $\Lambda(\bar{\Lambda})$  must fall within the range of  $1.111 < M_{p\pi^-/\bar{p}\pi^+} < 1.121 \text{ GeV}/c^2$ . The event selection efficiency is finally

determined to be 38.2%. The influence of the polarization of the electron beam on event selection efficiency has also been studied, and the selection efficiency is found to be unaffected by beam polarization.

Based on the joint angular distribution, a maximum likelihood fit is performed with four free parameters  $(\alpha_\psi, \alpha_-, \alpha_+, \Delta\Phi_\psi)$ . The joint likelihood function, as shown in Eq. (57), is used for this purpose.

$$\mathcal{L} = \prod_{i=1}^N \mathcal{P}(\xi^i, \alpha_\psi, \alpha_-, \alpha_+, \Delta\Phi) = \prod_{i=1}^N \mathcal{C}\mathcal{W}(\xi^i, \alpha_\psi, \alpha_-, \alpha_+, \Delta\Phi)\epsilon(\xi^i), \quad (57)$$

The probability density function of the kinematic variable  $\xi^i$  for event  $i$  denoted as  $\mathcal{P}(\xi^i, \alpha_\psi, \alpha_-, \alpha_+, \Delta\Phi)$  is used in a maximum likelihood fit. The detection efficiency is represented by  $\epsilon(\xi^i)$  and  $N$  denotes the total number of events. The normalization factor, denoted as  $\mathcal{C}^{-1} = \frac{1}{N_{MC}} \sum_{j=1}^{N_{MC}} \mathcal{W}(\xi^j, \alpha_\psi, \alpha_-, \alpha_+, \Delta\Phi)\epsilon(\xi^j)$ , is estimated the  $N_{MC}$  events generated with the phase space model, which is about ten times the size of mDIY MC. Usually, the minimization of  $-\ln\mathcal{L}$  is performed by using MINUIT:

$$-\ln\mathcal{L} = - \sum_{i=1}^N \ln\mathcal{C}\mathcal{W}(\xi^i, \alpha_\psi, \alpha_-, \alpha_+, \Delta\Phi)\epsilon(\xi^i). \quad (58)$$

In this analysis, we extrapolate the sensitivity of  $CP$  violation for a large number of  $J/\psi$  events generated at future STCF, taking into account the effects of excessive storage pressure. This extrapolation is based on the relationship between the sensitivity of  $CP$  violation and generated 0.1 trillion  $J/\psi$  events. We investigate this relation using a sample size ranging from 0.01 to 0.1 trillion  $J/\psi$ , with a step size of 0.01 trillion  $J/\psi$ . The sensitivity analysis is presented in Fig. 5(a), where we examine the impact of event statistics on the sensitivity of  $CP$  violation. The sensitivity can be described using the following formula:

$$\sigma_{ACP} \times \sqrt{N_{\text{fin}}} = k. \quad (59)$$

The variable  $N_{\text{fin}}$  represents the number of events that pass the final selection criteria, while  $k$  is a constant with a value of 7.82. As shown in Fig. 5(b), the sensitivity improves proportionally with the polarization. This observation provides a foundation for extrapolating  $CP$  violation sensitivity from the size of the data sample.

Five different beam polarizations were utilized to generate a sample of 0.1 trillion MC events, with the specific aim of investigating the quantity  $\sigma_{ACP}$ . The resulting five sets of data points were fit using Eq. (60) [19]:

$$\sigma_{ACP} \approx \sqrt{\frac{3}{2}} \frac{1}{\alpha_- \sqrt{N_{sig}} \sqrt{\langle P_\Lambda^2 \rangle}}. \quad (60)$$

Under the same sample size, the obtained results align with those in Ref. [70], maintaining consistency at the order of magnitude level. By extrapolating the number of  $J/\psi$  events based on the 3.4 trillion events expected to be generated annually by future STCF, the statistical sensitivity of  $CP$  violation will reach the order of  $\mathcal{O}(10^{-4})$ , and a beam polarization of 80% will further improve the sensitivity by a factor of 3.

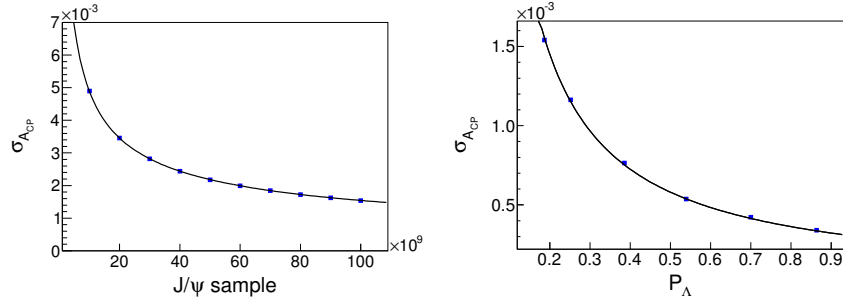


Figure 5: The blue dots represent the statistical errors of  $CP$  violation, while the black line is fitted using Eq. (59). The blue dots represent the values of  $\sigma_{ACP}$  under different  $\Lambda$  polarization.

A comparison of the hyperon  $CP$  sensitivity at STCF with various experiments, namely the LHCb and BelleII experiments, is presented as follows.

- **Production mechanism of hyperons**

The LHCb experiment produces hyperons mainly via promote production, and the decay of  $B$  meson or charmed/bottom baryons. With the data collected in run2, about 13 million of  $\Xi^-$  and 5 million of  $\Omega^-$  hyperons have been reconstructed inclusively. The Hyperons are not polarized from promote production, and may have polarization from decays, *e.g.* from charmed baryon. It is therefore essential to distinguish the hyperons from promote production or from decay. With the run3 data, five times more hyperons can be produced than that of run2. As for run4 and run5, the integrated luminosities of  $40 \text{ fb}^{-1}$  and  $300 \text{ fb}^{-1}$  are expected, respectively.

The Belle and Belle II experiments produce hyperons depending on the running strategy, mainly from decays of  $B$  meson and charmed baryons (and also  $\Upsilon(nS)$  ( $n = 1, 2, 3$ ) at Belle), and  $e^+e^- \rightarrow q\bar{q}$  ( $q = u, d, s$ ). The cross sections of  $e^+e^- \rightarrow b\bar{b}$  and  $c\bar{c}$  are about 1.1 nb and 1.3 nb, respectively. Using the  $\Lambda_c^+ \rightarrow \Lambda\pi^+$  decay where the  $\Lambda_c^+$  is produced from  $e^+e^- \rightarrow c\bar{c}$  process with  $1 \text{ ab}^{-1}$  integrated luminosity at Belle experiment, more than  $10^5$   $\Lambda$  events are reconstructed with the precision of decay asymmetry parameters determined to be at the level of  $\mathcal{O}(10^{-3})$ . The  $\Lambda_c$  is supposed to be not polarized via the process  $e^+e^- \rightarrow c\bar{c}$  and the final  $\Lambda$  is polarized due to the weak decay of  $\Lambda_c$ . With the inclusive process  $e^+e^- \rightarrow [\Xi^- \rightarrow \Lambda\pi^-] + X$ , where  $X$  denotes anything, Belle ( $980 \text{ fb}^{-1}$ ) has reconstructed over  $10^6$   $\Xi^-$  hyperons with high purity, and may reach a precision of  $\mathcal{O}(10^{-3})$  level for  $\alpha_{\Xi}\alpha_{\Lambda}$ . With full Belle II data set ( $50 \text{ ab}^{-1}$ ), this  $\Xi^-$  inclusive sample will be exceed the  $5 \times 10^7$  level.

The STCF produces hyperons mainly from their pair production. With 3.4 trillions of  $J/\psi$  events foreseen and the branching fraction of  $J/\psi \rightarrow B\bar{B}$  to be  $\mathcal{O}(10^{-3})$ , a rough estimation of hyperons pair produced via  $J/\psi$ , as well as the maximum polarization of hyperons, are presented in Table 6.

Table 6: Expected number of hyperon pairs at STCF, where the Br is cited from Ref. [15].  $\epsilon$  is the reconstruction efficiency of the exclusive decay from BESIII.  $N_{rec}$  is the expected reconstructed number of hyperon events at STCF, with similar efficiency as BESIII, and  $P_y^{\max}$  is the maximum transverse polarization of hyperon in  $J/\psi$  decay.

Sample	Br( $\times 10^{-3}$ )	$\epsilon$	$N_{rec}$	$P_y^{\max}$
$J/\psi \rightarrow \Lambda\bar{\Lambda}$	$1.89 \pm 0.09$	40%	$1 \times 10^9$	25%
$J/\psi \rightarrow \Sigma^+\bar{\Sigma}^-$	$1.07 \pm 0.04$	24%	$2.2 \times 10^8$	16%
$J/\psi \rightarrow \Sigma^0\bar{\Sigma}^0$	$1.172 \pm 0.032$	20%	$3.3 \times 10^8$	-
$J/\psi \rightarrow \Sigma^-\bar{\Sigma}^+$	$1.51 \pm 0.06$	6%	$3.0 \times 10^8$	-
$J/\psi \rightarrow \Xi^0\bar{\Xi}^0$	$1.17 \pm 0.04$	14%	$2.3 \times 10^8$	27%
$J/\psi \rightarrow \Xi^-\bar{\Xi}^-$	$0.97 \pm 0.08$	19%	$2.5 \times 10^8$	30%

- **Expected statistical sensitivity**

From the reconstructed number of hyperon samples at LHCb with data collected in run2, the  $CP$  observable  $A_{\Xi\Lambda} = \frac{\alpha_{\Xi}\alpha_{\Lambda} + \alpha_{\Xi}\bar{\alpha}_{\bar{\Lambda}}}{\alpha_{\Xi}\alpha_{\Lambda} + \alpha_{\Xi}\bar{\alpha}_{\bar{\Lambda}}}$  can be constructed, where  $\alpha_{\Xi}$  and  $\alpha_{\Lambda}$  is the decay asymmetry parameter of  $\Xi^-$  and  $\Lambda$ , respectively. The sensitivity is in a level of  $\mathcal{O}(10^{-3})$ . The expected statistical

sensitivity is better than  $\mathcal{O}(3 \times 10^{-4})$  with  $50 \text{ fb}^{-1}$  integrated luminosity reached in till run4.

At Belle and Belle II, with  $\Lambda_c^+ \rightarrow \Lambda\pi^+$  inclusive sample, the  $\alpha$ -induced  $CP$  violation observable of  $\Lambda \rightarrow p\pi^-$  decay is constructed to be  $A_\Lambda = \frac{\alpha_\Lambda + \alpha_{\bar{\Lambda}}}{\alpha_\Lambda - \alpha_{\bar{\Lambda}}}$  under the assumption of  $CP$  conservation in Cabibbo-favored decay  $\Lambda_c^+ \rightarrow \Lambda\pi^+$  (i.e  $\alpha_{\Lambda_c^+} = -\alpha_{\bar{\Lambda}_c^-}$ ). Based on  $980 \text{ fb}^{-1}$  of data set at Belle, the statistical uncertainty of  $A_\Lambda$  is determined to be  $7 \times 10^{-3}$  [71]. With  $50 \text{ ab}^{-1}$  integrated luminosity collected at Belle II foreseen, the statistical sensitivity of  $A_\Lambda$  is estimated to be  $10^{-3}$ .

At STCF,  $CP$  observables of  $\Lambda$ ,  $\Sigma^+$ ,  $\Xi^0$  and  $\Xi^-$  can be constructed via  $A_Y = \frac{\alpha_Y + \alpha_{\bar{Y}}}{\alpha_Y - \alpha_{\bar{Y}}}$ , where  $\alpha_Y$  is the decay asymmetry parameter of the hyperon. The sensitivity follows the empirical formula as in Eq. 60. With unpolarized electron-positron beam, the maximum polarization of hyperons can be found in Table 6. The average polarization of  $\Lambda$ ,  $\Sigma^+$  and  $\Xi^-$  with unpolarized beam is 18%, 10%, and 22%, respectively [19]. When the electron beam is 80% polarized, the average polarization of  $\Lambda$ ,  $\Sigma^+$  and  $\Xi^-$  is 70%, 70% and 60%, respectively. The corresponding sensitivity of  $A_Y$  is summarized in Table 7.

Table 7: Expected statistical sensitivity of  $A_Y$  with different polarization at STCF.

Hyperon	$\alpha_Y$	$\langle P_Y^2 \rangle_{(P_e=0)}$	$\sigma_{A_Y(P_e=0)}$	$\langle P_Y^2 \rangle_{(P_e=80\%)}$	$\sigma_{A_Y(P_e=80\%)}$
$\Lambda$	0.75	18%	$3 \times 10^{-4}$	70%	$7 \times 10^{-5}$
$\Sigma^+$	-0.98	10%	$8 \times 10^{-4}$	70%	$1 \times 10^{-4}$
$\Xi^-$	-0.376	22%	$9 \times 10^{-4}$	60%	$3 \times 10^{-4}$

- **Systematic uncertainty** The systematic uncertainty from LHC hyperon  $CP$  test mainly comes from the asymmetry of detector, and the uncertainty from the simulation model. Several assumptions should be made under the law that Cabibbo allowed decay produces unpolarized hyperons, while Cabibbo suppressed decay produces polarized hyperons. The systematic uncertainty will be a dominant limiting factor of the results.

The systematic uncertainty from Belle  $\Lambda$  hyperon  $CP$  test via  $\Lambda_c^+$  Cabibbo-favored decay is determined to be  $1.1 \times 10^{-2}$ , that is larger than statistical uncertainty, and dominated by the source of the fit bias. Other systematic sources contribute a systematic uncertainty of  $3 \times 10^{-3}$ . Naively, the uncertainty from fit bias can be likely to improve with a better fit procedure,

therefore, the final sensitivity of such  $A_\Lambda$  measurement at Belle II is promisingly estimated to be at the  $10^{-3}$  level.

At STCF, the uncertainty sources of hyperon  $CP$  test is the selection criteria related, those including tracking, vertex fitting and kinematic fit; the background contamination and the fit method. These are statistically related, and are estimated to be in a level of  $10^{-4} \sim 10^{-5}$ . Apart from that, the effects from regeneration, decoherence, or non-uniformity of magnetic field will play an important role in the systematic uncertainty, thus demands detailed detector design and simulation in future.

Overall, the STCF offers great potential to search of new  $CP$  violation source via through direct measurements of  $CP$  violation and EDM measurements in hyperon sector. It is expected to produce billions of quantum-correlated hyperon-antihyperon with almost background free. Numerous  $CP$  observables can be constructed. From the feasibility study, the  $CP$  violation in hyperon non-leptonic decays will reach  $\mathcal{O}(10^{-4})$  and the EDM of hyperons will reach  $\mathcal{O}(10^{-20}) \sim \mathcal{O}(10^{-21}) e \text{ cm}$ .

### 3. $CP$ violation in $\tau$ sector

As the only lepton that is massive enough to open the hadronic decay channels, the SL  $\tau$  decay provides an excellent platform to explore the nonperturbative QCD dynamics and is one of the leading research subjects at the electron-positron colliders. In the meanwhile, the rich patterns of the  $\tau$  lepton decaying into different hadrons offer valuable opportunities to study the  $CP$  violation phenomena. In this section, we first give a brief review about the current status of the various hadron form factors and structure functions entering the SL  $\tau$  decays. Then we elaborate on different types of  $CP$  violation observables in the hadronic final states in  $\tau$  decays, and pay special attention to the  $CP$  violation study in the  $\tau \rightarrow K_S^0 \pi \nu_\tau$  channel. The  $\tau$  EDM is shortly discussed as well. At the end of this section, we give some prospects for the  $CP$  violation measurements of the  $\tau$  lepton at STCF.

#### 3.1. Hadronic form factors in semileptonic $\tau$ decays

In the SM, hadronization in two-meson tau decays is described by two form factors,  $f_{0,+}(Q^2)$ , carrying angular momenta  $J = 0, 1$ , respectively ( $D = d, s$  below)

$$\begin{aligned} & \langle P_1(q_1) P_2(q_2) | \bar{u} \gamma^\mu D + h.c. | 0 \rangle \\ &= C^{12} \left\{ \frac{\Delta_{12}}{Q^2} f_0^{12}(Q^2) (q_1 + q_2)^\mu + f_+^{12}(Q^2) \left[ (q_1 - q_2)^\mu - \frac{\Delta_{12}}{Q^2} (q_1 + q_2)^\mu \right] \right\}, \end{aligned} \quad (61)$$

where  $C^{\pi^- \pi^0} = \sqrt{2}$ ,  $Q^2 = (q_1 + q_2)^2$ ,  $\Delta_{12} = m_1^2 - m_2^2$ , and the finiteness of the matrix element at the origin imposes  $f_0(0) = f_+(0)$ , which depart from unity only by flavor symmetry breaking corrections.

Using the angle  $\alpha$ , defined by the momenta of  $P_1$  and  $\tau$  in the hadronic rest frame, the double differential decay rate reads [72]

$$\begin{aligned} \frac{d\Gamma(\tau^- \rightarrow (P_1 P_2)^- \nu_\tau)}{d \cos \alpha d\sqrt{Q^2}} &= \frac{(C^{12} G_F |V_{uD}|)^2}{128 \pi^3} \left( \frac{M_\tau^2}{Q^2} - 1 \right)^2 \frac{\lambda^{1/2}(Q^2, M_1^2, M_2^2)}{2\sqrt{Q^2} M_\tau} \\ & \left\{ |f_0^{12}(Q^2)|^2 \Delta_{12}^2 + |f_+^{12}(Q^2)|^2 \lambda(Q^2, M_1^2, M_2^2) \left( \frac{Q^2}{M_\tau^2} + \left( 1 - \frac{Q^2}{M_\tau^2} \right) \cos^2 \alpha \right) \right. \\ & \quad \left. - 2 \text{Re}[f_0^{12}(Q^2) f_+^{12}(Q^2)^*] \Delta_{12} \lambda^{1/2}(Q^2, M_1^2, M_2^2) \cos \alpha \right\}, \end{aligned} \quad (62)$$

where  $\lambda(a, b, c) = a^2 + b^2 + c^2 - 2(ab + ac + bc)$ .

In the three-meson case, the most general decomposition of the matrix element encoding the hadronization of the left-handed  $W$ -mediated current in presence of strong interactions is [72]

$$\langle P_1(q_1)P_2(q_2)P_3(q_3)|\bar{u}\gamma^\mu(1-\gamma_5)D+h.c.|0\rangle = V_1^\mu F_1 + V_2^\mu F_2 + V_3^\mu F_3 + Q^\mu F_4, \quad (63)$$

where  $Q^\mu = (q_1+q_2+q_3)^\mu$ ,  $V_{1\mu} = \left(g_{\mu\nu} - \frac{Q_\mu Q_\nu}{Q^2}\right)(q_2-q_1)^\nu$ ,  $V_{2\mu} = \left(g_{\mu\nu} - \frac{Q_\mu Q_\nu}{Q^2}\right)(q_3-q_1)^\nu$ ,  $V_{3\mu} = i\epsilon_{\mu\nu\rho\sigma}q_1^\nu q_2^\rho q_3^\sigma$ . The  $F_{1,2,4}$  form factors carry axial-vector quantum numbers and  $F_3$  stems from the vector current (anomalous sector).

The differential decay width contains information on four angles and is most conveniently written in terms of structure functions [72], which are bilinears of form factors depending also on kinematical invariant variables. More information on this formalism is given in the next subsection.

Beyond the Standard Model, the two-meson matrix elements can also correspond to a scalar or a tensor current [73]. The form factor associated to the hadronization of the scalar current is related to  $f_0(Q^2)$  via the divergence of the vector current hadron matrix element [74], while the tensor current form factor can be related to  $f_+(s)$  in the elastic region [75]. For three mesons, new form factors from hadronizing possible pseudoscalar and tensor currents appear [76]. The former is proportional to  $F_4$ , while for the latter simplifications to the involved three-body unitary treatment arise thanks to (approximate and useful) discrete symmetries of QCD.

Dispersive descriptions of the  $f_{0,+}(Q^2)$  form factors in Eq. (61) exploit their analytic properties and are best suited to comply with unitarity, according to

$$f_{0,+}^{12}(Q^2) = P_N(Q^2)\Omega_{0,+}^{12}(Q^2), \quad (64)$$

where the Omnès function is

$$\Omega_{0,+}^{12}(Q^2) = \exp\left[\frac{Q^2}{\pi}\int_{s'_0}^{\infty} ds' \frac{\phi_{0,+}^{12}(s')}{s'(s'-Q^2)}\right]. \quad (65)$$

In this way, knowledge of the form factor phase ( $\tan\phi = \text{Im}\phi/\text{Re}\phi$ ) everywhere encodes this whole complex function. With a perfect description of the phase, the degree  $N$  of the polynomial  $P_N(Q^2)$  is immaterial. Increasing  $N$  (which brings in additional subtraction constants to  $f_{0,+}(0)$ ) reduces the weight of the high-energy region of the integrand, where data are worse.  $N$  is chosen to be as small as possible, while keeping a close description of the measurements. In addition to

experimental input, theory also restricts  $f_{0,+}(Q^2)$ . Asymptotically, they must fall off as  $1/Q^2$  [77], with their phase being an integer multiple of  $\pi$  at infinite  $Q^2$ . Watson's Theorem ensures the equality of the form factors phase with the corresponding phase shift of di-meson scattering in the elastic region. Close enough to threshold, the chiral symmetry of QCD [78, 79] predicts the low- $Q^2$  behaviours of the form factors. The intermediate energy region phase depends on the properties of the various resonance states (particularly their pole positions and relative phases) that can be exchanged in the process.

The best understood form factor is  $f_+^{\pi\pi}(Q^2)$ . Roy equations constrain stringently the relevant (iso)vector phaseshift in the elastic region [80, 81] for  $Q^2 \lesssim 1 \text{ GeV}^2$ , allowing for dispersive representations of  $f_+(Q^2)$ , which are phenomenologically successful up to  $M_\tau^2$  [82, 83]. See also Refs. [84–89] for discussing additional scattering channels. A similar approach is pursued for  $f_+^{K\pi}$ . In this instance, the dispersive form factor has been obtained in Refs. [90–94]. Dispersive vector form factors for partner decay modes  $f_+^{K\bar{K}(K\eta^{(\prime)})}$  have been determined based on  $f_+^{\pi\pi(K\pi)}$  in Refs. [83]([94, 95]). A thorough analysis of the electromagnetic kaon form factor was recently performed in Ref. [96]. The  $\tau^- \rightarrow \pi^- \eta^{(\prime)} \nu_\tau$  decays are more subtle, due to their strong  $G$ -parity suppression [97, 98] and Refs. [99, 100] differ substantially in their predictions for  $f_+^{\pi^- \eta^{(\prime)}}$ .

Scalar and tensor two-meson form factors were computed in Ref. [101]. Specifically,  $f_0^{\pi\pi}$  (which determines  $f_0^{\pi^- \eta^{(\prime)}}$  [74, 99]) was addressed in Refs. [87, 99, 102, 103], although the  $K\pi$  sector is better known thanks to its relevance in  $K\pi$  scattering [104–106], which enables a precise determination of the coupled  $f_0^{K^-(\pi^0/\eta/\eta')}$  form factors [107]. Inelastic effects on  $f_0^{K\pi}$  were the focus of Ref. [108]. Finally,  $f_0^{K\bar{K}}$  was derived in Ref. [102]. Tensor form factors in Refs. [101, 109–111] are also subject to chiral dynamics.

For the three-meson final states, fully unitary dispersive determinations of the form factors are not yet available. There are, however, sound approximations implementing two-body dominance [90] (for  $K\pi\pi$ ), and chiral constraints beyond leading order: [112–116] ( $\pi\pi\pi$ ), [117] ( $KK\pi$ ), [118] ( $\eta\pi\pi$ ), [119] (vector meson and a light pseudoscalar), [120] ( $4\pi$ ).

One- and two-meson  $\tau$  decays can bring in additional useful information (particularly regarding  $CP$  or  $T$  violation) when including a real photon, or a virtual pair-converting one. The corresponding form factors and radiative corrections have been determined, according to the known chiral behaviour, in Refs. [121–128].

The timelike form factors of the light pseudoscalar mesons have also been de-

terminated recently by the lattice QCD simulations. Most of the existing lattice calculations focus on the  $\pi\pi$  electromagnetic form factors [129–132], which could be related to the charged vector  $\pi\pi$  form factor entering in the  $\tau$  decay via the isospin transformation. However, the lattice simulations are still done with unphysically large pion masses, and hence chiral extrapolations are generally needed to provide direct inputs for the study of  $\tau$  decays. Future developments in the lattice simulations to probe the electroweak timelike form factors involving kaons and multi-pions can provide alternative inputs, which will be definitely helpful for the precision studies of hadronic  $\tau$  decays.

### 3.2. Structure functions in $\tau$ decays with hadronic final states

This formalism was introduced in Ref. [72] and, barring interactions of tensor type in the lepton and hadron vertices [76], it gives the most general description of these decays in a model-independent way (including  $\tau$  polarization).

It is based on the introduction of two reference frames ( $S$  and  $S'$ ) and the use of the Euler rotation (with angles  $\alpha, \beta$  and  $\gamma$ ) connecting them.  $S$  simplifies the description of the hadron tensor and  $S'$  of the  $\tau$  spin and momentum.  $S$  is defined by a plane containing hadron momenta and its normal.  $S'$  is again specified by a plane and its normal, with the former containing the hadrons' direction in the lab system and the  $\tau$  flight direction seen from the hadronic rest frame (see Fig. 1 in Ref. [72]). The angle  $\alpha$  is unobservable unless the  $\tau$  momentum can be measured, which is the case for flavor factories. However, in  $\tau$  pair production near threshold at STCF, the lab frame coincides with the COM one, which facilitates the description of  $S'$  (see appendix B of Ref. [72] for explicit formulae in this case).

The matrix element factorizes in its lepton and hadron parts, with the most general description of its modulus squared (factoring the lepton part out) giving rise to the structure functions,  $W_i$ , which are bilinears of form factors, depending also on kinematical invariant variables.  $W_{E,F,H,SC,SE,SF}$  are odd under time reversal and others are sensitive to  $CP$ -violation through interferences among form factors (in presence of non-vanishing weak phase differences). These observations make structure functions in SL  $\tau$  decays particularly interesting for this section.

Ref. [72] quotes the relations between the  $W_i$  and the  $f_i$  ( $F_i$ ) for the two (three) meson cases. In principle, all 16 structure functions (and thus all hadronization information) can be determined in a data-driven way if decays of a polarized  $\tau$  are analyzed in its rest frame [72], which should be possible at a STCF running close to threshold production.

### 3.3. $CP$ violation observables in hadronic $\tau$ decays

Hadronic  $\tau$  decays provide rich sources to probe possible  $CP$  violation phenomena, since the multitude of kinematical variables from multi-meson channels can be helpful to construct proper quantities to isolate the  $CP$  violation signals from the  $CP$ -even ones. Generally speaking, three different types of observables are studied in literature [75, 133–148], which allow to discern different mechanisms for the generation of  $CP$  violation: the integrated/full rate asymmetry, local rate asymmetry (also referred as differential angular distribution asymmetry) and the triple-product asymmetry.

In order to have true  $CP$  violation signals, at least two different amplitudes that can interfere with each other with nonvanishing relative phases are required for a given  $\tau$  decay reaction, with the exception of the  $K^0 - \bar{K}^0$  mixing induced  $CP$  violation in the  $\tau^- \rightarrow K_S^0 X^- \nu_\tau$  decays, such  $X = \pi, K, \pi\pi$ , etc., as discussed later. The SM amplitude is given by the  $W$  exchange, while the other one can be mediated by a hypothetical charged Higgs, a new  $W'_L$  coupled to left-handed current<sup>1</sup> and/or a leptoquark field, among others.

The hadronic decay amplitudes of the  $\tau$  lepton can be conveniently described by numerous structure functions [72], which can receive contributions both from SM and BSM. On the one hand, the weak  $CP$ -violating phases in the hadronic  $\tau$  decays are expected to be much suppressed in the SM, since they can be only generated via higher-order weak interactions, *e.g.* the SM  $CP$  asymmetry in the  $\tau^\pm \rightarrow K^\pm \pi^0 \nu_\tau$  processes turns out to be at the level of  $10^{-12}$ , that is far below the current experimental sensitivity [138]. On the other hand, this also indicates that any experimental observation of the  $CP$  violation in  $\tau$  decays, except the ones caused by  $K^0 - \bar{K}^0$  mixing, will be a smoking gun for BSM NP. As a result, it is convenient to only introduce the weak  $CP$ -violating phase to the BSM part in the  $\tau$  decay amplitude. Therefore, for a given  $\tau$  decay reaction, one can write its amplitude sketchily as

$$T = \sum_i A_i e^{i\phi_i^A} + \sum_j B_j e^{i(\delta_j + \phi_j^B)}, \quad (66)$$

where  $A_i$  and  $B_j$  stand for the magnitudes of amplitudes from SM and BSM contributions respectively, and the phases  $\phi_j^A$  and  $\phi_j^B$  denote the  $CP$ -even strong

---

<sup>1</sup>The interference of a right-handed  $W_R$  and  $W$  from SM is proportional to the neutrino mass. Therefore the possible effect from  $W_R$  in the  $CP$  violation discussion of  $\tau$  decays can be ignored in a first approximation.

phases and the weak  $CP$ -odd phases are represented by  $\delta_j$  (defined relative to the SM weak phase). In general, it is reasonable to assume  $|B_j| \ll |A_j|$  in Eq. (66), although -due to the symmetry constraints- sometimes specific form factors  $A_j$  could be vanishing or suppressed in the SM.

The nonzero  $CP$  violation observable can be calculated via the decay amplitude (Eq. (66)) squared, *i.e.*,

$$|T|^2 = \left| \sum_i A_i e^{i\phi_i^A} \right|^2 + 2\text{Re} \left[ \left( \sum_i A_i e^{i\phi_i^A} \right) \left( \sum_j B_j e^{i(\delta_j + \phi_j^B)} \right)^* \right] + \left| \sum_j B_j e^{i(\delta_j + \phi_j^B)} \right|^2. \quad (67)$$

For the  $CP$  conjugate process, the sign of the  $CP$ -odd phases  $\delta_j$  should be reversed, *i.e.*, by taking  $\delta_j \rightarrow -\delta_j$ , while the rest remain the same. The second term with  $A_i B_j$  interference and the third one with  $B_i B_j$  interference are responsible for the  $CP$  violation strengths. Furthermore, the final  $CP$  violation observables that can be measured in experiments should be calculated by performing the kinematical phase space integrals for the squared decay amplitude, Eq. (66).

To enhance the  $CP$  violation features in the multi-meson  $\tau$  decay processes, it is crucial to investigate the various differential distributions of the sub-hadron systems with respect to specific kinematical variables. Many theoretical efforts have been completed to pursue such research goals.

For the integrated rate asymmetry, one simply performs the full integration of the phase spaces for the  $\tau^\pm$  processes and take the difference afterwards. A nonzero difference between the partial widths of the  $\tau^\pm$  would signalize the  $CP$  violation interaction. In many cases, especially when the charged Higgs is responsible for the BSM interaction, it is usually found that only the interference parts between the BSM and (generally suppressed) scalar SM form factors in the  $\tau$  decay, contribute to the integrated rate asymmetries, *e.g.*, for the  $\tau \rightarrow \rho\pi\nu_\tau$ ,  $\tau \rightarrow \omega\pi\nu_\tau$ ,  $\tau \rightarrow a_1\pi\nu_\tau$  and  $\tau^- \rightarrow K^-\pi\pi\nu_\tau$  processes [140, 141], which makes the integrated rate asymmetries less appealing in such cases.

Interestingly, by taking properly weighted kinematical variables, typically the cosine/sine of some specific angles, into the integration of phase-space, it is possible to isolate the substantial interference parts between the dominant form factors from the SM and the term with nonvanishing  $CP$ -violating phases, so as to enhance the  $CP$  violation signals as much as possible. Those weighted rate asymmetries are usually proportional to  $\sin \delta_i \sin \phi_j$ , namely both nonzero relative strong

and weak phases are needed for such  $CP$  violation observables [133, 140, 141]. *E.g.*, several weighted asymmetries are proposed for the  $\tau^\pm \rightarrow K^\pm \pi \pi \nu_\tau$  [141, 149] and  $\tau^\pm \rightarrow PP' \nu_\tau$  [133] (being  $P$  a light-flavor pseudoscalar meson).

Another type of  $CP$  violation observable can be constructed with the  $T$ -odd kinematical variable, also often referred as triple product  $\xi = \vec{v}_1 \cdot (\vec{v}_2 \times \vec{v}_3)$ , being  $\vec{v}_i$  the momentum or spin of the involved particles. To take spin to construct the triple product  $\xi$  means that the spin of the involved particle has to be measured and it is usually quite a challenge for the experiments [146, 147]. Meanwhile, when only taking momenta in the construction of  $\xi$ , one needs to consider at least a four-body decay process. It should be noted that the triple product asymmetries from a single  $\tau$  lepton could be also mimicked by the final-state interactions from the SM [127]. Conversely, the differences of the triple product asymmetries from  $\tau^\pm$  will definitely signalize the genuine  $CP$  violation interactions. A significant difference of the  $CP$  violation signals between the weighted rate asymmetries and triple-product asymmetries is that the former is proportional to  $\sin \delta_i \sin \phi_j$ , implying nonzero phases from the strong and weak parts, while the latter is proportional to  $\sin \delta_i \cos \phi_j$ , indicating that the strong phase is not required in such  $CP$  violation signals. Early studies about the triple product asymmetries in the  $\tau \rightarrow K \pi \pi \nu$  have been given in Ref. [144] and later refined in Refs. [141, 149].

We also point out that in the four- and five-body  $\tau$  decays, one can also access  $CP$  violation by  $T$ -odd observables [150, 151] without the information of the  $\tau$  polarization. The global as well as the local  $CP$  violation could be probed. Another direct  $CP$  violation observable constructed by comparing the forward-backward asymmetry of  $\tau^-$  and  $\tau^+$ , namely,  $A_{FB}(\tau^- \rightarrow K^- \pi^0 \nu_\tau) - \bar{A}_{FB}(\tau^+ \rightarrow K^+ \pi^0 \bar{\nu}_\tau)$ , could be also examined, although it takes a very small value in a two Higgs doublet model [152]. Note that  $A_{FB}$  itself is a manifestation of parity violation [153–155]. These topics are certainly worth to analyze in future experiments with higher-statistics data samples.

### 3.4. $CP$ violation in $\tau \rightarrow K_S^0 \pi \nu_\tau$ decays: the BaBar anomaly and the Belle measurement

In the SM, there is no genuine observable  $CP$  violation signal in the hadronic  $\tau$  decays. Any existence of such signal would manifest some novel kind of NP beyond SM. In fact, only the known  $CP$  violation in the neutral kaon system will lead to a nonzero  $CP$ -violating signal in the  $\tau$  decay channels containing the  $K_S^0$

or  $K_L^0$  state. As Bigi and Sanda first pointed out [136], the asymmetry

$$\begin{aligned} A_{CP}^\tau &= A_{CP}(\tau^- \rightarrow K_S^0 \pi^- \nu_\tau) \\ &= \frac{\Gamma(\tau^+ \rightarrow K_S^0 \pi^+ \bar{\nu}_\tau) - \Gamma(\tau^- \rightarrow K_S^0 \pi^- \nu_\tau)}{\Gamma(\tau^+ \rightarrow K_S^0 \pi^+ \bar{\nu}_\tau) + \Gamma(\tau^- \rightarrow K_S^0 \pi^- \nu_\tau)} \end{aligned} \quad (68)$$

should be about  $2\text{Re}\epsilon_K \approx 3.3 \times 10^{-3}$  due to the decay rate difference in  $\Gamma(\tau^+ \rightarrow K_L^0 \pi^+ \bar{\nu}_\tau)$  vs.  $\Gamma(\tau^- \rightarrow K_L^0 \pi^- \nu_\tau)$ . In fact, one can include any  $\pi^0$  into Eq. (68) without changing the value. It is interesting to note that the relation between the  $CP$  asymmetry of  $\tau^\pm \rightarrow K_S^0 \pi^\pm \nu_\tau$  and the one of  $\tau^\pm \rightarrow K_L^0 \pi^\pm \nu_\tau$  required by  $CPT$  symmetry is also discussed in Ref. [136], and this issue is elegantly explained in Ref. [156]. Motivated by this prediction, BaBar collaboration measured  $A_{CP}(\tau^- \rightarrow K_S^0 \pi^- (\geq 0\pi^0) \nu_\tau)$ :  $(-0.36 \pm 0.23 \pm 0.11)\%$ , with statistical and systematic error bars in order [157]. Noticeably, its sign is opposite to the prediction stemming from neutral kaon mixing. In fact, the prediction of  $3.3 \times 10^{-3}$  should be more carefully examined, as pointed out by Grossman and Nir in Ref. [158]. That is, the above mentioned asymmetry means the time-integrated decay rate asymmetry, where the interference of the  $K_S^0 - K_L^0$  term is as important as the pure  $K_S^0$  amplitude; the result crucially depends on the time interval over which the integration is done, and also the above theoretical value ought to be obtained by the convolution with the efficiency as a function of time (which should be part of the experimental analysis). The number  $3.3 \times 10^{-3}$  does correspond to the time interval  $[t_1, t_2]$  where  $t_1 \ll \tau_S$  and  $\tau_S \ll t_2 \ll \tau_L$  with  $\tau_S$  and  $\tau_L$  being the lifetime of  $K_S^0$  and  $K_L^0$  respectively, and also to the ideal efficiency  $\epsilon = 1$  within this range. BaBar considered its efficiency and find that there should be a multiplicative factor of  $1.08 \pm 0.01$  applied as a correction to the neutral kaon mixing result. Consequently, a realistic prediction is  $A_{CP}(\tau^- \rightarrow K_S^0 \pi^- \nu_\tau) = (0.36 \pm 0.01)\%$ , which deviates from the experimental result by 2.8 standard deviations. A more elaborate analysis may be to probe  $A_{CP}(\tau \rightarrow \nu_\tau K_S^0 \pi)$ ,  $A_{CP}(\tau \rightarrow \nu_\tau K_S^0 2\pi)$ ,  $A_{CP}(\tau \rightarrow \nu_\tau K_S^0 3\pi)$  separately to explore the existence of NP and impact of intermediate resonances [150], which would require more data.

This discrepancy aroused great interest, and various NP models were proposed. One typical example is given in Ref. [159], which found that a charged scalar interaction fails to yield the above rate asymmetry, although the  $CP$  violation could appear in angular observables; and instead, the non-standard tensor interaction could account for the measured rate asymmetry. More precisely speaking, the NP term was parametrized by its coupling strength and weak phase,

and these parameters could be accommodated by the PDG branching fraction value and the BaBar’s rate asymmetry measurement. However, as pointed out by Cirigliano, Crivellin and Hoferichter [75], the authors of Ref. [159] overlooked the Watson final-state interaction theorem in their treatment of the form factors, and thus the conclusion therein was challenged. This theorem states that the phase of the form factor should coincide with the corresponding scattering phase shift in the elastic scattering region [160]. Once considering this constraint, the effect of the tensor operator estimated in Ref. [159] would be strongly suppressed unless the coupling strength was very large, which -however- would conflict with the bounds from neutron EDM and  $D - \bar{D}$  mixing [75]. Later, Ref. [110] confirmed the result in Ref. [75] by allowing for more realistic variations of the tensor form factor (its modulus and phase) in the inelastic region. That is, the  $A_{CP}$  could reach the level of  $10^{-6}$  at most. Such a methodology was adopted by Refs. [161, 162] but with a more detailed analysis (extending to  $CP$ -violating asymmetries with angular information)<sup>2</sup>. Again, the  $CP$  violation measured by BaBar is hard to understand, given the various constraints from branching fraction, decay spectrum, (semi-)leptonic kaon decays, neutron EDM as well as  $D - \bar{D}$  mixing; one exception being a fine tuning (extreme cancellation between the NP contributions) or the NP occurring below the electroweak scale (see, however, Ref. [164]).

*In one word, the anomaly in the  $CP$ -violation value measured by BaBar gave rise to a bunch of dedicated studies, with extremely interesting outcomes.* Therefore more input from the experimental side should further revitalize this field, a new measurement from either Belle II or the proposed STCF considered here is absolutely essential, with results that will undoubtedly guide our future efforts to find NP signals in these searches.

Correspondingly, Belle II is studying this observable and the STCF will measure it after some years of data-taking [165] and will contribute to solving this conundrum, if not settled before.

Before BABAR’s result on  $A_{CP}^\tau$ , Belle [166] measured, in four  $Q^2$ -bins, a  $CP$ -violating asymmetry as the mean value of the  $\cos \beta \cos \Psi$  distributions<sup>3</sup> for the considered decays. The measured asymmetry was small ( $\mathcal{O}(10^{-3,-2})$ ) and,

---

<sup>2</sup>This effective treatment has just been extended to the other two-meson tau decays in Ref. [163], emphasizing the interest of similar measurements for the  $K_S K^\pm$  decay channels that can, moreover, provide an independent data-driven check of the BaBar anomaly.

<sup>3</sup>Here  $\beta$  is the second angle in the Euler rotation introduced in section 3.2 and  $\Psi$  is the angle between the direction of the COM frame and the direction of the  $\tau$ , as seen from the hadronic rest frame [72].

except for the lowest mass bin, within one standard deviation from zero. Given the achieved precision, this result cannot shed light on the BaBar anomaly<sup>4</sup>, which motivates further near-future measurements of  $CP$ -violating asymmetries in  $\tau \rightarrow K_S^0 \pi \nu_\tau$  and related channels.

### 3.5. $CP$ violation proposed via EDM

The EDM of the  $\tau$  can be introduced to the SM  $\bar{\tau}\tau\gamma$  vertex with the following Lorentz-invariant ansatz:

$$e\Gamma^\mu = -d_\tau(q^2)\sigma^{\mu\nu}\gamma^5 q_\nu, \quad (69)$$

where  $q$  stands for the photon momentum.

In the SM, a non-zero value of  $d_\tau$  is forbidden by both  $P$  invariance and  $T$  invariance. If  $CPT$  symmetry is assumed, observation of a non-zero value of  $d_\tau$  would imply new  $CP$ -violation sources beyond the KM mechanism and only upper bounds for fermion EDMs exist [168]. Due to its short lifetime, direct measurement of the  $\tau$  lepton's static dipole moment is extremely challenging, and currently, indirect information comes from measurements of processes involving  $\tau\bar{\tau}\gamma$  vertex in experiments.

For processes such as those considered by the LEP experiment ( $e^+e^- \rightarrow e^+e^-\tau^+\tau^-$ ,  $|d_\tau| \lesssim 10^{-16} e \text{ cm}$ ) [169–172] and by the Belle collaboration ( $e^+e^- \rightarrow \tau^+\tau^-$ ,  $|d_\tau| \lesssim 10^{-17} e \text{ cm}$ ) [173], the focus is on measuring the total cross-section to determine the EDM of the  $\tau$  lepton. As for the process  $e^+e^- \rightarrow \gamma\tau^+\tau^-$ , current research mostly involves measuring the total cross-section [174, 175]. The L3 collaboration considered data from running at Z-pole, including simple photon energy distribution and angular distribution information, which can determine the  $\tau$  lepton's EDM to be  $d_\tau = (0 \pm 1.5 \pm 1.3) \times 10^{-16} e \text{ cm}$  [176].

Kinematics of the final particles can be fully utilized to improve the constraints on  $d_\tau$  from experimental measurements. Theoretical studies based on the formalism of optimal observables applied to  $CP$ -odd quantities in the process  $e^+e^- \rightarrow \tau^+\tau^-$  [177–179] predict that Belle II experiment could measure the  $\tau$  lepton's EDM to the level of  $|d_\tau| < 2.04 \times 10^{-19} e \text{ cm}$  [178]. While for the the process  $e^+e^- \rightarrow \gamma\tau^+\tau^-$ , the main challenge lies in extracting useful information to the maximum extent from the rich angular distribution of final-state particles, calling for future studies.

---

<sup>4</sup>Neither can the earlier CLEO analysis [167].

The inherent  $CP$  properties of the  $\tau$  lepton also include the weak EDM, which is introduced to the  $\bar{\tau}\tau Z$  vertex in a similar way as EDM, with  $d_\tau^W = eF_3(q^2 = m_Z^2)$  being the weak EDM. By utilizing data collected near the Z-pole energy and considering the angular distribution information of the  $\tau$  lepton decay products in the  $e^+e^- \rightarrow \tau^+\tau^-$  process, the LEP experiments were able to constrain the weak EDM to the order of  $d_\tau^W < 10^{-17} e \text{ cm}$  [180, 181], leaving significant room for achieving the precision required to test the SM prediction (which is  $d_\tau^W \lesssim 8 \cdot 10^{-34} e \text{ cm}$  [182]). Future studies, *e.g.* with dedicated constructions of  $CP$ -sensitive observables for  $e^+e^- \rightarrow \gamma\tau^+\tau^-$  process at Z-pole, are expected to improve the constraints on the weak EDM.

Experiments like Belle II and STCF will gather more data in the future. Plans are in place to build new generations of electron-positron colliders across different regions, *e.g.* China, Japan and Europe, with their primary missions including running at the Z-pole energy for high-precision measurements. This presents a great opportunity for measuring the  $\tau$  lepton's EDMs. Research on  $\tau$  lepton EDM at future electron-positron colliders is still quite limited, mainly focusing on information related to scattering cross-sections [183–185]. Exploring  $CP$  sensitive observables and machine learning methods for these measurements would push the boundary of future experiments in constraining  $d_\tau$ . A preliminary feasibility study shows that STCF can test the tau EDM form factor with a sensitivity of  $10^{-18} e \text{ cm}$  in a wide energy range [186].

### 3.6. Prospect of $\tau$ $CP$ violation study at STCF

The peak of  $\tau$  pair production cross section  $e^+ + e^- \rightarrow \tau^+ + \tau^-$  is around 4.26 GeV, where it is 3.5 nb, which would yield  $3.5 \times 10^9$   $\tau$  pairs per year at STCF. The STCF has several advantages in the  $\tau$  physics study, such as the excellent ratio of signal to background, the perfect detection efficiency, the well-controlled systematic uncertainty and the capability of full event reconstruction, etc. In the following, the feasibility study of  $CP$  violation in  $\tau^- \rightarrow K_S^0 \pi^- \nu_\tau$  decay from  $e^+e^- \rightarrow \tau^+\tau^-$  at  $\sqrt{s} = 4.26$  GeV will be introduced with the fast simulation software package [187].

MC events corresponding to  $1 \text{ ab}^{-1}$  of integrated luminosity at  $\sqrt{s} = 4.26$  GeV are simulated. The  $e^+e^- \rightarrow \tau^+\tau^-$  process is generated with KKMC [188], which implement TAUOLA [189] to describe the production of  $\tau$  pairs and does not include asymmetry effect. Passage of the particles through the detector is simulated by the fast simulation software.

The signal process  $\tau^- \rightarrow K_S^0 \pi^- \nu_\tau$  is generated with vector and scalar config-

urations of  $K_S^0\pi$  and the parameterized spectrum is described by:

$$\frac{d\Gamma}{d\sqrt{s}} \propto \frac{1}{s} \left(1 - \frac{s}{m_\tau^2}\right)^2 \left(1 + \frac{2s}{m_\tau^2}\right) P(s) \times \left\{ P^2(s)|f_+|^2 + \frac{3(m_{K_S^0}^2 - m_\pi^2)^2|f_0|^2}{4s(1 + \frac{2s}{m_\tau^2})} \right\}, \quad (70)$$

which is the form inherited from Eq. (62) by integrating over the angle  $\alpha$ , where  $s$  is the squared invariant mass of  $K_S^0\pi^-$ . The masses of  $\tau$ ,  $K_S^0$  and charged  $\pi^-$  are  $m_\tau$ ,  $m_{K_S^0}$  and  $m_\pi$ , respectively.  $P(s)$  is the momentum of the  $K_S^0$  in the  $(K_S^0\pi^-)$  centre of mass frame, given by:

$$P(s) = \frac{\sqrt{(s - (m_{K_S^0} + m_\pi)^2)(s - (m_{K_S^0} - m_\pi)^2)}}{2\sqrt{s}}. \quad (71)$$

The  $f_0$  and  $f_+$  are the scalar and vector form factors to parameterize the amplitudes of  $K_0^*(800)$ ,  $K^*(892)$  and  $K^*(1410)$ :

$$f_0 = a_{K_0^*(800)} \cdot BW_{K_0^*(800)}, \quad (72)$$

$$f_+ = \frac{BW_{K^*(892)} + a_{K^*(1410)} \cdot BW_{K^*(1410)}}{1 + a_{K^*(1410)}}, \quad (73)$$

where BW denotes Breit-Wigner function, and  $a_{K_0^*(800)}$  and  $a_{K^*(1410)}$  are complex coefficients for the fractions of the  $K_0^*(800)$  and  $K^*(1410)$  resonances as presented in Ref. [190]. It should be noted that here simplified form factors are given, as compared to Sec. 3.1, for the sake of yielding faster evaluation with sensible results.

We consider signal events with  $\tau^+$  decaying to leptons,  $\tau^+ \rightarrow l^+\nu_l\bar{\nu}_\tau$  ( $l = e$  for  $e$ -tag,  $l = \mu$  for  $\mu$ -tag), and  $\tau^- \rightarrow K_S^0\pi^-\nu_\tau$  with  $K_S^0 \rightarrow \pi^+\pi^-$ . The existence of a  $K_S^0$  candidate is selected from pairs of oppositely charged tracks with invariant mass  $0.485 < M_{\pi^+\pi^-} < 0.512 \text{ GeV}/c^2$ . Moreover, to suppress the background from  $\tau^- \rightarrow \pi^+\pi^-\pi^-\nu_\tau$ , the flight significance of  $K_S^0$  candidates are required to be larger than 2 and the decay length of  $K_S^0$  larger than 0.5 cm.  $\mu^+$  is selected with an efficiency over 90% at momentum larger than 0.9 GeV/c and 40% at momentum 0.5 GeV/c for  $\mu$ -tag. The  $\pi/\mu$  mis-identification is 3% based on current design of the STCF detector. To suppress the background from  $\tau^- \rightarrow K_S^0\pi^-\pi^0\nu_\tau$  process, we veto a  $\pi^0$  candidate with two photons with invariant mass in the region between 0.115 and 0.15 GeV/c<sup>2</sup>. A machine learning technique is further implemented to suppress the hadronic final states. After the above selection, there are still backgrounds from  $\tau$  decays and the hadronic final states containing multiple  $\pi$

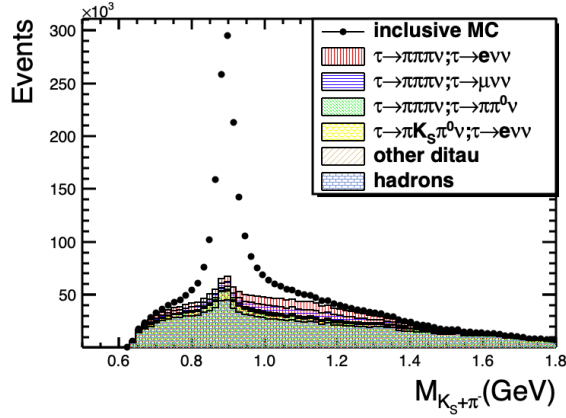


Figure 6: Invariant masses of  $K_S^0\pi^-$  with combined  $e$ -tag and  $\mu$ -tag from  $\tau^+$  decay after selection. Normalized according to the luminosity of  $1 \text{ ab}^{-1}$  at  $\sqrt{s} = 4.26 \text{ GeV}$ .

final states remain. The mass spectrum of  $K_S^0\pi^-$  after the above selections is shown in Fig. 6.

With the above selection criteria, the number of signal events  $\tau^-$  and  $\tau^+$  decay mode in  $1 \text{ ab}^{-1}$  inclusive MC at  $\sqrt{s} = 4.26 \text{ GeV}$  are obtained by fitting the  $K_S^0\pi$  invariant mass, where the signal can be parameterized by the function as shown in Eq. (70) and background is described with simulated background. The efficiency corrected numbers for  $\tau^- \rightarrow K_S^0\pi^-\nu_\tau$  and  $\tau^+ \rightarrow K_S^0\pi^+\bar{\nu}_\tau$  are  $3681017 \pm 5034$  and  $3681127 \pm 5091$ , respectively. It shows a good consistency with input values. The statistical sensitivity of  $CP$  asymmetry with decay rate according to Eq. (68) can be calculated accordingly, to be  $9.7 \times 10^{-4}$ .

Though the analysis is performed with purely MC simulation, a discussion of possible systematic uncertainties that may bias the decay-rate asymmetry measurement between  $\tau^- \rightarrow K_S^0\pi^-\nu_\tau$  and  $\tau^+ \rightarrow K_S^0\pi^+\bar{\nu}_\tau$  can be given. The uncertainty sources will be introduced and estimated as follows:

- The detection asymmetry for charged particles, which can be studied from the control sample of  $\tau \rightarrow \pi^+\pi^-\pi^-\nu_\tau$  decays, which is the sample with largest branching fractions. The effects can be corrected by comparing the asymmetry between MC simulation and data, and the remaining uncertainty is related to the statistics uncertainty of the control sample. Since the branching fraction of the control sample is over one order of magnitude larger than the signal process, the uncertainty will be significantly smaller than the statistical uncertainty.

- The uncertainty related with the selection criteria, which can be studied by varying the criteria. By performing the Barlow test [191], and any bias from selection will be studied and corrected until the systematic accuracy matches the statistical precision.
- The uncertainty from the MC generator. In this analysis, no  $CP$  violation is modeled and the output asymmetry in MC is about  $3 \times 10^{-5}$ , which can be neglected. The uncertainty associated with the background contamination. In this analysis, no decay-rate asymmetry is observed in background, and the uncertainty can be tested by applying different criteria on the background between data and MC simulation.
- The different nuclear-interaction cross sections of the  $K^0$  and  $\bar{K}^0$  mesons. In Ref. [192], a correction to the asymmetry accounting from  $K^0$  and  $\bar{K}^0$  mesons interacting with the material in the detector is applied by taking the  $K^\pm$  nucleon cross sections as an analogy, under the assumption of isospin invariance. Similar attempts can be made at STCF according to its material setup around the beam pipe.

As the selection efficiency for  $\tau \rightarrow K_S \pi \nu$  with c.m. energy from  $\sqrt{s} = 4.0$  GeV to 5.0 GeV, where the cross section for  $e^+e^- \rightarrow \tau^+\tau^-$  does not vary a lot around the peak value, is also quite stable, within 3% relative difference. The sensitivity of the  $CP$  asymmetry is found to be proportional to  $1/\sqrt{L}$ . With  $10 \text{ ab}^{-1}$  luminosity collected at STCF in the future, the sensitivity can be at a level of  $3.1 \times 10^{-4}$ , which is comparable to the uncertainty of the SM theoretical prediction. The clean topology and threshold production characteristics of the tau lepton pair further ensure high-precision measurements with excellent systematic uncertainty control. Combing with the tau EDM studies at STCF, with a precision of  $\mathcal{O}(10^{-18}) e \text{ cm}$ , STCF is expected to test the  $CP$  violation in the tau sector with very high precision.

## 4. $CP$ violation in charm sector

### 4.1. CKM unitarity triangle in the charm sector

In the SM,  $CP$  violations are generated by the weak phase in the quark flavor mixing matrix, *i.e.* the CKM matrix. The unitarity relation of the CKM matrix allows six unitarity triangles. The so-called *charmed* CKM unitarity triangle illustrated in Fig. 7 is closely associated with the strength of  $CP$  violation in the charm sector [193], because its three sides are just the CKM matrix elements appearing in both the box diagrams of  $D^0$ - $\bar{D}^0$  mixing and the penguin diagrams of the  $D^0 \rightarrow \pi^+\pi^-$  decay shown in Fig. 8. Unfortunately, the bottom quark plays a negligibly small role in both the box and penguin diagrams because its contributions are suppressed both by  $m_b^2/m_W^2 \sim \mathcal{O}(10^{-3})$  and by

$$\left| \frac{V_{ub}^* V_{cb}}{V_{ud}^* V_{cd}} \right| \simeq \left| \frac{V_{ub}^* V_{cb}}{V_{us}^* V_{cs}} \right| \simeq A^2 \lambda^3 \sqrt{\rho^2 + \eta^2} \sim \mathcal{O}(10^{-3}), \quad (74)$$

where  $A$ ,  $\lambda$ ,  $\rho$  and  $\eta$  are the Wolfenstein parameters introduced in Eq. (3). That is why  $CP$  violation in the charm sector is mainly associated with the first and second families of quarks, and the magnitudes of  $CP$ -violating asymmetries between various charm quark decays and their  $CP$ -conjugated processes are expected to be of order

$$\mathcal{A}_{CPV} \sim \frac{\text{Im}(V_{ud} V_{cs} V_{us}^* V_{cd}^*)}{\text{Re}(V_{ud} V_{cs} V_{us}^* V_{cd}^*)} \simeq A^2 \lambda^4 \eta \simeq 6 \times 10^{-4}, \quad (75)$$

up to an uncertainty factor of two or three. In other words, it is the smallest inner angle of the charmed unitarity triangle that essentially determines the size of charmed  $CP$  violation in the SM.

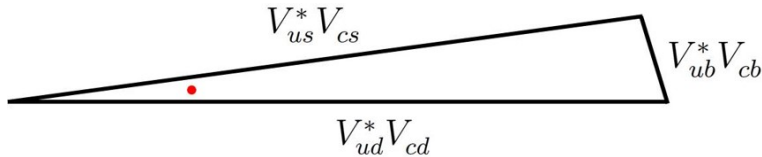


Figure 7: The *charmed* CKM unitarity triangle associated with  $V_{ud}^* V_{cd} + V_{us}^* V_{cs} + V_{ub}^* V_{cb} = 0$  in the complex plane. The relevant angle determining charmed  $CP$  violation in the SM is highlighted with a red dot.

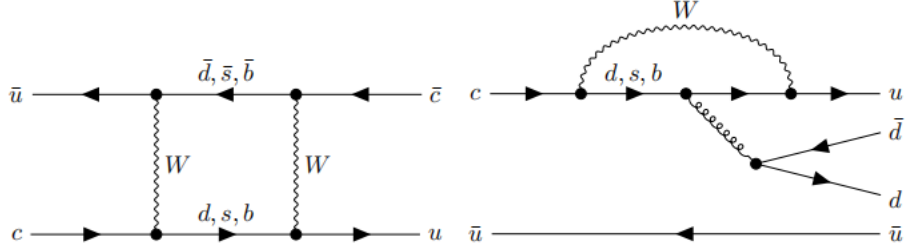


Figure 8: An illustration of the box diagrams for  $D^0$ - $\bar{D}^0$  mixing and the penguin diagrams for the  $D^0 \rightarrow \pi^+\pi^-$  decay.

#### 4.2. $CP$ violation in the direct decays

As given in Eq. (4), at least two amplitude components with different weak phases and different strong phases are the necessary conditions to arrive at a nonzero  $CP$ -violating asymmetry. These two requirements mean that direct  $CP$  violation will not take place unless the decay mode under consideration involves at least two different tree-level amplitudes, or one tree-level amplitude and the penguin amplitudes, or only the penguin amplitudes mediated by the three down-type quarks in the loop.

For the time being, the only convincingly established signal of  $CP$  violation in the charm sector is just direct  $CP$  violation in a combination of  $D^0 \rightarrow K^+K^-$  and  $D^0 \rightarrow \pi^+\pi^-$  decays [194]:  $\mathcal{A}_{K^+K^-} - \mathcal{A}_{\pi^+\pi^-} = (-1.54 \pm 0.29) \times 10^{-3}$ , whose magnitude is essentially compatible with the naive estimate made in Eq. (75). The time-integrated asymmetry can be further decomposed into a direct  $CP$  asymmetry  $a_{CP}^{\text{dir}}$  and a mixing-induced indirect  $CP$  asymmetry characterized by the parameter  $\Delta Y_f$ , which measures the asymmetry between  $D^0 \rightarrow f$  and  $\bar{D}^0 \rightarrow f$  effective decay widths; that is,

$$A_{CP}(f) \approx a_f^{\text{dir}} + \frac{\langle t \rangle_f}{\tau_{D^0}} \Delta Y_f, \quad (76)$$

where  $\langle t \rangle_f$  is the mean decay time of the  $D^0$  mesons. Based on the LHCb average of  $\Delta Y$ , it follows that the direct  $CP$  asymmetry difference is given by [194]

$$\Delta a_{CP}^{\text{dir}} = a_{K^+K^-}^{\text{dir}} - a_{\pi^+\pi^-}^{\text{dir}} = (-1.57 \pm 0.29) \times 10^{-3}. \quad (77)$$

Notice that the  $D^0$  meson is the only neutral meson system where direct  $CP$  violation can overcome indirect  $CP$  violation.

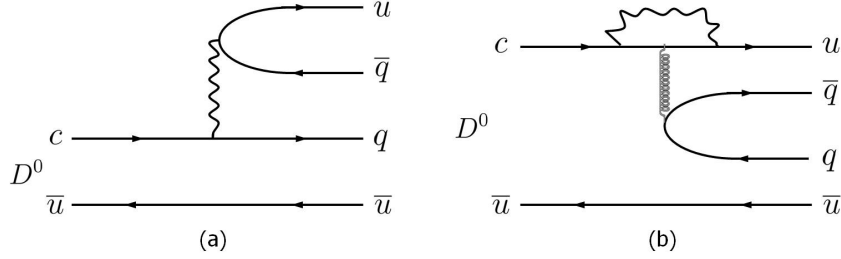


Figure 9: The tree and penguin Feynman diagrams for  $D^0 \rightarrow K^+K^-$  and  $\pi^+\pi^-$  decays with  $q = d$  and  $s$  [197].

In 2022, the time-integrated  $CP$  asymmetry in  $D^0 \rightarrow K^+K^-$  was measured by LHCb [195] to be

$$A_{CP}(K^+K^-) = (6.8 \pm 6.4 \pm 1.6) \times 10^{-4}. \quad (78)$$

The direct  $CP$  asymmetries in  $D^0 \rightarrow K^+K^-$  and  $D^0 \rightarrow \pi^+\pi^-$  decays are derived by combining  $A_{CP}(K^+K^-)$  with  $\Delta A_{CP}$ , giving

$$a_{K^+K^-}^{\text{dir}} = (7.7 \pm 5.7) \times 10^{-4}, \quad a_{\pi^+\pi^-}^{\text{dir}} = (23.2 \pm 6.1) \times 10^{-4}. \quad (79)$$

Hence, the direct  $CP$  asymmetries deviate from zero by 1.4 and 3.8 standard deviations for  $D^0 \rightarrow K^+K^-$  and  $D^0 \rightarrow \pi^+\pi^-$ , respectively. This implies a breaking of  $U$ -spin symmetry in charm decays. In the limit of  $U$ -spin symmetry, there exists a sum rule implying that  $a_{K^+K^-}^{\text{dir}} + a_{\pi^+\pi^-}^{\text{dir}} = 0$ , so that the  $CP$  asymmetries of these two modes have different signs. The above measurement breaks the  $U$ -spin symmetry by  $2.7\sigma$ . If the future measurements hold the above result, it may indicate a signal of new physics [196]. Therefore, it requires more precise measurements on the  $CP$  asymmetries of individual decay channels.

In view of Fig. 9, let us write out the amplitudes of  $D^0 \rightarrow \pi^+\pi^-$  and  $D^0 \rightarrow K^+K^-$  decay modes in a universal way as follows:

$$\begin{aligned} A(D^0 \rightarrow f_q) &= T_q (V_{cq}V_{uq}^*) e^{i\delta_q} + P_q (V_{cb}V_{ub}^*) e^{i\delta'_q}, \\ A(\bar{D}^0 \rightarrow f_q) &= T_q (V_{cq}^*V_{uq}) e^{i\delta_q} + P_q (V_{cb}^*V_{ub}) e^{i\delta'_q}, \end{aligned} \quad (80)$$

where  $T_q$  and  $P_q$  (for  $q = d, s$ ) are real,  $\delta_q$  and  $\delta'_q$  stand respectively for the strong phases of the tree and penguin amplitudes, and only the dominant bottom-quark contribution to the penguin loop has been taken into account as a reasonable approximation [197]. If the penguin contribution is neglected and the standard phase convention for the CKM matrix is taken, one will simply arrive at

$A(D^0 \rightarrow K^+K^-) \simeq -A(D^0 \rightarrow \pi^+\pi^-)$  under U-spin symmetry because this  $d \leftrightarrow s$  interchange symmetry assures  $T_s = T_d$ ,  $\delta_s = \delta_d$  and  $\delta'_s = \delta'_d$  to hold. But the penguin contribution proves to be important and hence cannot be neglected. To see this point, let us figure out the direct  $CP$ -violating asymmetry in the following approximation:

$$\mathcal{A}_{f_q} \simeq \mathcal{U}_{f_q} \simeq 2\eta_q (A^2\lambda^4\eta) \frac{P_q}{T_q} \sin(\delta_q - \delta'_q) , \quad (81)$$

where the Wolfenstein parametrization of the CKM matrix  $V$  has been used, and the coefficient  $\eta_d = -1$  for the final state  $f_d = \pi^+\pi^-$  or  $\eta_s = +1$  for  $f_s = K^+K^-$ . As a result, the combined  $CP$ -violating asymmetry

$$\mathcal{A}_{K^+K^-} - \mathcal{A}_{\pi^+\pi^-} \simeq 2 (A^2\lambda^4\eta) \left[ \frac{P_s}{T_s} \sin(\delta_s - \delta'_s) + \frac{P_d}{T_d} \sin(\delta_d - \delta'_d) \right] \quad (82)$$

is expected to be  $(-1.54 \pm 0.29) \times 10^{-3}$ , as measured in the LHCb experiment [194]. This result requires that the quantities in the square brackets of Eq. (82) should be as large as about 1.2, implying that both the penguin contribution and final-state interactions are significant (see, *e.g.*, Refs. [198–200]).

In 2012 there existed two independent studies in which direct  $CP$  violation in charmed meson decays was explored, based on the Topological diagrammatic approach (Topo) for tree amplitudes and the QCD-inspired approach for penguin amplitudes [198, 199], and the Factorization-Assisted Topological-amplitude approach (FAT) [200]. Interestingly, both works predicted a  $\Delta A_{CP}$  at the per mille level seven years before the LHCb's announcement of the first observation of  $CP$  violation in the charm sector. The comparison between the experimental measurements and the theoretical predictions is shown in Fig. 10, taken from Ref. [201]. These two works are the only ones with correct predictions before the observation by LHCb. Under topological-diagram methods, the dynamics of charm decays at the scale of 1GeV can be understood by the data of the branching fractions. Then the penguin contributions can be reliably obtained at the same scale.

The correct predictions are based on the precise measurements of branching fractions of  $D$  meson decays by BESIII and other experiments. The dynamics of charm decays are polluted by large non-perturbative contributions which are difficult to be calculated using the current theoretical methods. But the branching fractions of  $D$  meson decays can provide very useful information on the dynamics of charm decays. Using the topological diagrammatic approach and factorization hypothesis, the non-perturbative hadronic matrix elements can be well extracted

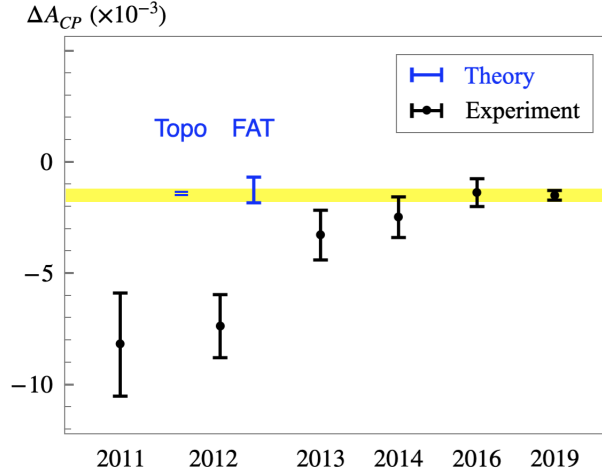


Figure 10: Comparison between experimental measurements (in black) and theoretical predictions (in blue) on  $\Delta A_{CP}$  as a function of time [201]. Experimental results are corresponding to the world-average values for a specific year. The theoretical approaches are the Topological diagrammatic approach (Topo) under the flavor  $SU(3)$  symmetry limit and the Factorization-Assisted Topological-amplitude approach (FAT), respectively. The yellow band is the 2019 experimental result, shown for comparison.

from the data of branching fractions. Therefore, the measurements of branching fractions at BESIII and STCF are very important, even though these experiments cannot directly observe the  $CP$ -violation of charm decays.

One may similarly discuss direct  $CP$  violation in the charged  $D$ -meson decays. The magnitude of direct  $CP$  violation in such decay modes is also expected to be of  $\mathcal{O}(10^{-3})$  or smaller (see, *e.g.*, Refs. [198–200, 202–208]), but a striking and reliable signal has not been observed in the present-day experiments.

The STCF, as an electron-positron collider, has only a marginal power for observation of direct  $CP$  violation in charm decays. However, its measurements on the branching fractions and any other observables would be very helpful for the theoretical prediction on the  $CP$  violation of charm-meson and charm-baryon decays, which is important in the comparison with experimental measurements to precisely test the SM and explore NP.

A lot of data have been collected for charmed anti-triplet baryons  $\Lambda_c$ ,  $\Xi_c^0$  and  $\Xi_c^+$ . The final-state-interaction effect can generate  $CP$  asymmetries of charm-baryon decays [209]. The leading decay amplitude for two-body charmed anti-

triplet baryon  $B_c$  decays into an octet low-lying baryon  $B$  and an pseudoscalar octet  $P$  have been studied [210–212]. The penguin contributions in the charmed baryon decays have been addressed in [213], in which a possible enhancement effect to the  $CP$  violation is found similarly to what happened to  $D \rightarrow \pi\pi, KK$  decays.

The search for  $CP$  violation in charmed baryon decays has taken on new momentum with the large samples of  $\Lambda_c^+$  obtained by BESIII and LHCb. For two-body decays of the  $\Lambda_c^+$ ,  $CP$  violation through the measurement of  $CP$ -violating decay parameter asymmetry,  $\mathcal{A} = (\alpha + \bar{\alpha})/(\alpha - \bar{\alpha})$  had been carried out with the current result given by  $\mathcal{A} = -0.07 \pm 0.19 \pm 0.24$  for  $\Lambda_c^+ \rightarrow \Lambda\pi^+$  and  $\bar{\Lambda}_c^- \rightarrow \bar{\Lambda}\pi^-$  [214] and  $(1.5 \pm 5.2 \pm 1.7)\%$  for  $\Xi_c^0 \rightarrow \Xi^-\pi^+$  and  $\bar{\Xi}_c^0 \rightarrow \bar{\Xi}^+\pi^-$  [215]. These measurements are still an order of magnitude away from SM expectations [213].

As for three-body decays, LHCb has measured the difference between  $CP$  asymmetries in  $\Lambda_c^+ \rightarrow pK^+K^-$  and  $\Lambda_c^+ \rightarrow p\pi^+\pi^-$  decay channels, in analogy to  $D^0 \rightarrow K^+K^-$  and  $D^0 \rightarrow \pi^+\pi^-$  [216]. The result is  $\Delta A_{CP}(\Lambda_c^+) = A_{CP}(pK^+K^-) - A_{CP}(p\pi^+\pi^-) = (0.30 \pm 0.91 \pm 0.61)\%$ , to be compared with a generic SM prediction of a fraction of 0.1% [217]. In order to probe the SM level, one has to multiply the available statistics by at least a factor of 100. LHCb has also looked for local  $CP$  asymmetry in  $\Xi_c^+ \rightarrow pK^-\pi^+$  decays and found null results [218].

For multi-hadrons in the final state of  $\Lambda_c^+$  decays such as  $\Lambda_c^+ \rightarrow pK^-\pi^+\pi^0$ ,  $\Lambda_c^+ \rightarrow \Lambda\pi^+\pi^+\pi^-$  and  $\Lambda_c^+ \rightarrow pK_S^0\pi^+\pi^-$ ,  $CP$  violation can be exploited through several  $T$ -odd observables [219]. Owing to its features of high luminosity, broad c.m. energy acceptance, abundant production and clean environment, STCF may provide a great platform for this kind of study. A fast Monte Carlo simulation study in [151] by using the  $e^+e^-$  annihilation data of  $1 \text{ ab}^{-1}$  at  $\sqrt{s} = 4.64 \text{ GeV}$ , which are expected to be available at the future STCF, indicates that a sensitivity at the level of (0.25-0.5)% is accessible for the above-mentioned three decay modes. This will be enough to measure non-zero  $CP$ -violating asymmetries as large as 1%.

STCF will be able to produce also charmed baryon-antibaryon pairs. Having the c.m. energy range up to 7 GeV, the pairs of  $\Lambda_c^+\bar{\Lambda}_c^-$ ,  $\Xi_c^0\bar{\Xi}_c^0$  and  $\Xi_c^+\bar{\Xi}_c^-$  can be created. According to the BESIII data, there is no evident resonance that could increase production yields. For example, the cross section of  $e^+e^- \rightarrow \Lambda_c^+\bar{\Lambda}_c^-$  increases quickly above the threshold and stays approximately constant with the value of about 200 pb [220, 221]. Charmed baryon decays have many competing decay modes, since all branching fractions are small and do not exceed 7% [222].

Therefore, decay measurements require a double tagging technique that combines a set of common decay modes. With  $1 \text{ ab}^{-1}$  data sample collected at STCF,  $2 \times 10^8$   $\Lambda_c^+ \bar{\Lambda}_c^-$  pairs can be produced, which might not be sufficient for  $CP$  symmetry studies using entangled baryon-antibaryon systems. One of the most useful decays for tagging and polarization measurement is  $\Lambda_c^+ \rightarrow p K^- \pi^+$  with the branching fraction as  $\mathcal{B} = 6.26(29)\%$  and the effective polarimeter constant (weighted average over the Dalitz plot) of 65% [223].

Here we comment on how the production and decay properties of charmed baryon differ from those of hyperons.

- There are many hadronic decays into three or more final-state particles. Several processes include hyperons, which allows to determine their spin via sequential weak decays.
- The range of the  $q^2$  variable in the SL decays of charmed baryons is large enough for the form factors in Eq. (37) to acquire imaginary part due to on-shell contribution of hadronic states. For  $CP$  symmetry test it means that the elements of the aligned decay matrix in Eq. (40) terms  $b_{20}, b_{21}, b_{23}, b_{02}, b_{12}$  and  $b_{32}$  are nonzero [45]. This allows for  $T$ -odd  $CP$  tests which are complementary to the  $T$ -even tests such as a comparison of the partial decay widths. There are also Lattice QCD calculations for SL decays of heavy quarks [224].
- In the SM, the direct  $CP$  violation vanishes for Cabibbo-favoured decays of charmed baryons. But for processes involving  $K_{S,L}$  in the final states,  $CP$  violation can show up due to  $K^0 - \bar{K}^0$  mixing with a size of order  $10^{-3}$  [225].
- Exclusive reconstruction of decays with one unmeasured particle.
- Selection of the c.m. Energy has to include effects such as the total cross section, detection efficiency and the transverse polarization of the baryon, given by the value of the relative phase  $\Delta\Phi = \text{Arg}(G_E/G_M)$ . For the  $\Lambda_c^+ \bar{\Lambda}_c^-$  channels, the cross section is largest close to threshold. The angular distribution parameter  $\eta$  changes from zero at threshold to  $-0.26(9)$  at 4.2619 GeV and then raises to  $+0.63(21)$  at the BESIII highest energy of 4.9559 GeV. The  $\Delta\Phi$  phase and the natural polarization is zero at threshold since  $G_E = G_M$ . The relative phases are not measured yet by BESIII. However, beam polarization can play an important role for the precision of the

measurements. For example, the absolute value of baryon polarization at threshold is equal to the electron beam polarization and it does not depend on the production angle  $\theta$  [19].

#### 4.3. *CP violation associated with $D^0$ - $\bar{D}^0$ mixing*

The theoretical study of *CP* violation in  $D^0$ - $\bar{D}^0$  mixing can be traced back to the seminal papers by Okun, Zakharov and Pontecorvo [226] and by Pais and Treiman [227] in 1975, just one year after the experimental discoveries of the charm quark [228, 229]. The key point is that the box diagrams illustrated in Fig. 8 allow  $D^0$  and  $\bar{D}^0$  mesons to form the mass eigenstates

$$\begin{aligned} |D_1\rangle &= p|D^0\rangle + q|\bar{D}^0\rangle, \\ |D_2\rangle &= p|D^0\rangle - q|\bar{D}^0\rangle, \end{aligned} \quad (83)$$

where the complex parameters  $p$  and  $q$  satisfy the normalization condition  $|p|^2 + |q|^2 = 1$ , and *CPT* invariance has been assumed. Let us use the dimensionless parameters,

$$\begin{aligned} x &\equiv \frac{\Delta m}{\Gamma} \equiv \frac{m_2 - m_1}{\Gamma}, \\ y &\equiv \frac{\Delta\Gamma}{2\Gamma} \equiv \frac{\Gamma_2 - \Gamma_1}{2\Gamma}, \end{aligned} \quad (84)$$

to describe the effects of  $D^0$ - $\bar{D}^0$  mixing, where  $m_{1,2}$  and  $\Gamma_{1,2}$  denote the masses and decay widths of  $D_{1,2}$ , and  $\Gamma = (\Gamma_1 + \Gamma_2)/2$  is the mean decay width of these two particles. It is notoriously difficult to reliably calculate  $x$  and  $y$ , simply because the long-distance effects on  $D^0$ - $\bar{D}^0$  mixing at the hadron level are essentially nonperturbative and hence involve a lot of theoretical uncertainties (see, *e.g.*, Refs. [230–234]). Some order-of-magnitude estimates have given  $x \sim y \sim \mathcal{O}(10^{-3})$ , consistent with their allowed regions extracted from current experimental data shown in Fig. 11.

The definition of  $D_{1,2}$  in Eq. (83) tells us that these two mass eigenstates would be the *CP* eigenstates if  $p = \pm q$  held. So  $|p| \neq |q|$  is a rephrasing-invariant measure of *CP* violation in  $D^0$ - $\bar{D}^0$  mixing. In the SL decays of neutral  $D$  mesons, the *CP*-violating observable is [226, 227]

$$\Delta_{\text{mixing}} \equiv \frac{|p|^4 - |q|^4}{|p|^4 + |q|^4}. \quad (85)$$

It is expected that the magnitude of  $\Delta_{\text{mixing}}$  is at most of  $\mathcal{O}(10^{-3})$  in the SM, but the calculations suffer from large long-distance uncertainties [232–234]. Fig. 12

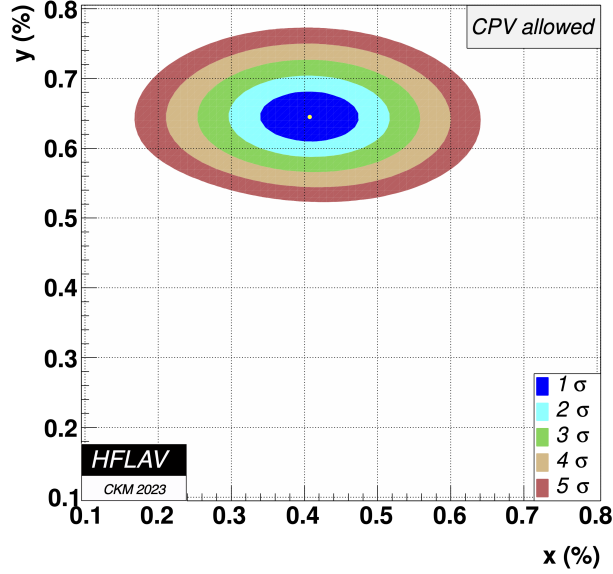


Figure 11: Constraints on the  $D^0$ - $\bar{D}^0$  mixing parameters  $x$  and  $y$  as obtained by the HFLAV group from current data [235].

illustrates the present experimental constraints on the argument and modulus of  $q/p$ , which are consistent with the SM expectation. NP might contribute to  $D^0$ - $\bar{D}^0$  mixing via the box diagrams and enhance the size of  $\Delta_{\text{mixing}}$  to some extent (see, *e.g.*, Refs. [236–238]), but a significant enhancement seems quite unlikely in this regard.

In the  $e^+e^-$  collisions at the threshold of  $D\bar{D}$ , it has a particular advantage to investigate the indirect  $CP$  violation of  $D^0 - \bar{D}^0$  mixing where  $D^0$  and  $\bar{D}^0$  are quantum correlated to each other.

*Formulas for incoherent neutral D meson decays.* Given the parameters of  $D^0$ - $\bar{D}^0$  mixing defined in Eqs. (83) and (84) the time-independent decay rates can be

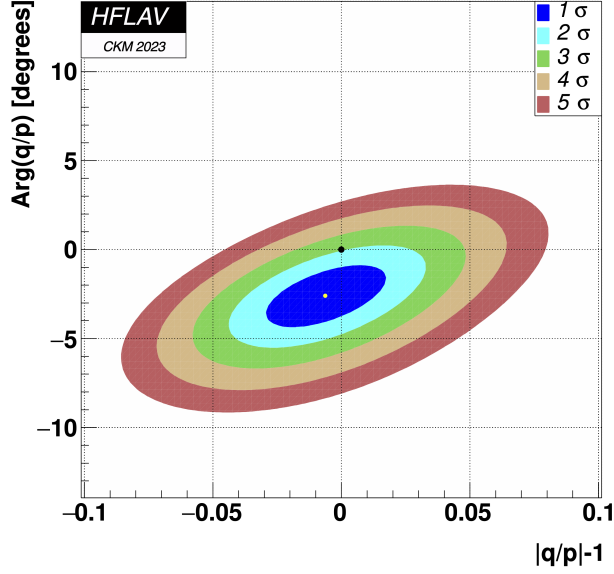


Figure 12: Constraints on the modulus and argument of  $q/p$  in  $D^0$ - $\bar{D}^0$  mixing as obtained by the HFLAV group from currently available experimental data [235].

expressed as [239]

$$\begin{aligned}
\Gamma(D^0 \rightarrow f) &\propto |A(D^0 \rightarrow f)|^2 \left[ \frac{1}{1-y^2} \cdot \frac{1+|\lambda_f|^2}{2} + \frac{y}{1-y^2} \text{Re}\lambda_f \right. \\
&\quad \left. + \frac{1}{1+x^2} \cdot \frac{1-|\lambda_f|^2}{2} - \frac{x}{1+x^2} \text{Im}\lambda_f \right], \\
\Gamma(\bar{D}^0 \rightarrow f) &\propto |A(D^0 \rightarrow f)|^2 \left[ \frac{1}{1-y^2} \cdot \frac{1+|\lambda_f|^2}{2} + \frac{y}{1-y^2} \text{Re}\lambda_f \right. \\
&\quad \left. - \frac{1}{1+x^2} \cdot \frac{1-|\lambda_f|^2}{2} + \frac{x}{1+x^2} \text{Im}\lambda_f \right] \left| \frac{p}{q} \right|^2. \tag{86}
\end{aligned}$$

Here, we define

$$\begin{aligned}
\lambda_f &\equiv \frac{q}{p} \cdot \frac{A(\bar{D}^0 \rightarrow f)}{A(D^0 \rightarrow f)}, \\
\bar{\lambda}_{\bar{f}} &\equiv \frac{p}{q} \cdot \frac{A(D^0 \rightarrow \bar{f})}{A(\bar{D}^0 \rightarrow \bar{f})}, \tag{87}
\end{aligned}$$

and  $f$  and  $\bar{f}$  are required to be common to the decay of  $D^0$  (or  $\bar{D}^0$ ). Therefore, one may calculate the time-independent decay rates of neutral  $D$  mesons into  $\bar{f}$ , the  $CP$ -conjugate state of  $f$ , in the same way.

As shown in Fig. 11, the  $D^0$ - $\bar{D}^0$  mixing parameters  $x$  and  $y$  are both positive and smaller than 1%. It is therefore safe to make analytical approximations for the time-independent decay rates of  $D^0 \rightarrow f$ ,  $D^0 \rightarrow \bar{f}$ ,  $\bar{D}^0 \rightarrow f$  and  $\bar{D}^0 \rightarrow \bar{f}$  by neglecting the terms of  $\mathcal{O}(x^2)$  and  $\mathcal{O}(y^2)$ . With the help of Eq. (86), we easily arrive at

$$\begin{aligned}\Gamma(D^0 \rightarrow f) &\propto |A(D^0 \rightarrow f)|^2 (1 + y\text{Re}\lambda_f - x\text{Im}\lambda_f) , \\ \Gamma(\bar{D}^0 \rightarrow \bar{f}) &\propto |A(\bar{D}^0 \rightarrow \bar{f})|^2 \left(1 + y\text{Re}\bar{\lambda}_{\bar{f}} - x\text{Im}\bar{\lambda}_{\bar{f}}\right) ;\end{aligned}\quad (88)$$

and

$$\begin{aligned}\Gamma(\bar{D}^0 \rightarrow f) &\propto |A(D^0 \rightarrow f)|^2 (|\lambda_f|^2 + y\text{Re}\lambda_f + x\text{Im}\lambda_f) (1 + \Delta_{\text{mixing}}) , \\ \Gamma(D^0 \rightarrow \bar{f}) &\propto |A(\bar{D}^0 \rightarrow \bar{f})|^2 \left(|\bar{\lambda}_{\bar{f}}|^2 + y\text{Re}\bar{\lambda}_{\bar{f}} + x\text{Im}\bar{\lambda}_{\bar{f}}\right) (1 - \Delta_{\text{mixing}}) ,\end{aligned}\quad (89)$$

where  $\bar{\lambda}_{\bar{f}}$  has been defined in Eq. (87), and  $|p/q|^4 = (1 + \Delta_{\text{mixing}})/(1 - \Delta_{\text{mixing}}) \simeq 1 + 2\Delta_{\text{mixing}}$  derived from Eq. (85) has been used. As the magnitude of  $\Delta_{\text{mixing}}$  is at most of  $\mathcal{O}(10^{-3})$  in the SM, it can also be omitted from Eq. (89) in most cases.

*Formulas for coherent  $(D^0\bar{D}^0)_{C=\pm 1}$  decays.* On the  $\psi(3770)$  or  $\psi(4140)$  resonance, which possess the quantum number  $J^{\text{PC}} = 1^{--}$ , a  $C$ -odd or  $C$ -even  $D^0\bar{D}^0$  pair can be coherently produced as follows [240, 241]:

$$\begin{aligned}\psi(3770) &\longrightarrow (D^0\bar{D}^0)_{C=-1} , \\ \psi(4140) &\longrightarrow D^0\bar{D}^{*0} \text{ or } D^{*0}\bar{D}^0 \longrightarrow (D^0\bar{D}^0)_{C=-1} + \pi^0 , \\ \psi(4140) &\longrightarrow D^0\bar{D}^{*0} \text{ or } D^{*0}\bar{D}^0 \longrightarrow (D^0\bar{D}^0)_{C=+1} + \gamma .\end{aligned}\quad (90)$$

For such a coherent pair at rest, its time-dependent wave function can be written as

$$|D^0\bar{D}^0(t)\rangle_C = \frac{1}{\sqrt{2}} \left[ |D^0(\mathbf{K}, t)\rangle |\bar{D}^0(-\mathbf{K}, t)\rangle + C |D^0(-\mathbf{K}, t)\rangle |\bar{D}^0(\mathbf{K}, t)\rangle \right] , \quad (91)$$

where  $\pm\mathbf{K}$  stand for the three-momentum vectors of the two neutral  $D$ -mesons, and  $C = \pm 1$  denotes the even or odd charge-conjugation parity of this coherent system. The joint decay mode

$$(D^0\bar{D}^0)_{CP\pm} \longrightarrow (f_1 f_2)_{CP\mp} , \quad (92)$$

where  $f_{1,2}$  stand for the proper hadronic  $CP$  eigenstates (*e.g.*,  $\pi^+\pi^-$ ,  $K^+K^-$  and  $K_S\pi^0$ ), must be a  $CP$ -forbidden process. In other words, such a decay cannot take place unless there exists  $CP$  violation in the  $D^0 \rightarrow f_{1,2}$  and  $\bar{D}^0 \rightarrow f_{1,2}$  decays. As  $CP$ -odd and  $CP$ -even  $D^0\bar{D}^0$  pairs are expected to be produced in a huge amount at STCF, it will be important to measure the  $CP$ -forbidden  $D^0\bar{D}^0$  decays on the  $\psi(3770)$  and  $\psi(4140)$  resonances, although such a measurement is very challenging in practice [197].

One may also start from Eq. (91) and consider that one of the two neutral  $D$  mesons (with momentum  $\mathbf{K}$ ) decays into a final state  $f_1$  at and the other (with  $-\mathbf{K}$ ) to  $f_2$ , and therefore derive the time-independent joint decay rate as

$$\begin{aligned} \Gamma(f_1; f_2)_C &\propto |A(D^0 \rightarrow f_1)|^2 |A(D^0 \rightarrow f_2)|^2 \\ &\times \left[ \frac{1 + Cy^2}{(1 - y^2)^2} (|\xi_C|^2 + |\zeta_C|^2) + \frac{2(1 + C)y}{(1 - y^2)^2} \text{Re}(\xi_C^* \zeta_C) \right. \\ &\quad \left. - \frac{1 - Cx^2}{(1 + x^2)^2} (|\xi_C|^2 - |\zeta_C|^2) + \frac{2(1 + C)x}{(1 + x^2)^2} \text{Im}(\xi_C^* \zeta_C) \right], \quad (93) \end{aligned}$$

where

$$\begin{aligned} \xi_C &\equiv \frac{p}{q} \left( 1 + C\lambda_{f_1}\lambda_{f_2} \right), \\ \zeta_C &\equiv \frac{p}{q} \left( \lambda_{f_2} + C\lambda_{f_1} \right), \end{aligned} \quad (94)$$

It is obvious that the two interference terms,  $\text{Re}(\xi_C^* \zeta_C)$  and  $\text{Im}(\xi_C^* \zeta_C)$ , disappear in the  $C = -1$  case, no matter what the final states  $f_1$  and  $f_2$  are. Of course, the joint decay rates of  $\Gamma(f_1; \bar{f}_2)_C$ ,  $\Gamma(\bar{f}_1; f_2)_C$  and  $\Gamma(\bar{f}_1; \bar{f}_2)_C$  can similarly be calculated, where  $\bar{f}_{1,2}$  denote the  $CP$ -conjugate states of  $f_{1,2}$ .

Taking into account the approximation  $|p/q|^2 \simeq 1 + \Delta_{\text{mixing}}$  and neglecting

the terms of  $\mathcal{O}(x^2)$ ,  $\mathcal{O}(y^2)$  and smaller in Eq. (93), we find

$$\begin{aligned}
\Gamma(f_1; f_2)_{C=-1} &\propto 2|A(D^0 \rightarrow f_1)|^2 |A(D^0 \rightarrow f_2)|^2 \\
&\quad \times \left[ |\lambda_{f_1}|^2 + |\lambda_{f_2}|^2 - 2 \left( \text{Re}\lambda_{f_1} \text{Re}\lambda_{f_2} + \text{Im}\lambda_{f_1} \text{Im}\lambda_{f_2} \right) \right] \\
&\quad \times (1 + \Delta_{\text{mixing}}) , \\
\Gamma(f_1; f_2)_{C=+1} &\propto 2|A(D^0 \rightarrow f_1)|^2 |A(D^0 \rightarrow f_2)|^2 \\
&\quad \times \left\{ |\lambda_{f_1}|^2 + |\lambda_{f_2}|^2 + 2 \left( \text{Re}\lambda_{f_1} \text{Re}\lambda_{f_2} + \text{Im}\lambda_{f_1} \text{Im}\lambda_{f_2} \right) \right. \\
&\quad \left. + 2y \left[ \left( 1 + |\lambda_{f_1}|^2 \right) \text{Re}\lambda_{f_2} + \left( 1 + |\lambda_{f_2}|^2 \right) \text{Re}\lambda_{f_1} \right] \right. \\
&\quad \left. + 2x \left[ \left( 1 - |\lambda_{f_1}|^2 \right) \text{Im}\lambda_{f_2} + \left( 1 - |\lambda_{f_2}|^2 \right) \text{Im}\lambda_{f_1} \right] \right\} \\
&\quad \times (1 + \Delta_{\text{mixing}}) . \tag{95}
\end{aligned}$$

The above formulas can be further simplified if  $f_1 = f_2$  is taken. Here a key observation is that a combination of the measurements of  $\Gamma(f_1; f_2)_{C=-1}$  and  $\Gamma(f_1; f_2)_{C=+1}$  at STCF will allow us to extract much more information about  $D^0$ - $\bar{D}^0$  mixing and  $CP$  violation in neutral  $D$ -meson decays, although the events of coherent  $D^0$  and  $\bar{D}^0$  mesons on the  $\psi(4140)$  resonance are much fewer than those on the  $\psi(3770)$  resonance.

The decays of  $D^0 \rightarrow K^+\pi^-$  and  $K^-\pi^+$  are of particular interest for the study of both  $D^0$ - $\bar{D}^0$  mixing and  $CP$  violation. The reason is simply that both  $D^0$  and  $\bar{D}^0$  can decay into the final states  $K^\pm\pi^\mp$  via just the tree-level quark diagrams, assuring that their amplitudes are hardly contaminated by any kind of new physics [242]. Let us factorize the transition amplitudes of  $D^0 \rightarrow K^\pm\pi^\mp$  and  $\bar{D}^0 \rightarrow K^\pm\pi^\mp$  as [239]:

$$\begin{aligned}
A(D^0 \rightarrow K^-\pi^+) &= (V_{cs}V_{ud}^*) T_a e^{i\delta_a} , \\
A(D^0 \rightarrow K^+\pi^-) &= (V_{cd}V_{us}^*) T_b e^{i\delta_b} , \\
A(\bar{D}^0 \rightarrow K^+\pi^-) &= (V_{cs}^*V_{ud}) T_a e^{i\delta_a} , \\
A(\bar{D}^0 \rightarrow K^-\pi^+) &= (V_{cd}^*V_{us}) T_b e^{i\delta_b} , \tag{96}
\end{aligned}$$

where  $T_{a,b}$  denote the real hadronic matrix elements, and  $\delta_{a,b}$  are the corresponding strong phases. Defining  $h_{K\pi} \equiv T_b/T_a$  and  $\delta_{K\pi} \equiv \delta_b - \delta_a$  for the decay modes under consideration and  $q/p \equiv |q/p|e^{i\phi}$  for the weak phase of  $D^0$ - $\bar{D}^0$  mixing, we

obtain

$$\begin{aligned}\lambda_{K^-\pi^+} &= \frac{q}{p} \cdot \frac{A(\bar{D}^0 \rightarrow K^-\pi^+)}{A(D^0 \rightarrow K^-\pi^+)} \simeq -\lambda^2 h_{K\pi} \left| \frac{q}{p} \right| e^{i(\delta_{K\pi} + \phi)}, \\ \bar{\lambda}_{K^+\pi^-} &= \frac{p}{q} \cdot \frac{A(D^0 \rightarrow K^+\pi^-)}{A(\bar{D}^0 \rightarrow K^+\pi^-)} \simeq -\lambda^2 h_{K\pi} \left| \frac{p}{q} \right| e^{i(\delta_{K\pi} - \phi)},\end{aligned}\quad (97)$$

for  $f = K^-\pi^+$  and  $\bar{f} = K^+\pi^-$ , where the standard phase convention for the CKM matrix elements taken in Eq. (3) (namely,  $V_{ud} \simeq V_{cs} \simeq 1$  and  $V_{cd} \simeq -V_{us} \simeq -\lambda$ ) has been used. The magnitude of  $h_{K\pi}$  is expected to be of  $\mathcal{O}(1)$ , but an explicit calculation of this quantity involves some uncertainties arising from the relevant hadronic matrix elements.

On the  $\psi(3770)$  resonance, one may easily obtain the time-independent joint decay rates

$$\begin{aligned}\Gamma(K^-\pi^+; K^-\pi^+)_{C=-1} &\propto 2|A(D^0 \rightarrow K^-\pi^+)|^4 r \left| \frac{p}{q} \right|^2, \\ \Gamma(K^+\pi^-; K^+\pi^-)_{C=-1} &\propto 2|A(D^0 \rightarrow K^-\pi^+)|^4 r \left| \frac{q}{p} \right|^2,\end{aligned}\quad (98)$$

which are highly suppressed due to the smallness of  $r \equiv (x^2 + y^2)/2$ . On the  $\psi(4140)$  resonance, the corresponding joint decay rates turn out to be [239]

$$\begin{aligned}\Gamma(K^-\pi^+; K^-\pi^+)_{C=+1} &\propto 2|A(D^0 \rightarrow K^-\pi^+)|^4 \left\{ 3r \left| \frac{p}{q} \right|^2 + 4\lambda^4 h_{K\pi}^2 \right. \\ &\quad \left. - 4\lambda^2 h_{K\pi} \left| \frac{p}{q} \right| [y \cos(\delta_{K\pi} + \phi) + x \sin(\delta_{K\pi} + \phi)] \right\}, \\ \Gamma(K^+\pi^-; K^+\pi^-)_{C=+1} &\propto 2|A(\bar{D}^0 \rightarrow K^+\pi^-)|^4 \left\{ 3r \left| \frac{q}{p} \right|^2 + 4\lambda^4 h_{K\pi}^2 \right. \\ &\quad \left. - 4\lambda^2 h_{K\pi} \left| \frac{q}{p} \right| [y \cos(\delta_{K\pi} - \phi) + x \sin(\delta_{K\pi} - \phi)] \right\},\end{aligned}\quad (99)$$

as a good approximation. The difference between these two joint decay rates is also a direct measure of  $D^0$ - $\bar{D}^0$  mixing and  $CP$  violation.

It is well known that the above decay modes have played an important role in the experimental constraints of  $D^0$ - $\bar{D}^0$  mixing, but so far no  $CP$  violation has been observed in them [15].

*CP violation in  $D^0 \rightarrow \pi^+\pi^-$  and  $K^+K^-$  decays.* Both  $f_d \equiv \pi^+\pi^-$  and  $f_s \equiv K^+K^-$  are the *CP*-even eigenstates, as  $\bar{f}_q = f_q$  holds in either case (for  $q = d$  or  $s$ ). In particular, the decay modes  $D^0 \rightarrow \pi^+\pi^-$  and  $D^0 \rightarrow K^+K^-$  satisfy the so-called U-spin symmetry — a kind of invariance under the  $d \leftrightarrow s$  interchange, as shown in Fig. 9. For such a decay mode, one may simply define

$$\mathcal{U}_f \equiv \frac{1 - |\lambda_f|^2}{1 + |\lambda_f|^2}, \quad \mathcal{V}_f \equiv \frac{-2\text{Im}\lambda_f}{1 + |\lambda_f|^2}, \quad \mathcal{W}_f \equiv \frac{2\text{Re}\lambda_f}{1 + |\lambda_f|^2}, \quad (100)$$

which satisfy the sum rule  $\mathcal{U}_f^2 + \mathcal{V}_f^2 + \mathcal{W}_f^2 = 1$  [239]. It is obvious that  $\mathcal{U}_f$  and  $\mathcal{V}_f$  correspond respectively to direct and indirect *CP*-violating effects, while  $\mathcal{W}_f$  is a *CP*-conserving quantity.

It is naturally expected that the joint decays of a pair of coherent  $D^0$  and  $\bar{D}^0$  mesons into  $(K^+K^-)(\pi^+\pi^-)$  on the  $\psi(3770)$  resonance cannot happen unless there exists *CP* violation in them. Taking into account Eqs. (95) and (100), we find

$$\begin{aligned} \Gamma(K^+K^-; \pi^+\pi^-)_{C=-1} &\propto |\tilde{A}(D^0 \rightarrow K^+K^-)|^2 |\tilde{A}(D^0 \rightarrow \pi^+\pi^-)|^2 \left| \frac{p}{q} \right|^2 \\ &\times \left( \frac{1 - \mathcal{W}_{KK}\mathcal{W}_{\pi\pi}}{1 - y^2} - \frac{\mathcal{U}_{KK}\mathcal{U}_{\pi\pi} + \mathcal{V}_{KK}\mathcal{V}_{\pi\pi}}{1 + x^2} \right), \end{aligned} \quad (101)$$

as well as

$$\begin{aligned} \Gamma(K^+K^-; K^+K^-)_{C=-1} &\propto |\tilde{A}(D^0 \rightarrow K^+K^-)|^4 \left| \frac{p}{q} \right|^2 \\ &\times \left( \frac{1}{1 - y^2} - \frac{1}{1 + x^2} \right) (\mathcal{U}_{KK}^2 + \mathcal{V}_{KK}^2), \\ \Gamma(\pi^+\pi^-; \pi^+\pi^-)_{C=-1} &\propto |\tilde{A}(D^0 \rightarrow \pi^+\pi^-)|^4 \left| \frac{p}{q} \right|^2 \\ &\times \left( \frac{1}{1 - y^2} - \frac{1}{1 + x^2} \right) (\mathcal{U}_{\pi\pi}^2 + \mathcal{V}_{\pi\pi}^2). \end{aligned} \quad (102)$$

Note that the  $D^0$ - $\bar{D}^0$  mixing parameters  $x$  and  $y$  play an important role in Eq. (102), simply because  $1/(1 - y^2) - 1/(1 + x^2) \simeq x^2 + y^2$  holds. In practice, it will be extremely challenging to observe such a suppressed signal of *CP* violation on the  $\psi(3770)$  resonance even in STCF [197]. But we remark that this kind of *CP* violation is conceptually interesting and deserves our special attention and penetrating search, as it is simply a rate rather than a conventional *CP*-violating asymmetry.

*CP violation in  $D^0 \rightarrow K^{*+}K^-$  and  $K^+K^{*-}$  decays.* In the SM the singly Cabibbo-suppressed decays  $D^0 \rightarrow K^{*\pm}K^\mp$  can take place through both the tree-level and penguin diagrams. The former is essentially *CP*-conserving because it is proportional to the CKM factor  $V_{cs}V_{us}^*$ , and the latter may not be very small with respect to the former as can be seen in the  $D^0 \rightarrow K^+K^-$  case discussed above. But for the sake of simplicity and illustration, here we assume that the tree-level contribution to  $D^0 \rightarrow K^{*\pm}K^\mp$  decays is dominant. In this approximation, we have [243]

$$\begin{aligned}\lambda_{K^{*+}K^-} &= \frac{q}{p} \cdot \frac{A(\bar{D}^0 \rightarrow K^{*+}K^-)}{A(D^0 \rightarrow K^{*+}K^-)} \simeq h_{K^*K} \left| \frac{q}{p} \right| e^{i(\delta_{K^*K} + \phi)}, \\ \bar{\lambda}_{K^{*-}K^+} &= \frac{p}{q} \cdot \frac{A(D^0 \rightarrow K^{*-}K^+)}{A(\bar{D}^0 \rightarrow K^{*-}K^+)} \simeq h_{K^*K} \left| \frac{p}{q} \right| e^{i(\delta_{K^*K} - \phi)},\end{aligned}\quad (103)$$

where  $h_{K^*K}$  is real and of  $\mathcal{O}(1)$ ,  $\delta_{K^*K}$  denotes the relevant strong phase difference, and the standard phase convention  $\arg(V_{cs}V_{us}^*) \simeq 0$  has been taken as an excellent approximation. where only the terms of  $\mathcal{O}(x)$  and  $\mathcal{O}(y)$  are kept, and the so-called ‘‘strong-phase-rotated’’  $D^0$ - $\bar{D}^0$  mixing parameters  $x'_\pm$  and  $y'_\pm$  are defined as

$$\begin{aligned}x'_\pm &= x \cos \delta_{K^*K} \pm y \sin \delta_{K^*K}, \\ y'_\pm &= y \cos \delta_{K^*K} \pm x \sin \delta_{K^*K}.\end{aligned}\quad (104)$$

So it is possible to determine  $h_{K^*K}$  and constrain the magnitudes of both  $D^0$ - $\bar{D}^0$  mixing and *CP* violation from the measurements of these four decay modes. In particular, a remarkable difference between  $y'_+$  and  $y'_-$  will imply that both  $x$  and  $\delta_{K^*K}$  should not be very small [244].

On the  $\psi(3770)$  resonance, where a pair of  $D^0$  and  $\bar{D}^0$  mesons with  $C = -1$  can be coherently produced, their joint decays into the final states  $(K^{*\pm}K^\mp)(K^{*\pm}K^\mp)$  have the following rates to the accuracy of  $\mathcal{O}(x^2)$  and  $\mathcal{O}(y^2)$  [243]:

$$\begin{aligned}\Gamma(K^{*+}K^-; K^{*+}K^-)_{C=-1} &\propto 2|A(D^0 \rightarrow K^{*+}K^-)|^4 r \\ &\times \left[ \left| \frac{p}{q} \right|^2 - 2h_{K^*K}^2 \cos(\delta_{K^*K} + \phi) + h_{K^*K}^4 \left| \frac{q}{p} \right|^2 \right], \\ \Gamma(K^{*-}K^+; K^{*-}K^+)_{C=-1} &\propto 2|A(\bar{D}^0 \rightarrow K^{*-}K^+)|^4 r \\ &\times \left[ \left| \frac{q}{p} \right|^2 - 2h_{K^*K}^2 \cos(\delta_{K^*K} - \phi) + h_{K^*K}^4 \left| \frac{p}{q} \right|^2 \right],\end{aligned}\quad (105)$$

where  $r \equiv (x^2 + y^2)/2$  as defined below Eq. (98). On the  $\psi(4140)$  resonance, with  $C = +1$  for the coherent  $D^0\bar{D}^0$  pairs, the rates of their joint decays into  $(K^{*\pm}K^\mp)(K^{*\pm}K^\mp)$  are given as follows to the accuracy of  $\mathcal{O}(x)$  and  $\mathcal{O}(y)$  [243]:

$$\begin{aligned} \Gamma(K^{*+}K^-; K^{*+}K^-)_{C=+1} &\propto 8|A(D^0 \rightarrow K^{*+}K^-)|^4 h_{K^*K} \\ &\times \left[ h_{K^*K} + \left| \frac{p}{q} \right| (y'_+ \cos \phi + x'_- \sin \phi) \right. \\ &\quad \left. + h_{K^*K}^2 \left| \frac{q}{p} \right| (y'_- \cos \phi - x'_+ \sin \phi) \right], \\ \Gamma(K^{*-}K^+; K^{*-}K^+)_{C=+1} &\propto 8|A(\bar{D}^0 \rightarrow K^{*-}K^+)|^4 h_{K^*K} \\ &\times \left[ h_{K^*K} + \left| \frac{q}{p} \right| (y'_+ \cos \phi - x'_- \sin \phi) \right. \\ &\quad \left. + h_{K^*K}^2 \left| \frac{p}{q} \right| (y'_- \cos \phi + x'_+ \sin \phi) \right], \end{aligned} \quad (106)$$

where only the terms of  $\mathcal{O}(x)$  and  $\mathcal{O}(y)$  are kept, and the so-called ‘‘strong-phase-rotated’’  $D^0$ - $\bar{D}^0$  mixing parameters  $x'_\pm$  and  $y'_\pm$  are defined as

$$\begin{aligned} x'_\pm &= x \cos \delta_{K^*K} \pm y \sin \delta_{K^*K}, \\ y'_\pm &= y \cos \delta_{K^*K} \pm x \sin \delta_{K^*K}. \end{aligned} \quad (107)$$

So it is possible to determine  $h_{K^*K}$  and constrain the magnitudes of both  $D^0$ - $\bar{D}^0$  mixing and  $CP$  violation from the measurements of these four decays. In particular, a remarkable difference between  $y'_+$  and  $y'_-$  will imply that both  $x$  and  $\delta_{K^*K}$  should not be very small [244]. A nonzero difference between the two joint decay rates in either Eq. (105) or Eq. (106) is a clear signal of  $D^0$ - $\bar{D}^0$  mixing and  $CP$  violation.

It is worth emphasizing that studying the  $K^{*\pm}K^\mp$  events of neutral  $D$ -meson decays are important as they can be complementary to the  $K^\pm\pi^\mp$  and  $K^+K^-$  (or  $\pi^+\pi^-$ ) events for the experimental searches for both  $D^0$ - $\bar{D}^0$  mixing and  $CP$  violation. A quite similar idea, which utilizes the  $D^{*\pm}D^\mp$  events of neutral  $B$ -meson decays to probe  $CP$  violation and test the factorization hypothesis [245], has already been applied to the Belle [246] and BaBar [247] experiments.

#### 4.4. $CP$ violation from the interplay between decay and mixing

As for the neutral  $D$ -meson decays,  $CP$  violation may arise from the ‘‘double-slit’’ interference effect of the form  $D^0 \rightarrow \bar{D}^0 \rightarrow f$  versus  $D^0 \rightarrow f$  (or  $\bar{D}^0 \rightarrow$

$D^0 \rightarrow \bar{f}$  versus  $\bar{D}^0 \rightarrow \bar{f}$ ) [239, 248–252], where the final hadronic state  $f$  and its  $CP$ -conjugated state  $\bar{f}$  are unnecessarily the  $CP$  eigenstates. In this case, the interplay between the direct decay and  $D^0$ - $\bar{D}^0$  mixing can be described by the following rephasing-invariant quantities  $\lambda_f$  and  $\bar{\lambda}_{\bar{f}}$  as defined in Eq. 87. Then the difference

$$\text{Im}\lambda_f - \text{Im}\bar{\lambda}_{\bar{f}} \neq 0 \quad (108)$$

characterizes the effects of *indirect*  $CP$  violation, which may include both the contribution of  $\Delta_{\text{mixing}}$  in Eq. (85) and that from direct  $CP$  violation in Eq. (??).

Note that  $D^0$ - $\bar{D}^0$  mixing affects  $\text{Im}\lambda_f$  and  $\text{Im}\bar{\lambda}_{\bar{f}}$  even in the special case of  $\Delta_{\text{mixing}} = 0$  (*i.e.*,  $|q/p| = 1$ ), if  $q/p$  has a nontrivial complex phase. In this case  $\lambda_{\bar{f}} = \lambda_f^*$  will hold if  $D^0 \rightarrow f$  and  $\bar{D}^0 \rightarrow \bar{f}$  are both dominated by a single amplitude component and  $\bar{f} = f$  is a hadronic  $CP$  eigenstate (*e.g.*,  $K^+K^-$  and  $\pi^+\pi^-$ ). Such a *purely indirect*  $CP$ -violating effect, without the contamination from either  $CP$  violation in  $D^0$ - $\bar{D}^0$  mixing or direct  $CP$  violation in the direct decays of  $D^0$  and  $\bar{D}^0$  mesons, is of great interest in the charm sector. A typical example of this kind in the bottom sector is  $CP$  violation in  $B_d^0 \rightarrow \bar{B}_d^0 \rightarrow J/\psi K_S$  versus  $B_d^0 \rightarrow J/\psi K_S$  decays, which has played an important role in testing the KM mechanism of  $CP$  violation in the SM.

#### 4.5. $CP$ violation due to the final-state $K^0$ - $\bar{K}^0$ mixing

In some decay modes of neutral or charged  $D$  mesons with  $K_S$  or  $K_L$  in the final states,  $CP$  violation of  $\mathcal{O}(10^{-3})$  arising from  $K^0$ - $\bar{K}^0$  mixing is expected to show up. It is well known that the mass and flavor eigenstates of neutral  $K$  mesons are correlated with each other via

$$\begin{aligned} |K_S\rangle &= \frac{1}{\sqrt{2(1+|\epsilon_K|^2)}} [(1+\epsilon_K)|K^0\rangle + (1-\epsilon_K)|\bar{K}^0\rangle] , \\ |K_L\rangle &= \frac{1}{\sqrt{2(1+|\epsilon_K|^2)}} [(1+\epsilon_K)|K^0\rangle - (1-\epsilon_K)|\bar{K}^0\rangle] , \end{aligned} \quad (109)$$

where  $\epsilon_K$  is the complex  $K^0$ - $\bar{K}^0$  mixing parameter, and the strength of  $CP$  violation in  $K^0$ - $\bar{K}^0$  mixing is characterized by  $|\epsilon_K| = (2.228 \pm 0.011) \times 10^{-3}$  and  $\arg(\epsilon_K) = 43.52^\circ \pm 0.05^\circ$  [15]. Let us consider the decay modes  $D^\pm \rightarrow X^\pm K_S$  with  $X$  being a SL or nonleptonic state, and assume them to occur mainly through the tree-level quark diagrams. In this case the amplitudes of these two transitions

can be parameterized as [253]

$$\begin{aligned} A(D^+ \rightarrow X^+ K_S) &= \kappa \left[ (1 + \epsilon_K^*) T_1 e^{i(\delta_1 + \phi_1)} + (1 - \epsilon_K^*) T_2 e^{i(\delta_2 + \phi_2)} \right], \\ A(D^- \rightarrow X^- K_S) &= \kappa \left[ (1 - \epsilon_K^*) T_1 e^{i(\delta_1 - \phi_1)} + (1 + \epsilon_K^*) T_2 e^{i(\delta_2 - \phi_2)} \right], \end{aligned} \quad (110)$$

where  $\kappa = 1/\sqrt{2(1 + |\epsilon_K|^2)}$ ,  $T_{1,2}$ ,  $\delta_{1,2}$  and  $\phi_{1,2}$  are the moduli, strong and weak phases of the two amplitude components associated respectively with  $K^0$  and  $\bar{K}^0$  in the  $D^+$  decay mode. Then the  $CP$ -violating asymmetry between  $D^- \rightarrow X^- K_S$  and  $D^+ \rightarrow X^+ K_S$  is given as

$$\begin{aligned} \mathcal{A}_{X^\pm K_S} &\equiv \frac{\Gamma(D^- \rightarrow X^- K_S) - \Gamma(D^+ \rightarrow X^+ K_S)}{\Gamma(D^- \rightarrow X^- K_S) + \Gamma(D^+ \rightarrow X^+ K_S)} \\ &= 2 \frac{\text{Re}\epsilon_K (T_2^2 - T_1^2) + 2\text{Im}\epsilon_K T_1 T_2 \cos(\phi_2 - \phi_1) \sin(\delta_2 - \delta_1)}{T_1^2 + T_2^2 + 2T_1 T_2 \cos(\phi_2 - \phi_1) \cos(\delta_2 - \delta_1)} \\ &\quad + 2 \frac{T_1 T_2 \sin(\phi_2 - \phi_1) \sin(\delta_2 - \delta_1)}{T_1^2 + T_2^2 + 2T_1 T_2 \cos(\phi_2 - \phi_1) \cos(\delta_2 - \delta_1)}, \end{aligned} \quad (111)$$

in which the first term arises from  $K^0$ - $\bar{K}^0$  mixing and the second term results from the direct  $D^\pm$  decays. The former is very likely to be comparable with and even dominant over the latter in magnitude for some explicit decay modes of this category [253–256]. Of course, one may similarly consider the  $D^\pm \rightarrow X^\pm K_L$  transitions and their  $CP$ -violating asymmetries. As for the decay modes of  $D^0$  and  $\bar{D}^0$  mesons,  $K^0$ - $\bar{K}^0$  mixing in their final states can also give rise to similar  $CP$ -violating effects characterized by  $\text{Re}\epsilon_K$  and  $\text{Im}\epsilon_K$ .

In practice, a precision measurement of the  $\epsilon_K$ -induced  $CP$  violation in charged or neutral  $D$ -meson decays will be very helpful to calibrate the experimental systematics of STCF sensitive to a  $CP$ -violating asymmetry of  $\mathcal{O}(10^{-3})$ , in order to search for the genuine charmed  $CP$  violation of the same order in  $D$ -meson decays.

#### 4.6. $CP$ violation due to $D^0 - \bar{D}^0$ and $K^0 - \bar{K}^0$ oscillating interference

In Cascade decays involving both neutral  $D$  mesons and neutral kaons,  $CP$  violation may arise from the interference effect of different  $D$  and kaon oscillating paths, such as  $D^0 \rightarrow \bar{K}^0 \rightarrow K^0$  and  $D^0 \rightarrow \bar{D}^0 \rightarrow K^0$ . The decay products of the primary decay associated with kaons, such as  $\pi^0$ ,  $\rho^0$   $\pi^+\pi^-$ , etc., have been omitted, and the final state  $f$  is not necessarily a  $CP$  eigenstate. This  $CP$ -violation effect is referred to as double-mixing  $CP$  violation, as introduced in

Refs. [257, 258]. It offers an opportunity for a two-dimensional time-dependent analysis of  $CP$ -violation effects, depending on the weak decaying time durations of the primary and secondary decaying mesons. Furthermore, as  $CP$  violation arises from the interplay between decay and mixing, its presence does not necessitate a nonzero strong phase, providing a direct test of the KM mechanism of  $CP$  violation in the SM.

The cascade decay  $D^0 \rightarrow K f_{CP} \rightarrow (\pi^- \ell^+ \nu_\ell) f_{CP}$  can serve as an illustrative example. Owing to the frequent kaon oscillations, the dominant amplitude of the process is  $D^0 \rightarrow \bar{K}^0 f_{CP} \rightarrow K^0 f_{CP} \rightarrow (\pi^- \ell^+ \nu_\ell) f_{CP}$ . The subdominant amplitudes are  $D^0 \rightarrow K^0 f_{CP} \rightarrow (\pi^- \ell^+ \nu_\ell) f_{CP}$  and  $D^0 \rightarrow \bar{D}^0 \rightarrow K^0 f_{CP} \rightarrow (\pi^- \ell^+ \nu_\ell) f_{CP}$ , which are suppressed by  $\lambda^2$  and  $x_D(y_D)$ , respectively. The  $CP$ -violation effects can be induced by the magnitude squares and interferences of the three amplitudes, including the  $CP$  violation from neutral meson mixing,  $CP$  violation from the interplay between decay and mixing, as discussed previously, and also the double-mixing  $CP$  violation [257, 258]. The double-mixing  $CP$  violation arises from the interplay between  $D$  mixing and kaon mixing, specifically between the  $D^0 \rightarrow \bar{K}^0 f_{CP} \rightarrow K^0 f_{CP} \rightarrow (\pi^- \ell^+ \nu_\ell) f_{CP}$  and  $D^0 \rightarrow \bar{D}^0 \rightarrow K^0 f_{CP} \rightarrow (\pi^- \ell^+ \nu_\ell) f_{CP}$  amplitudes. It can be characterized by the difference  $(q/p)_D^* (p/q)_K A(D^0 \rightarrow \bar{K}^0 f_{CP}) - (p/q)_D^* (q/p)_K A(\bar{D}^0 \rightarrow K^0 f_{CP}) \neq 0$ . The corresponding time dependence of the double-mixing  $CP$  violation is given by

$$A_{CP}^{\text{dm}}(t_1, t_2) \propto e^{-\Gamma_D t_D - \Gamma_K t_K} \left[ \sinh \frac{\Delta \Gamma_D t_D}{2} S_h(t_K) + \sin(\Delta m_D t_D) S_n(t_K) \right] \quad (112)$$

where

$$\begin{aligned} S_h(t_K) &\approx -\sin(\Delta m_K t_K) \sin \Phi_{DK} + 2 \sinh \frac{\Delta \Gamma_K t_K}{2} \text{Re}(\epsilon_K - \epsilon_D) \cos \Phi_{DK}, \\ S_n(t_K) &\approx \sinh \frac{\Delta \Gamma_K t_K}{2} \sin \Phi_{DK} + 2 \sin(\Delta m_K t_K) \text{Re}(\epsilon_K - \epsilon_D) \cos \Phi_{DK}, \end{aligned} \quad (113)$$

with  $\Phi_{DK} = \phi_D + \phi_K + \omega$  and  $e^{i\omega} \equiv A(D^0 \rightarrow \bar{K}^0 f_{CP})/A(\bar{D}^0 \rightarrow K^0 f_{CP})$ . Apart from the overall exponential factor, the four terms exhibit distinct sine and hyper-sine dependencies on  $t_D$  and  $t_K$ , allowing for a two-dimensional time-dependent analysis to extract their contributions individually. Similarly, in the decay  $D^0 \rightarrow K f_{CP} \rightarrow (\pi^+ \ell^- \bar{\nu}_\ell) f_{CP}$ , the double-mixing  $CP$  violation arises from the interplay between  $D^0 \rightarrow \bar{K}^0 f_{CP} \rightarrow (\pi^+ \ell^- \bar{\nu}_\ell) f_{CP}$  and  $D^0 \rightarrow \bar{D}^0 \rightarrow K^0 f_{CP} \rightarrow \bar{K}^0 f_{CP} \rightarrow (\pi^+ \ell^- \bar{\nu}_\ell) f_{CP}$ . It is characterized by the difference  $(q/p)_D^* (q/p)_K A(D^0 \rightarrow \bar{K}^0 f_{CP}) - (p/q)_D^* (p/q)_K A(\bar{D}^0 \rightarrow K^0 f_{CP}) \neq 0$ , and the corresponding time-dependent

functions in Eq. (112) are given by

$$\begin{aligned}
S_h(t_K) &\approx -\sin(\Delta m_K t_K) \sin \Phi_{DK} - 2 \sinh \frac{\Delta \Gamma_K t_K}{2} \operatorname{Re}(\epsilon_K + \epsilon_D) \cos \Phi_{DK}, \\
S_n(t_K) &\approx -\sinh \frac{\Delta \Gamma_2 t_2}{2} \sin \Phi_{DK} + 2 \sin(\Delta m_2 t_2) \operatorname{Re}(\epsilon_K + \epsilon_D) \cos \Phi_{DK}. \quad (114)
\end{aligned}$$

#### 4.7. Prospects of charm $CP$ violation studies at STCF

Mixing and indirect  $CP$  violation effects in the neutral  $D$  meson system can be investigated with the quantum-correlated (QC) neutral  $D\bar{D}$  pairs produced at STCF. On the resonance  $\psi(4010)$  where the production cross-section of neutral  $D\bar{D}^*$  is 3320 pb [259], the integrated luminosity of the data sample that STCF is expected to collect annually is around  $1 \text{ ab}^{-1}$ , corresponding to  $3.32 \times 10^9$   $D\bar{D}^*$  pairs. The  $D\bar{D}$  pairs are  $C$ -odd and even correlated with the subsequent decays  $D^{*0} \rightarrow D^0\pi^0$  and  $D^{*0} \rightarrow D^0\gamma$ , respectively. Taking the branching fraction of  $D^{*0} \rightarrow D^0\gamma$ , the number of pairs of  $C$ -even  $D\bar{D}$  can reach approximately  $1.2 \times 10^9$ . At the c.m. energy  $\sqrt{s} = 4.01 \text{ GeV}$ , the production cross-section of  $D^{*+}\bar{D}^-$  is 3300 pb [259]. The number of  $D^{*+}\bar{D}^-$  pairs produced at STCF annually is about  $N_{D^{*+}\bar{D}^-} = 3.30 \times 10^9$ . Taking the branching fraction of  $D^{*+} \rightarrow D^0\pi^+$ , the number of  $D^0$  mesons is approximately  $2.23 \times 10^9$ . Flavour-specific neutral  $D$  meson decays can be accessed by reconstructing the soft pion from  $D^*$  decay or the charged  $D$  meson.

The two  $D$  mesons decay coherently with the double decay rates given by Eq. (95). A "double tag" (DT) method is needed to exploit the QC effects, where the signal  $D$  decay is reconstructed against the tag-side decay. Multiple-body decays are more sensitive to the charm mixing and indirect  $CP$  violation measurements due to the amplitude variations in phase space. Time-integrated measurements, referred as "single tag" (ST) method, with flavor-specific neutral  $D$  meson decays can add to the sensitivity. The decay rates are given by Eq. (89). We summarize the status of the future prospects at STCF with the three and four-body decays  $D \rightarrow K^-\pi^+\pi^0$ ,  $K_S^0\pi^+\pi^-$  and  $K^-\pi^+\pi^+\pi^-$ . They proceed through tree-level decays, where the direct  $CP$  violation can be neglected.

*Measurements of the  $D \rightarrow K^-\pi^+\pi^+\pi^-$  decay.* With the  $C$ -even correlated  $D\bar{D}$  pairs, the  $D \rightarrow K^-\pi^+\pi^+\pi^-$  decay can be reconstructed against the flavour tags  $K^\mp\pi^\pm\pi^+\pi^-$ ,  $K^\mp\pi^\pm\pi^0$ ,  $K^\mp\pi^\pm$ , the  $CP$ -even eigenstates  $K^+K^-$ ,  $\pi^+\pi^-$  and  $CP$ -odd eigenstates  $K_S^0\pi^0$ ,  $K_S^0\eta$ ,  $K_S^0\omega$  and  $K_S^0\eta'$  and the self-conjugate decay  $K_S^0\pi^+\pi^-$ . By exploiting the signal decays in four phase-space regions, the sensitivity is obtained as listed in Table 8 and 1, 2 and  $3\sigma$  regions of the parameters are shown in

Fig. 13. The  $CP$ -conserving strong-phase differences between  $D^0$  and  $\bar{D}^0$  decays in phase-space regions are required as inputs to such studies. These parameters can be accessed with the  $C$ -odd correlated  $D\bar{D}$  pairs produced at the same energy point [260].

Table 8: Statistical sensitivity of the charm mixing and indirect  $CP$  violation parameters by analyzing the  $C$ -even correlated and flavor specific  $D \rightarrow K^- \pi^+ \pi^+ \pi^-$  decays at STCF, and comparison with the LHCb Upgrade I.

	STCF (DT)	STCF (DT&ST)	LHCb ( $50 \text{ fb}^{-1}$ )
$x(\%)$	0.056	0.047	—
$y(\%)$	0.027	0.025	—
$r_{CP}$	0.050	0.042	0.005
$\phi(^{\circ})$	3.64	3.10	0.30

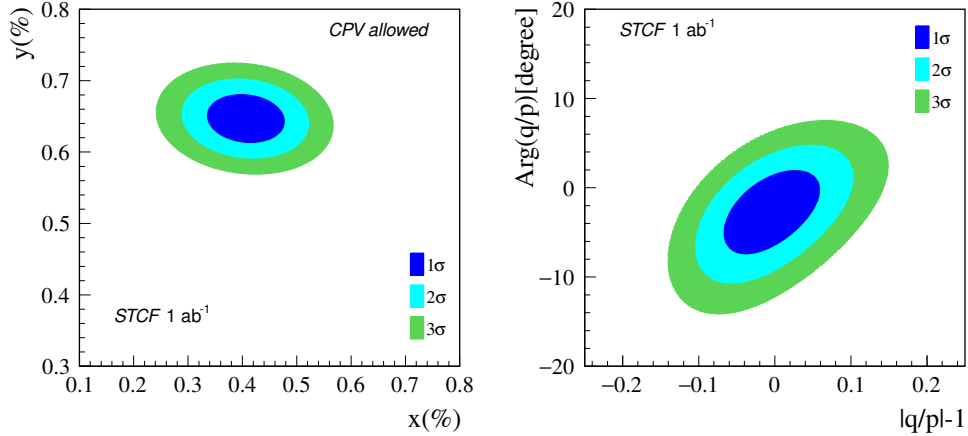


Figure 13: 1, 2 and  $3\sigma$  regions of the charm mixing parameters and indirect  $CP$  violation parameters by analyzing the  $D \rightarrow K^- \pi^+ \pi^+ \pi^-$  decay.

*Measurements of the  $D \rightarrow K_S^0 \pi^+ \pi^-$  decay.* Studies with  $D \rightarrow K_S^0 \pi^+ \pi^-$  decay also include the various tags used for  $D \rightarrow K^- \pi^+ \pi^+ \pi^-$  decay. With one-year data taking, the sensitivity that STCF is expected to achieve is shown in Table 9 and 1, 2 and  $3\sigma$  regions of the parameters are shown in Fig. 14. The strong-phase parameters in the exploit eight phase-space regions can be accessed with the corresponding  $C$ -odd correlated  $D\bar{D}$  decays [261]. Utilizing the same method, a

recent time-dependent measurement performed by the LHCb experiment determined that  $x = (0.398^{+0.056}_{-0.054})\%$ ,  $y = (0.46^{+0.15}_{-0.14})\%$  and  $r_{CP} = 0.996 \pm 0.052$ ,  $\phi = (3.2^{+2.7}_{-2.9})^\circ$  [262].

Table 9: Statistical sensitivity of the charm mixing and indirect  $CP$  violation parameters by analyzing the  $C$ -even correlated and flavor specific  $D \rightarrow K_S^0 \pi^+ \pi^-$  decays at STCF and comparison with the LHCb Upgrade I and Belle II.

	STCF (DT)	STCF (DT&ST)	LHCb ( $50 \text{ fb}^{-1}$ )	Belle II ( $50 \text{ ab}^{-1}$ )
$x(\%)$	0.076	0.069	0.012	0.030
$y(\%)$	0.054	0.050	0.013	0.020
$r_{CP}$	0.084	0.077	0.011	0.022
$\phi(^\circ)$	5.00	4.57	0.48	1.50

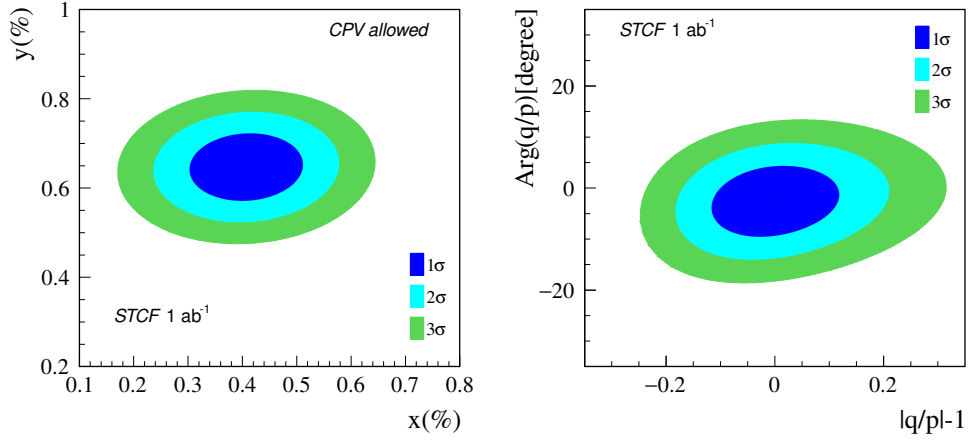


Figure 14: 1, 2 and  $3\sigma$  regions of the charm mixing parameters and indirect  $CP$  violation parameters by analyzing the  $D \rightarrow K_S^0 \pi^+ \pi^-$  decay.

*Measurements of the  $D \rightarrow K^- \pi^+ \pi^0$  decay.* Similar to the  $D \rightarrow K^- \pi^+ \pi^+ \pi^-$  decay, the  $D \rightarrow K^- \pi^+ \pi^0$  decay can be studied with the  $C$ -even correlated  $D\bar{D}$  pairs and the flavor-specific  $D$  mesons. Currently, the sensitivity is obtained by taking the inputs of average strong-phase and associated hadronic parameters over the whole phase-space [260]. This decay is found to be dominant for the charm mixing and indirect  $CP$  violation study at STCF, with the sensitivity shown in

Table 9 and 1, 2 and  $3\sigma$  regions of the parameters shown in Fig. 15. A binned study can further improve the sensitivity and again the strong-phase parameters can be determined simultaneously with the  $C$ -odd correlated  $D\bar{D}$  decays.

Table 10: Statistical sensitivity of the charm mixing and indirect  $CP$  violation parameters by analysing the  $C$ -even correlated and flavor specific  $D \rightarrow K^- \pi^+ \pi^0$  decays at STCF.

	STCF (DT)	STCF (DT&ST)
$x(\%)$	0.055	0.044
$y(\%)$	0.019	0.017
$r_{CP}$	0.048	0.034
$\phi(^{\circ})$	3.34	2.51

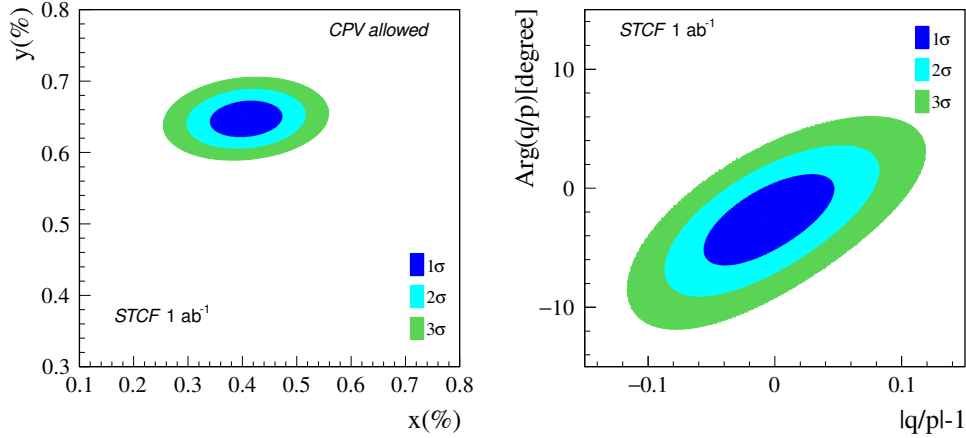


Figure 15: 1, 2 and  $3\sigma$  regions of the charm mixing parameters and indirect  $CP$  violation parameters by analyzing the  $D \rightarrow K^- \pi^+ \pi^0$  decay.

*Overall prospects.* A global fit of the DT  $D \rightarrow K^- \pi^+ \pi^0$ ,  $K_S^0 \pi^+ \pi^-$  and  $K^- \pi^+ \pi^+ \pi^-$  signal decays and flavor-specific ST gives the sensitivities of the charm mixing and indirect  $CP$  violation parameters to be  $\sigma(x) = 0.036\%$ ,  $\sigma(y) = 0.015\%$ ,  $\sigma(r_{CP}) = 0.028$  and  $\sigma(\phi) = 2.14^{\circ}$ , as shown in Fig. 16. Such studies indicate that indirect charm  $CP$  violation can be studied at the  $10^{-4}$  level in STCF and would complement the studies in upgraded LHCb and Belle II experiments.

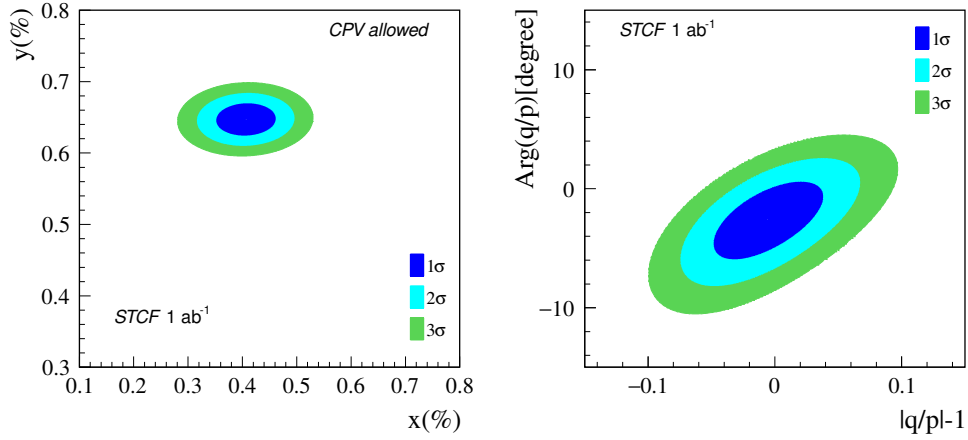


Figure 16: 1, 2 and 3 $\sigma$  regions of the charm mixing parameters and indirect  $CP$  violation parameters by analyzing the  $D \rightarrow K^- \pi^+ \pi^0$ ,  $K_S^0 \pi^+ \pi^-$  and  $K^- \pi^+ \pi^+ \pi^-$  decays.

Prerequisites for the charm mixing and indirect  $CP$  violation studies at charm and  $B$  factories are the strong-phase differences with ultimate uncertainties. The  $C$ -odd correlated  $D\bar{D}$  data samples collected with the BESIII and CLEO experiments at the  $\psi(3770)$  energy point have been the best laboratory to perform such measurements. Currently, the uncertainties of the dilution parameters are non-vanishing. STCF would collect more than 100 times the  $C$ -odd correlated  $D\bar{D}$  pairs at BESIII per year, which would be another important contribution to the whole community.

## 5. Tests of the $CPT$ invariance with $J/\psi$ decays

The  $CPT$  theorem [263] states that any quantum field theory that is *Lorentz invariant*, has *local point-like interaction vertices*, and is *hermitian* (*i.e.*, conserves probability) is invariant under the combined operations of  $C$ ,  $P$  and  $T$ . Since the three quantum field theories that make up the SM—QED, QCD, and Electroweak theory—all satisfy these criteria,  $CPT$  symmetry is a fundamental and inescapable prediction of the theory. Any deviation from  $CPT$  invariance would be unambiguous evidence for new, beyond the SM physics. Given the central role that the  $CPT$  theorem plays in our understanding of the most basic properties of space and time, it is essential that its validity should be tested at the highest level of sensitivity that the experimental technology permits.

Fortunately, the  $K^0$ - $\bar{K}^0$  mixing process, coupled with the requirements of unitarity, provides sensitive ways to search for violations of the  $CPT$  theorem. This is embodied in a remarkable equation called the *Bell-Steinberger relation*, that unambiguously relates a fundamental  $CPT$  violating amplitude called  $\delta$  to well defined measurable quantities. The relation is exact and, unlike most other experimental tests of the SM, there are no loose ends such as long-distance QCD-corrections or theoretical assumptions about anything other than unitarity and time independence of the Hamiltonian. If a non-zero value of  $\delta$  is established, the only possible interpretations are that either the  $CPT$  theorem is invalid or unitarity is violated, or that kaon mass or lifetime changes with time.

The measurement involves studies of the proper-time-dependence of the decay rates of large numbers of neutral kaons that have well established (*i.e.*, tagged) strangeness quantum numbers at the time of their production  $K^0(\tau)$  for  $\mathcal{S}=+1$  and  $\bar{K}^0(\tau)$  for  $\mathcal{S}=-1$ . The most sensitive limits to date are from experiments in the 1990s that used data samples that contained tens of millions of  $K^0$  and  $\bar{K}^0$  decays. A  $\sim 10^{12}$ -event sample of  $J/\psi$  decays will contain  $\sim 2$  billion  $J/\psi \rightarrow K^- \pi^+ K^0$  events and an equivalent number of  $J/\psi \rightarrow K^+ \pi^- \bar{K}^0$  events where the neutral kaon decays to  $\pi^+ \pi^-$ , and  $\sim 1$  billion events for each mode in which the kaon decays to  $\pi^0 \pi^0$ . In these reactions, the initial strangeness of the neutral kaon is tagged by the sign of the accompanying charged-kaon's electric charge: a  $K^-$  tags an  $\mathcal{S}=+1$   $K^0(\tau)$  and a  $K^+$  tags an  $\mathcal{S}=-1$   $\bar{K}^0(\tau)$ . These data samples would support a revisit of previous measurements with  $\sim$ fifty-times larger data samples.

In this report we discuss:

- i) why we expect  $CPT$  to be violated somewhere below the Planck mass-scale;
- ii) why the neutral kaon system is well suited for tests of the  $CPT$  theorem;

- iii) the quantum-mechanics of neutral kaons with restrictions on  $CPT$  relaxed;
- iv) estimated experimental sensitivities with  $10^{12}$   $J/\psi$  decays;
- v) applications of the Bell-Steinberger relation at a  $\tau$ -charm factory.

### 5.1. $CPT$ and the Theory of Everything

One of the requirements for a  $CPT$ -invariant theory is that it is *local*, which means that the couplings at each vertex occur at a single point in space-time. But theoretical physics always has troubles with point-like quantities. For example, the classical Coulombic self-energy of the electron is

$$W_e = \frac{e^2}{4\pi\epsilon_0 r_e}, \quad (115)$$

which diverges for  $r_e \rightarrow 0$ . The *classical radius of the electron*, i.e., the value of  $r_e$  that makes  $W_e = m_e c^2$ , is  $r_e^{\text{c.r.e.}} = 2.8 \times 10^{-13}$  cm (2.8 fermis), which is three times the radius of the proton, and  $\sim 3000$  times larger than the experimental upper limit on the electron radius, which is of  $\mathcal{O}(10^{-16}$  cm) [264]. Infinities associated with point-like objects persist in quantum field theories, where they are especially troublesome. In second- and higher-order perturbation theory, all diagrams that have virtual-particle loops involved integrals over all possible configurations of the loops that conserve energy and momentum. Whenever two of the point-like vertices coincide, the integrands become infinite and cause the integrals to diverge.

In the QED, QCD and Electroweak quantum field theories that make up the SM, these infinities are removed by the well established methods of renormalization [265–267]. In all these three theories, the perturbative expansions are in increasing powers of a dimensionless coupling strength,  $\alpha_{\text{QED}}$ ,  $\alpha_s$  and,  $\alpha_{\text{EW}} = \sqrt{2}M_W^2 G_F / \pi$ .<sup>5</sup> As a result of this, in the renormalization procedure, relations that exist between different orders of the perturbation expansion reduce the number of observed quantities that are needed to subtract off divergences. In QED, for example, there are only two, the electron’s mass, and charge (four, if the diagram includes muons and tau-leptons). However, in quantum theories of gravity, where a massless spin=2 *graviton* plays the role of the photon in QED, the expansion constant is Newton’s gravitational constant  $G_N = \hbar c / M_P^2$ , where  $M_P \equiv \sqrt{\hbar c / G_N} = 1.24 \times 10^{19}$  GeV is the *Planck mass*. Because this has dimension  $\text{mass}^{-2}$ , every order in the perturbation expansion has different dimensions and, thus, would need a

---

<sup>5</sup>Specifically not just  $G_F$ , which has dimensions of  $\text{mass}^{-2}$ .

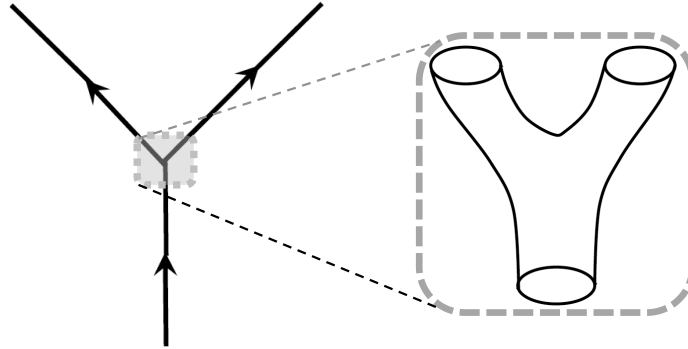


Figure 17: In string theories, elementary particles are tiny loops of oscillating strings with no point-like vertices and their associated infinities.

distinct observed quantity to carry out the subtraction. This means that a complete renormalization would require an infinite number of observed quantities, with the end effect that a quantum theory of gravity with point-like vertices would, in principle, be *nonrenormalizable* [268]. A viable theory of everything would have to include a mechanism for avoiding these divergences by somehow smearing out the vertices, for example by treating particles as loops of strings like in Fig. 17, and this *non-locality* would eliminate one of the necessary conditions for *CPT* invariance. Thus, a Theory of Everything, which, by definition, would have to include gravity <sup>6</sup>, would not be local and include *CPT* violations at some mass scale.

Although difficulties associated with non-renormalizability (*i.e.*, higher-order perturbative effects) will never show up at scales below the Planck mass, the fact that this problem exists at all demonstrates that there is nothing especially sacred about *CPT*-invariance, and nothing prevents it from being violated at a lower mass scale. Because of this close connection with the fundamental assumptions of the SM, stringent experimental tests of *CPT* invariance should have high priority.

### 5.2. Neutral *K* mesons and tests of the *CPT* theorem

The main consequences of *CPT* symmetry are that particle and antiparticle masses and lifetimes are equal, being their electric charges opposite and higher electromagnetic multipoles identical. Since lifetime differences can only come from on-mass-shell intermediate states and do not probe short-distance high-mass

---

<sup>6</sup>Even cavemen were aware of gravity.

physics, these are unlikely to exhibit any  $CPT$ -violating asymmetry. Instead, the focus here is on the possibility that particle and antiparticle masses may be different.

The particles with the best measured masses are the stable electron and proton, and, according to the PDG20 [269]:

$$|m_{\bar{e}} - m_e| < 4 \times 10^{-9} \text{ MeV}, \quad (116)$$

$$|m_{\bar{p}} - m_p| < 7 \times 10^{-7} \text{ MeV}. \quad (117)$$

However, these limits do not provide the best tests of  $CPT$ ; the most stringent experimental restriction on  $CPT$  violation comes from the difference between the  $\bar{K}^0$  and  $K^0$  masses:

$$|M_{\bar{K}^0} - M_{K^0}| = < 5 \times 10^{-16} \text{ MeV}, \quad (118)$$

which is 7-9 orders of magnitude stricter than those from the electron and proton mass measurements, even though the value of  $M_{K^0}$  itself is only known to  $\pm 13$  keV. This is because of the Fig. 18 diagrams, taken together with the quantum mechanics of  $K^0$ - $\bar{K}^0$  mixing, map the  $M_{\bar{K}^0} - M_{K^0}$  difference into the quantity  $\Delta M \equiv M_{K_L^0} - M_{K_S^0} \approx 3.5 \times 10^{-12}$  MeV, which is 14 orders of magnitude lower than  $M_{\bar{K}^0}$  or  $M_{K^0}$  and the independent quantity  $\Delta\Gamma \equiv \Gamma_{K_S^0} - \Gamma_{K_L^0} \approx 7.4 \times 10^{-12}$  MeV (which is, coincidentally,  $\approx 2 \times \Delta M$ ).

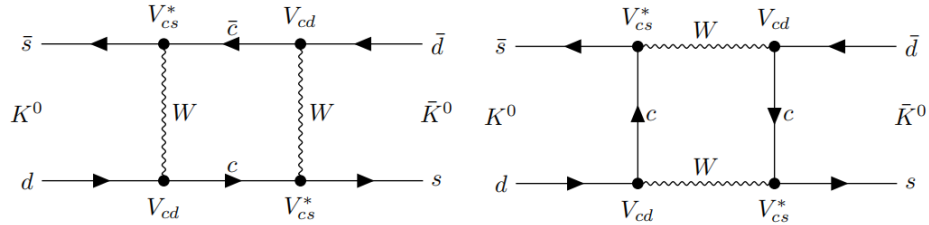


Figure 18: The box diagrams for the short-distance contributions to  $K^0$ - $\bar{K}^0$  mixing.

### 5.3. The neutral kaon mass eigenstates with no $CPT$ -invariance related restrictions

Any arbitrary neutral kaon state in its rest frame can be expressed as a linear combination of the strangeness eigenstates,  $|\psi\rangle = \alpha_1(\tau) |K^0\rangle + \alpha_2(\tau) |\bar{K}^0\rangle$ , where  $\alpha_1(\tau)$  and  $\alpha_2(\tau)$  are complex functions that are normalized as  $|\alpha_1(0)|^2 + |\alpha_2(0)|^2 = 1$ .

In the Wigner-Weisskopf formulation of quantum mechanics for exponentially decaying systems, the time-dependence is included by using  $\alpha_i(\tau) = \alpha_i^k e^{-i\lambda_k \tau}$  where  $\alpha_i^k$  are complex constants and the Schrödinger equation in the form

$$\mathcal{H}\psi(\tau) = \left( \mathcal{M} - \frac{i}{2}\Gamma \right) \Psi_k e^{-i\lambda_k \tau} = i \frac{d\psi_K}{d\tau} = \lambda_k \Psi_k e^{-i\lambda_k \tau}, \quad (119)$$

where the Hamiltonian  $\mathcal{H}$ , the *mass matrix*  $\mathcal{M}$  and the *decay matrix*  $\Gamma$  are  $2 \times 2$  matrices and  $\Psi_k$  is a two-dimensional spinor in  $(K^0, \bar{K}^0)$  space:

$$\mathcal{M} = \begin{pmatrix} M_{11} & M_{12} \\ M_{12}^* & M_{22} \end{pmatrix}, \quad \Gamma = \begin{pmatrix} \Gamma_{11} & \Gamma_{12} \\ \Gamma_{12}^* & \Gamma_{22} \end{pmatrix} \quad \text{and} \quad \Psi_k = \begin{pmatrix} \alpha_1^k \\ \alpha_2^k \end{pmatrix}. \quad (120)$$

Here  $\mathcal{M}$  and  $\Gamma$  are hermitian, which is ensured by setting  $M_{21} = M_{12}^*$  and  $\Gamma_{21} = \Gamma_{12}^*$ , while  $\mathcal{H}$ , which describes decaying particles and does not conserve probability, is not hermitian. Symmetry under *CP* requires  $M_{12}$  to be real; *CPT* invariance requires  $M_{11} = M_{22}$  and  $\Gamma_{11} = \Gamma_{22}$ . The mass eigenvalues and eigenstates for the most general case, *i.e.*, neither *CP* or *CPT* symmetry are [13, 270]

$$\begin{aligned} \lambda_S &= M_S - \frac{i}{\sqrt{2}}\Gamma_S, & |K_S^0\rangle &= \frac{1}{\sqrt{2(1+|\varepsilon_S|^2)}} [(1 + \varepsilon_S) |K^0\rangle + (1 - \varepsilon_S) |\bar{K}^0\rangle], \\ \lambda_L &= M_L - \frac{i}{\sqrt{2}}\Gamma_L, & |K_L^0\rangle &= \frac{1}{\sqrt{2(1+|\varepsilon_L|^2)}} [(1 + \varepsilon_L) |K^0\rangle - (1 - \varepsilon_L) |\bar{K}^0\rangle], \end{aligned} \quad (121)$$

where  $\varepsilon_S = \varepsilon + \delta$ ,  $\varepsilon_L = \varepsilon - \delta$ , and

$$\varepsilon = -\frac{i\text{Im}(M_{12}) + \frac{1}{2}\text{Im}(\Gamma_{12})}{\frac{i}{2}\Delta\Gamma + \Delta M}, \quad (122)$$

is the familiar neutral kaon mass-matrix *CP* violation parameter, while

$$\delta = \frac{(M_{\bar{K}^0} - M_{K^0}) - i(\Gamma_{\bar{K}^0} - \Gamma_{K^0})/2}{2\Delta M - i\Delta\Gamma}, \quad (123)$$

is the equivalent mass-matrix *CPT* violation parameter. A unique and important feature is that the  $K_L^0$  and  $K_S^0$  eigenstates are not orthogonal; according to Eq. (121),

$$\langle K_S^0 | K_L^0 \rangle = 2\text{Re}(\varepsilon) - 2i\text{Im}(\delta), \quad (124)$$

where here, and in (most of) the following, we drop second-order terms in  $|\varepsilon|$ .

In a commonly used phase convention,  $Im\Gamma_{12}$  is defined to be zero, in which case the phase of  $\varepsilon$  is directly related to the well measured quantities<sup>7</sup>  $\Delta M$  and  $\Delta\Gamma$  via

$$\phi_{\text{SW}} = \tan^{-1}\left(\frac{2\Delta M}{\Delta\Gamma}\right) = (43.5 \pm 0.1)^\circ, \quad \leftarrow \text{the Superweak phase} \quad (125)$$

that, since  $\Delta M \approx \Delta\Gamma/2$ , is very nearly  $45^\circ$ . Using this approximate relation for  $\phi_{\text{SW}}$ , we can rewrite the Eq. (123) expression for  $\delta$  as

$$\delta \approx \frac{i(M_{\bar{K}^0} - M_{K^0}) + (\Gamma_{\bar{K}^0} - \Gamma_{K^0})/2}{2\sqrt{2}\Delta M} e^{i\phi_{\text{SW}}} = (i\delta_\perp + \delta_\parallel) e^{i\phi_{\text{SW}}}, \quad (126)$$

where the real quantities  $\delta_\perp$  and  $\delta_\parallel$  are defined as

$$\delta_\perp \approx \frac{M_{\bar{K}^0} - M_{K^0}}{2\sqrt{2}\Delta M} \quad \text{and} \quad \delta_\parallel = \frac{(\Gamma_{\bar{K}^0} - \Gamma_{K^0})}{4\sqrt{2}\Delta M}. \quad (127)$$

In the complex plane,  $\delta_\perp$ , which is the short-distance component of  $\delta$ , is perpendicular to  $\varepsilon$ , and  $\delta_\parallel$ , the long-distance component, is parallel to  $\varepsilon$ . Thus, a signature for a non-zero short-distance  $CPT$  violation would be a difference between the phase of  $\varepsilon_L$  and  $\phi_{\text{SW}}$  by an amount

$$\Delta\phi^{CPT} = \phi_{\varepsilon_L} - \phi_{\text{SW}} = \frac{\delta_\perp}{|\varepsilon|}, \quad (128)$$

which means that

$$\begin{aligned} M_{\bar{K}^0} - M_{K^0} &= 2\sqrt{2}|\varepsilon|\Delta M\Delta\phi^{CPT} \\ &= 3.8 \times 10^{-16}(\text{MeV/deg}) \times \Delta\phi^{CPT}. \end{aligned} \quad (129)$$

The tiny proportionality constant between the mass difference and  $\Delta\phi^{CPT}$  is the reason why the Eq. (118) limit on  $M_{\bar{K}^0} - M_{K^0}$  is many orders of magnitude more stringent those for the  $m_{\bar{p}} - m_p$  (Eq. (117)) and  $m_{\bar{e}} - m_e$  (Eq. (116)). This is a feature that is unique to the neutral kaon system and does not apply to any other particle.

#### 5.4. Interference measurements of the $\phi_{+-}$ and $\phi_{00}$ phases

A simulated  $J/\psi \rightarrow K^- \pi^+ K^0(\tau); K^0(\tau) \rightarrow \pi^+ \pi^-$  event in the BESIII detector is shown in Fig. 19(a). Although it looks superficially like a  $K^- \pi^+ K_S^0$  event, the

<sup>7</sup>We use [168]  $\Delta M = (0.5289 \pm 0.0010) \times 10^{10} \text{s}^{-1}$  &  $\Delta\Gamma = (1.1149 \pm 0.0005) \times 10^{-10} \text{s}^{-1}$ .

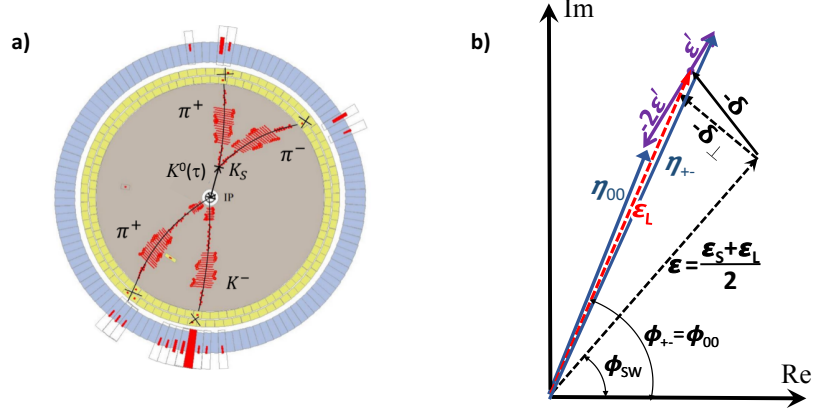


Figure 19: **a)** A simulated  $J/\psi \rightarrow K^- \pi^+ K^0(\tau); K^0(\tau) \rightarrow \pi^+ \pi^-$  event in the BESIII detector. **b)** The relative arrangements in the complex plane of the complex quantities discussed in the text. Here, for display purposes, the magnitudes of  $\delta$  and  $\varepsilon'$  relative to  $\varepsilon$  are exaggerated.

neutral kaon is not a  $K_S^0$  mass eigenstate and does not have a simple exponential decay curve. Instead, the neutral kaons produced in these reactions are coherent mixtures of interfering  $|K_S^0\rangle$  and  $|K_L^0\rangle$  eigenstates:

$$\begin{aligned} |K^0(\tau)\rangle &= \frac{1}{\sqrt{2}}[(1 + \varepsilon_L) |K_S^0\rangle e^{-i\lambda_S\tau} + (1 + \varepsilon_S) |K_L^0\rangle e^{-i\lambda_L\tau}] \\ |\bar{K}^0(\tau)\rangle &= \frac{1}{\sqrt{2}}[(1 - \varepsilon_L) |K_S^0\rangle e^{-i\lambda_S\tau} - (1 - \varepsilon_S) |K_L^0\rangle e^{-i\lambda_L\tau}], \end{aligned} \quad (130)$$

and have decay curves with opposite-sign  $K_S^0$ - $K_L^0$  interference terms:

$$\left[ \begin{array}{c} R(\tau)_{K^0 \rightarrow \pi\pi} \\ \bar{R}(\tau)_{\bar{K}^0 \rightarrow \pi\pi} \end{array} \right] \propto (1 \mp 2Re(\varepsilon_L)) [e^{-\Gamma_S\tau} + |\eta_j|^2 e^{-\Gamma_L\tau} \pm 2|\eta_j| e^{-\bar{\Gamma}\tau} \cos(\Delta M\tau - \phi_j)],$$

where  $\bar{\Gamma} = (\Gamma_S + \Gamma_L)/2 \approx \Gamma_S/2$  and  $|\eta_j|$  and  $\phi_j$  are the magnitudes and phases of  $\eta_{+-}$  and  $\eta_{00}$ :

$$\eta_{+-} = \frac{\langle \pi^+ \pi^- \rangle K_L^0}{\langle \pi^+ \pi^- \rangle K_S^0} = \varepsilon - \delta + \varepsilon' \quad \text{and} \quad \eta_{00} = \frac{\langle \pi^0 \pi^0 \rangle K_L^0}{\langle \pi^0 \pi^0 \rangle K_S^0} = \varepsilon - \delta - 2\varepsilon'. \quad (131)$$

Here  $\varepsilon' = \langle \pi\pi \rangle K_2 / \langle \pi\pi \rangle K_1$  is the ratio of the direct- $CP$ -violating amplitude of the  $CP$ -odd  $|K_2\rangle = \frac{1}{\sqrt{2}}(|K^0\rangle - |\bar{K}^0\rangle)$  eigenstate to  $CP$ -even  $\pi\pi$  final states, to that for  $CP$ -allowed  $\pi\pi$  decays of its  $CP$ -even counterpart:  $|K_1\rangle = \frac{1}{\sqrt{2}}(|K^0\rangle + |\bar{K}^0\rangle)$ . Measurements [271, 272] have established that  $\varepsilon'$  is much smaller than  $\varepsilon$ :

$$Re(\varepsilon'/\varepsilon) = (1.66 \pm 0.23) \times 10^{-3}, \quad (132)$$

and its phase, which is specified by low-energy  $\pi\pi$  scattering phase shifts to be  $\phi_{\varepsilon'} = (42.3 \pm 1.7)^\circ$  [273] and equal, within errors, to  $\phi_{\text{SW}}$ . This rather remarkable coincidence<sup>8</sup> means that  $\varepsilon'$  and  $\varepsilon$  are very nearly parallel, and the combined effect of this and the small magnitude of  $\varepsilon'$  reduces its impact on  $\delta\phi^{CPT}$  measurements to negligible,  $\mathcal{O}(0.01^\circ)$ , levels. The arrangement of the various quantities discussed above on the complex plane is indicated in Fig. 19(b).

### 5.5. Comment on the Bell-Steinberger relation

A general procedure for determining  $Im(\delta)$  that is based on unitarity and independent of any phase convention was devised by John Bell and Jack Steinberger in 1965 and is briefly summarized here [274].

In terms of the  $K_S^0$  and  $K_L^0$  eigenfunctions, a general solution to the Schrödinger equation can be written as

$$\psi(\tau) = \alpha_1 e^{-i\lambda_S \tau} |K_S^0\rangle + \alpha_2 e^{-i\lambda_L \tau} |K_L^0\rangle, \quad (133)$$

where  $\alpha_1$  and  $\alpha_2$  can be any complex constants subject only to the normalization condition  $|\alpha_1|^2 + |\alpha_2|^2 = 1$ . The time-dependent probability associated with this wave function is

$$|\psi(\tau)|^2 = |\alpha_1|^2 e^{-\Gamma_S \tau} + |\alpha_2|^2 e^{-\Gamma_L \tau} + 2Re(\alpha_1^* \alpha_2 e^{-\frac{1}{2}(\Gamma_S + \Gamma_L + 2i\Delta M)\tau} \langle K_S^0 | K_L^0 \rangle), \quad (134)$$

and the negative of its derivative at  $\tau=0$  is

$$-\left. \frac{d|\psi(\tau)|^2}{d\tau} \right|_{\tau=0} = |\alpha_1|^2 \Gamma_S + |\alpha_2|^2 \Gamma_L + Re(\alpha_1^* \alpha_2 (\Gamma_S + \Gamma_L + 2i\Delta M) \langle K_S^0 | K_L^0 \rangle). \quad (135)$$

In the Weisskopf-Wigner formalism, the Schrödinger equation is not hermitian and the solutions do not conserve probability. Instead, the overall normalization has a time dependence given by

$$|\psi(\tau)|^2 = |\psi(0)|^2 e^{-\Gamma_{\text{tot}} \tau}; \quad \frac{d|\psi(\tau)|^2}{d\tau} = -\Gamma_{\text{tot}} e^{-\Gamma_{\text{tot}} \tau}, \quad (136)$$

and unitarity requires that

$$-\left. \frac{d|\psi(\tau)|^2}{d\tau} \right|_{\tau=0} = \Gamma_{\text{tot}} = \sum_j \Gamma_j = \sum_j |\langle f_j | \psi(0) \rangle|^2, \quad (137)$$

---

<sup>8</sup> $\phi_{\varepsilon'}$  is a long-distance QCD effect while  $\phi_{\text{SW}}$  is due to short-distance EW physics.

where the summation index  $j$  runs over all of the accessible final states  $|f_j\rangle$ . Applying this unitarity condition to the Eq. (133) wave function, gives an independent expression for the derivative of  $|\psi(\tau)|^2$  at  $\tau=0$

$$-\left.\frac{d|\psi(\tau)|^2}{d\tau}\right|_{\tau=0} = \sum_j |\alpha_1|^2 |\langle f_j | K_S^0 |^2 + |\alpha_2|^2 |\langle f_j | K_L^0 |^2 + 2\text{Re}(\alpha_1^* \alpha_2 \langle f_j | K_S^{0*} \langle f_j | K_L^0). \quad (138)$$

Equations (135) and (138) have to apply for any values of  $\alpha_1$  and  $\alpha_2$  (subject to  $|\alpha_1|^2 + |\alpha_2|^2 = 1$ ), therefore the terms multiplying  $\alpha_1^* \alpha_2$  in each expression have to be equal

$$(\Gamma_S + \Gamma_L + 2i\Delta M) \langle K_S^0 | K_L^0 \rangle = 2 \sum_j \langle f_j | K_S^{0*} \langle f_j | K_L^0, \quad (139)$$

that, together with Eq. (124), becomes

$$\frac{1}{2} \langle K_S^0 | K_L^0 \rangle = \frac{\text{Re}(\varepsilon)}{1 + |\varepsilon|^2} - i\text{Im}(\delta) = \frac{\sum_j \langle f_j | K_S^{0*} \langle f_j | K_L^0}{\Gamma_S + \Gamma_L + 2i\Delta M}. \quad (140)$$

This is known as the *Bell-Steinberger relation*. Here the second-order term in  $|\varepsilon|$  is retained in order to emphasize that, with it, this equation is exact. A non-zero value of  $\text{Im}(\delta)$  could only occur if *CPT* is violated, or if unitarity is invalid, or if the  $M_{ij}$  and/or  $\Gamma_{ij}$  elements of the Hamiltonian were time-dependent. Because of the small number of  $K_S^0$  decay modes, the sum on the right-hand side of this equation only contains a few terms and is manageable. In contrast, the neutral *B*-mesons have hundreds of established decay modes and probably a similar number of modes that have yet to be detected; any attempt to apply a Bell-Steinberger-like unitarity constraint would be a hopeless task.

A Bell-Steinberger-relation-based evaluation of  $\text{Im}(\delta)$  and  $\text{Re}(\varepsilon)$  by Giancarlo D'Ambrosio and Gino Isidori in collaboration with the KLOE team, that used all the latest relevant measurements, was originally presented in 2006 [275] and recently updated in the PDG2020 review [276]. Their tabulation of relevant measurements that were available in 2022 is:

Channel	$\langle f_j \rangle K_S^{0*} \langle f_j \rangle K_L^0 (10^{-5} \Gamma_S)$
$\pi^+ \pi^- (\gamma)$	$112.1 \pm 1.0 + i(106.1 \pm 1.0)$
$\pi^0 \pi^0$	$49.3 \pm 0.5 + i(47.1 \pm 0.5)$
$\pi^+ \pi^- \gamma_{E1}$	$< 0.01$
$\pi^+ \pi^- \pi^0$	$0.0 \pm 0.2 + i(0.0 \pm 0.2)$
$\pi^0 \pi^0 \pi^0$	$< 0.15$
$\pi^\pm \ell^\mp \nu$	$-0.1 \pm 0.2 + i(-0.1 \pm 0.5),$

where: the  $\pi\pi(\gamma)$  values come from the PDG20 averages of many  $\eta_{+-}$  and  $\eta_{00}$  measurements; the  $\pi^+\pi^-\gamma_{E1}$  limit comes from theory [277, 278]; the  $\pi\pi\pi$  results are based on thirty-year-old  $\mathcal{B}(K_S^0 \rightarrow \pi^+\pi^-\pi^0)$  measurements [279, 280] and a 2013 KLOE upper bound on  $\mathcal{B}(K_S^0 \rightarrow \pi^0\pi^0\pi^0)$  [281]; and the  $\pi^\pm\ell^\mp\nu_\ell$  values come from twenty-five-year-old measurements of SL charge asymmetries for tagged  $K^0(\tau)$  and  $\bar{K}^0(\tau)$  decays from CPLEAR [12] and  $K_L^0$  decays from KTeV [282] plus a 2018 measurement for tagged  $K_S^0$  decays from KLOE-2 [283].

The bottom line of this analysis is

$$Im(\delta) = (-0.3 \pm 1.4) \times 10^{-5} \Rightarrow |M_{\bar{K}^0} - M_{K^0}| < 4 \times 10^{-16} \text{ MeV}, \quad (141)$$

and the  $Im(\delta)$  vs.  $Re(\varepsilon)$  and  $\Gamma_{\bar{K}^0} - \Gamma_{K^0}$  vs.  $M_{\bar{K}^0} - M_{K^0}$  allowed regions are shown in Figs. 20(a) & (b), respectively. The limit on  $|M_{\bar{K}^0} - M_{K^0}|$  is nearly the same as the Eq. (129) bound, that comes from simply comparing the PDG20 world average values for  $\phi_{+-}$  and  $\phi_{SW}$ . This is not surprising, since in both analyses the  $\pi\pi$

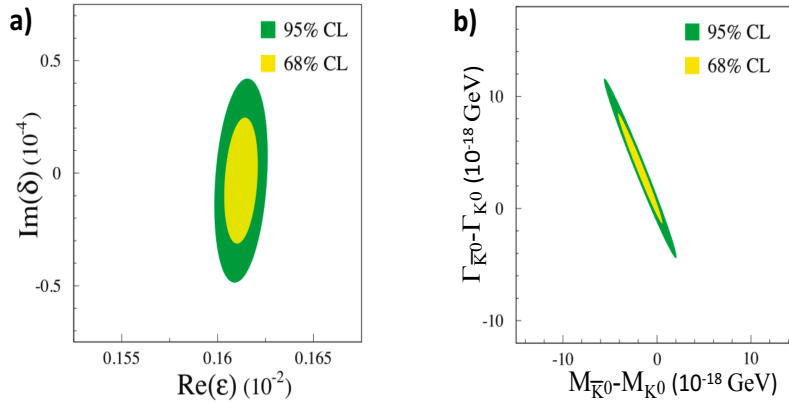


Figure 20: **a)** The 68% and 95% confidence level allowed region for  $Im\ m\delta$  and  $Re\ e\varepsilon$  from a Bell-Steinberger analysis. **b)** The corresponding allowed regions in  $\Delta\Gamma = \Gamma_{\bar{K}^0} - \Gamma_{K^0}$  and  $\Delta M = M_{\bar{K}^0} - M_{K^0}$ . From Ref. [269].

channels dominate, and the sensitivities are limited by the same  $\eta_{+-}$  and  $\eta_{00}$  measurement errors. Moreover, contributions from the uncertainties associated with the other modes are smaller than those from the  $\pi\pi$  modes. However, these contributions are not so small and future progress in Bell-Steinberger-relation analyses will require that improvements in the  $\eta_{+-}$  and  $\eta_{00}$  phase measurements are accompanied by similar improvements in the precision of the other terms.

The  $\pi^+\pi^-\pi^0$  entry in the above table comes from statistics limited time-dependent Dalitz-plot analyses of  $K_S^0$ - $K_L^0$  interference effects in strangeness-tagged  $K^0(\tau)$  and  $\bar{K}^0(\tau)$  decays to  $\pi^+\pi^-\pi^0$ , and will be improved with the higher statistics data samples that will be available at STCF. On the other hand, the  $\pi^0\pi^0\pi^0$  entry is based on a  $\mathcal{B}(K_S^0 \rightarrow 3\pi^0) < 2.6 \times 10^{-8}$  upper limit from KLOE that used tagged- $K_S^0$  mesons produced in a sample of 1.7 billion  $e^+e^- \rightarrow \phi \rightarrow K_S^0 K_L^0$  events [281]. Likewise, the precision of the  $\pi\ell\nu_\ell$  entry is limited by the measured value of the lepton charge asymmetry in a  $\sim 70$  K-event sample of reconstructed  $\pi e \nu_e$  decays of tagged  $K_S^0$  mesons in the same KLOE event sample [283]. Further improvements of these measurements would need substantially larger numbers of tagged  $K_S^0$  decays and will not be easy. The possibilities for improving these values using  $J/\psi \rightarrow \phi K_S^0 K_S^0$  and  $\omega K_S^0 K_S^0$  decays as sources of tagged  $K_S^0$  decays<sup>9</sup> at STCF are currently being investigated.

### 5.6. Prospects of kaon CPT study at STCF

Based on the data sample with  $10^{12}$  collected by STCF per year, the expected yields of  $J/\psi \rightarrow K^-\pi^+K^0(K^0 \rightarrow \pi^+\pi^-) + c.c.$  will be more than  $3.9 \times 10^9$  events. Based on this data sample, a significant improvement in the precision of CPT measurements in the kaon system can be achieved. The following sections will introduce the event reconstruction and the expected precision of measured parameters.

A Monte Carlo simulation sample with  $3.9 \times 10^9$   $J/\psi \rightarrow K^-\pi^+K^0(K^0 \rightarrow \pi^+\pi^-) + c.c.$  total events is generated by the phase space model. The time-dependent decay rates of  $K^0(\bar{K}^0) \rightarrow \pi^+\pi^-$  are shown at Eq. (131), and the input parameters are fixed to the PDG average values [15].

For the decay channels  $J/\psi \rightarrow K^-\pi^+K^0$  and  $J/\psi \rightarrow K^+\pi^-\bar{K}^0$ , the flavor of the neutral  $K$  meson produced at time  $t = 0$  is tagged by the charge sign of the charged kaon. Subsequently, the neutral  $K$  meson is reconstructed to the final state with CP of +1 through the decay channel  $K^0/\bar{K}^0 \rightarrow \pi^+\pi^-$ .

---

<sup>9</sup> $J/\psi \rightarrow \phi K_S^0 K_L^0$  and  $\omega K_S^0 K_L^0$  decays are forbidden by CP invariance.

For charged tracks not originating from the decay of neutral  $K$  mesons, the distance of closest approach to the collision point in the direction of the beam should be within  $\pm 10$  cm, and the projection onto the plane perpendicular to the beam direction should be less than 1 cm. A particle identification algorithm is performed on the selected charged tracks with information from sub-detectors, to get the probability ( $Prob$ ) that a charged particle is a certain type of particle. The kaon candidate is required that  $Prob(K) > Prob(p), Prob(K) > Prob(\pi)$  and for the pion candidate:  $Prob(\pi) > Prob(K)$ .

A vertex-constrained fit is carried out on the  $\pi^+\pi^-$  to obtain the decay vertex of  $K^0$ . The two charged pions are required to originate from a common vertex, and the corresponding fitting  $\chi^2$  should be less than 100. Subsequently, the production vertex of  $K^0$  is obtained by performing another vertex-constrained fit on  $K^-\pi^+$ . The invariant mass of the  $\pi^+\pi^-$  after vertex fitting is required to be within [482, 514] MeV. In order to reduce the background from random combinations of charged tracks in  $K^0$  and from  $\pi^+\pi^-$  combinations not originating from  $K^0$  decays, the secondary vertex fitting algorithm package is utilized to obtain the decay distance  $L_{K^0}$  and its corresponding error  $\sigma(L_{K^0})$  for  $K^0$ . The ratio of the decay distance to its error is required to be  $L_{K^0}/\sigma(L_{K^0}) > 2$ .

In each event, the sum of the charges of the charged tracks should be zero. A four-momentum constrained kinematic fit is applied to the  $\pi^+\pi^-K^-\pi^+$  hypothesis, and events with a minimum  $\chi^2 < 60$  are selected as best  $J/\psi$  candidates.

After all the event selections described above, the expected background ratio is less than 0.5%, resulting in a high-purity data sample.

Decay curves for  $K^0(\tau) \rightarrow \pi^+\pi^-$  and  $\bar{K}^0(\tau) \rightarrow \pi^+\pi^-$  for simulated BESIII events with 100 billion  $J/\psi$  that were generated with PDG values of the  $\eta_{+-}$  magnitude and phase are shown in Fig. 21(a), where there are strong interference effects between the steeply falling  $K_S^0 \rightarrow \pi^+\pi^-$  and nearly flat  $K_L^0 \rightarrow \pi^+\pi^-$  amplitudes that have opposite signs for  $K^0(\tau)$ - and  $\bar{K}^0(\tau)$ -tagged decays. The difference between the interference terms is displayed in a plot of the reduced

asymmetry [11]  $\mathcal{A}'_{\pi\pi}$ , where<sup>10</sup>

$$\begin{aligned}\mathcal{A}'_{\pi\pi} &\equiv \frac{\bar{N}(\bar{K}^0(\tau)) - N(K^0(\tau))}{\bar{N}(\bar{K}^0(\tau)) + N(K^0(\tau))} e^{-\frac{1}{2}\Delta\Gamma\tau} \\ &= 2\text{Re}(\varepsilon_L) e^{-\frac{1}{2}\Delta\Gamma\tau} - 2 \frac{|\eta_{+-}| \cos(\Delta M\tau - \phi_{+-})}{1 + |\eta_{+-}|^2 e^{\Delta\Gamma\tau}},\end{aligned}\quad (142)$$

and is shown for the simulated data in Fig. 21 (b), where  $\phi_{+-}$  shows up as a phase shift in the interference-generated cosine-like oscillation.

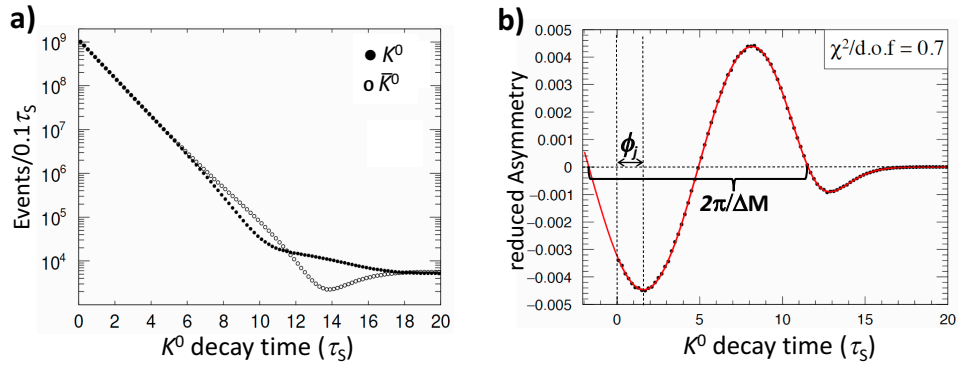


Figure 21: **a)** The solid circles show the proper time distribution for simulated strangeness-tagged  $K^0(\tau) \rightarrow \pi^+\pi^-$  decays (the open circles are  $\bar{K}^0(\tau) \rightarrow \pi^+\pi^-$  decays). **b)** The reduced asymmetry,  $\mathcal{A}'_{\pi^+\pi^-}$ , for the events shown in panel **a)**.

The simulated data shown in Figs. 21 (a) and (b) correspond to 3.8 billion tagged  $K \rightarrow \pi^+\pi^-$  decays that are almost equally split between  $J/\psi \rightarrow K^-\pi^+K^0$  and  $J/\psi \rightarrow K^+\pi^-\bar{K}^0$ , which were generated with  $\Delta\phi^{CPT}=0$  and  $\phi_{\text{SW}}=43.4^\circ$ . This corresponds to what one would expect for a total of  $10^{12}$   $J/\psi$  decays in a detector that covered a  $|\cos\theta| \leq 0.85$  solid angle and was otherwise almost perfect. The red curve in the figure is the result of a fit to the data that determined

$$\phi_{\text{SW}} + \Delta\phi^{CPT} = (43.51 \pm 0.05)^\circ, \quad (143)$$

where the errors are statistical only. According to Eq. (129), this  $\mathcal{O}(0.1^\circ)$  precision corresponds to  $|M_{\bar{K}^0} - M_{K^0}| \approx 4 \times 10^{-17}$  MeV. This is an order of magnitude improvement over the existing limit, which is based on the result in 1999

<sup>10</sup>In the unmodified asymmetry,  $\mathcal{A}_{\pi\pi} = [\bar{N}(\bar{K}^0(\tau)) - N(K^0(\tau))] / [\bar{N}(\bar{K}^0(\tau)) + N(K^0(\tau))]$ , the  $\cos(\Delta M\tau - \phi_j)$  oscillation term is multiplied by a factor  $e^{\frac{1}{2}\Delta\Gamma\tau}$  that, when displayed, emphasizes low-statistics, long-decay-time events that, in fact, have little influence on the  $\phi_j$  determination.

from the CPLEAR  $\bar{p}_{\text{stop}}p$  experiment at CERN [11] that used a sample of  $\sim 70$  million tagged  $K^0(\tau) \rightarrow \pi^+\pi^-$  and  $\bar{K}^0(\tau) \rightarrow \pi^+\pi^-$  events, and the result in 1995 from a Fermilab experiment E773 that used  $\sim 2$  million  $K \rightarrow \pi^+\pi^-$  and  $\sim 0.5$  million  $K \rightarrow \pi^0\pi^0$  decays produced downstream of a regenerator located in a high-energy  $K_L^0$  beam [284]:

$$\begin{aligned} \text{CPLEAR : } \phi_{\text{SW}} + \Delta\phi^{CPT} &= 42.91^\circ \pm 0.53^\circ(\text{stat}) \pm 0.28^\circ(\text{syst}), (144) \\ \text{E773 : } \phi_{\text{SW}} + \Delta\phi^{CPT} &= 42.94^\circ \pm 0.58^\circ(\text{stat}) \pm 0.49^\circ(\text{syst}). \end{aligned}$$

The CPLEAR systematic error includes a  $0.19^\circ$  component associated with the effects of regeneration in the high-pressure hydrogen gas in the stopping target and the walls of its containment vessel. In the E773 measurement, the phase offset that is introduced by the regenerator is unavoidable and large,  $\phi_{\text{regen}} \sim -130^\circ$ , and is evaluated from a dispersion relation with an assigned error of  $0.35^\circ$  [285]. In the STCF detector, the production and a significant fraction of the  $K \rightarrow \pi^+\pi^-$  decays will occur in a high vacuum, and the material traversed by rest of the decaying neutral kaons is very small. This will substantially reduce the effects of regeneration and its associated systematic error to be well below their level in these previous experiments.

The systematic uncertainty of this measurement includes the following sources: the decay time resolution of  $K^0$ , background contributions, regeneration effect of  $K^0$ , and uncertainty associated with parameters fixed in the fit. The decay time resolution depends on the  $K^-\pi^+$  vertex resolution, and the  $\pi^+\pi^-$  vertex resolution. The high performance of track detector of STCF will reconstruct the vertex of  $K^0$  efficiently and accurately. And its excellent position resolution and high resolution in the energy loss  $dE/dx$  will help to suppress the background of miscombinations and particle misidentification. Due to the high purity of the sample at 99.5%, the impact of the background can be neglected, and no decay-rate asymmetry is observed in the background. At the STCF, the flight of  $K^0$  will occur in the low-material detectors, therefore the effects of regeneration will be much lower compared to other experiments, resulting in a controllable systematic uncertainty.

### 5.7. Further comments

Even though the *CPT* theorem is a fundamental element of the SM, experimental constraints on its validity have not been significantly improved during the last three decades. This is not because these are uninteresting and not important but, instead, is a consequence of the fact that none of the world's active particle physics facilities have the capability of producing enough strangeness-tagged

neutral kaons to match, much less improve on, the CPLEAR and E773 results. Although currently operating experiments with huge numbers of charmed and beauty particles can address many interesting subjects, they will never be able to test the *CPT* theorem with the exquisite sensitivity that is uniquely provided by the neutral *K*-meson system. As noted in this report, the STCF project will provide the first practical opportunity to make an order of magnitude sensitivity improvement over earlier experiments. Note that in addition to probing *CPT* invariance, the CPLEAR experiment also produced the world's most sensitive search for violations of the  $\Delta S = \Delta Q$  rule, which can only occur in the SM as a second-order weak interaction. The CPLEAR result only limits  $\Delta S = -\Delta Q$  amplitudes to be less than a percent of the allowed  $\Delta S = \Delta Q$  ones. SCTF will test rule with an order of magnitude higher sensitivity.

The special requirements such measurements should be carefully considered during the design and implementation of the collider and its associated detector.

## 6. Summary

We have reviewed perspectives of using unprecedented large numbers of entangled light baryon-antibaryon, meson-antimeson, and tauon-antitauon pairs will be produced at the STCF to carry out high precision tests for  $CP$  violation in these systems.

With the implementation of STCF, studies of  $CP$  violation using spin-entangled and polarized baryon-antibaryon pairs, a program that was initiated by the BESIII experiment, will reach levels of precision that are compatible with SM predictions for hyperon non leptonic decays reaching  $\mathcal{O}(10^{-4})$ . Studies of the production process will provide stringent limits for electric dipole form factors that test  $C$  and  $P$  symmetry violation improve previous limit on Lambda EDM by five orders of magnitudes reaching  $\mathcal{O}(10^{-21}) e \text{ cm}$ , and to put on EDM limits on  $\Sigma$ ,  $\Xi$  to the level of  $\mathcal{O}(10^{-20}) e \text{ cm}$ . In principle, similar  $CP$  violation studies are possible for charmed baryons, however, the prospects for the attainable uncertainties will soon be known with the BESIII data after the completion of the BEPCII energy and luminosity upgrade. Although no vector resonances have been found that could enhance the production of charmed baryon-antibaryon pairs today, and the data samples for the charmed baryon measurements are not competitive with that at LHCb, the simplicity and complete kinematic of the production process of the charmed baryons at STCF will drive for several unique and complementary measurements.

The large data samples of  $\tau$  lepton pairs that are produced near threshold at STCF, with low background and well-controlled systematic uncertainties, will provide unique ways to make a number of precision and comprehensive studies of the  $\tau$ -lepton properties. Hadronic  $\tau$  decays offer rich perspective to probe possible  $CP$  violation phenomena, and the relevant form factors and structure functions are important inputs to construct  $CP$  violation observables in the  $\tau$  sector. Improved measurements of various hadronic  $\tau$  decay that can be performed at STCF will provide a solid foundation to search for diverse  $CP$  violation signals in  $\tau$  decays. These include a variety of differential observables, such as the integrated rate asymmetry, triple products and forward-backward asymmetries, that could potentially enhance  $CP$  violation features in multi-meson  $\tau$ -lepton decay channels. Specifically, measurements on the rate and forward-backward asymmetries of  $\tau \rightarrow K_S^0 \pi \nu_\tau$  decay at STCF will clear up the hint of a  $CP$  violation anomaly that has been reported by Babar, and shed light on BSM. Information on the  $\tau$  EDM can be indirectly extracted from processes involving  $\tau$  pair productions at lepton colliders. Together with dedicated studies with carefully optimized

observables, STCF can provide more data on relevant processes and improve significantly the measurements of the  $\tau$  EDM at the level of  $|d_\tau| < 10^{-18} e \text{ cm}$ .

Contrary to  $B$ -meson and kaon systems, non-perturbative long-distance effects have been found to be the prerequisites to explain the observed charm mixing and  $CP$  violation effects. Update to date, only direct  $CP$  violation has been measured in the singly Cabibbo-suppressed decays  $K^+K^-$  and  $\pi^+\pi^-$ . At STCF, despite the fact that the statistics of the charmed-meson samples will be orders of magnitudes lower than that in the LHCb experiment, and time-dependent measurements are not applicable, a unique time-integrated methodology can be adopted to access the charm mixing parameters and indirect  $CP$  violation by exploiting the quantum correlations in neutral  $D\bar{D}$  decays. Sensitivity studies have demonstrated that STCF has the potential to measure charm mixing parameters and the magnitude of  $CP$  violation at  $10^{-4}$  levels of precision. These are complementary to time-dependent measurements at the LHCb and Belle II experiments. Interestingly, the  $CP$ -conserving phase differences in  $D^0$  and  $\bar{D}^0$  decays, which are essential inputs to  $CP$  violation studies both in bottom and charm decays and have been determined by BESIII and CLEO experiments with great success, can be obtained with the correlated  $D\bar{D}$  decays in STCF with ultimate uncertainties.

During a year of operation at the peak of the  $J/\psi$  resonance, it is estimated that STCF will record 3.4 billion  $\pi^+\pi^-$  decays of neutral  $K$ -produced via  $J/\psi \rightarrow K^\mp\pi^\pm K^0$  processes that have well-defined strangeness at the time of production. These events will support studies of  $CP$  violation and tests of the  $CPT$  theorem with unprecedented precision. For comparison, the most stringent and theoretically robust current limit on the validity of the  $CPT$  theorem, a foundational principle of the SM, is the  $|M_{\bar{K}^0} - M_{K^0}| < 5 \times 10^{-16} \text{ MeV}$  result, that is based on a Bell-Steinberger analysis of 25 year-old CPLEAR, KLOE and KTeV measurements with  $\sim 70$  million event data samples [276]. The 3.4 billion STCF  $J/\psi$  event sample would advance the level of sensitivity on this most fundamental of all fundamental SM quantities by about an order of magnitude.

## Acknowledgements

We thank the Hefei Comprehensive National Science Center for their strong support on the STCF key technology research project. This work is supported in part by National Key R&D Program of China under Contracts No. 2022YFA1602200; International partnership program of the Chinese Academy of Sciences Grant No. 211134KYSB20200057; National Natural Science Foundation of China (NSFC) under Contracts Nos. 12375088, 12335003, 12305107, 12275023, 12475078, 12122509, 12221005, 12375086; National Research Foundation of Korea under Contract No. NRF-2022R1A2C1092335; Chinese Academy of Sciences President's International Fellowship Initiative; Polish National Science Centre through the grants 2019/35/O/ST2/02907 and 2024/53/B/ST2/00975; Swedish Research Council under grant No. 2021-04567. P. R. acknowledges Conahcyt funding (Mexico), through project CBF2023-2024-3226 and the support of MCIN/AEI/10.13039/501100011033, grant PID2020-114473GB-I00 and PID2023-146220NB-I00, and by Generalitat Valenciana, grant PROMETEO/2021 /071 (Spain, during his sabbatical).

## References

- [1] M. Achasov, et al., STCF conceptual design report (Volume 1): Physics & detector, *Front. Phys. (Beijing)* 19 (1) (2024) 14701. [arXiv:2303.15790](#), [doi:10.1007/s11467-023-1333-z](#).
- [2] S. Weinberg, Essay: Half a Century of the Standard Model, *Phys. Rev. Lett.* 121 (22) (2018) 220001. [doi:10.1103/PhysRevLett.121.220001](#).
- [3] N. Cabibbo, Unitary Symmetry and Leptonic Decays, *Phys. Rev. Lett.* 10 (1963) 531–533. [doi:10.1103/PhysRevLett.10.531](#).
- [4] M. Kobayashi, T. Maskawa, CP Violation in the Renormalizable Theory of Weak Interaction, *Prog. Theor. Phys.* 49 (1973) 652–657. [doi:10.1143/PTP.49.652](#).
- [5] L. Wolfenstein, Parametrization of the Kobayashi-Maskawa Matrix, *Phys. Rev. Lett.* 51 (1983) 1945. [doi:10.1103/PhysRevLett.51.1945](#).
- [6] S. Navas, et al., Review of particle physics, *Phys. Rev. D* 110 (3) (2024) 030001. [doi:10.1103/PhysRevD.110.030001](#).

- [7] J. Tandean, G. Valencia, CP violation in hyperon nonleptonic decays within the standard model, *Phys. Rev. D* 67 (2003) 056001. [doi:10.1103/PhysRevD.67.056001](https://doi.org/10.1103/PhysRevD.67.056001).
- [8] M. Ablikim, et al., Probing CP symmetry and weak phases with entangled double-strange baryons, *Nature* 606 (7912) (2022) 64–69. [arXiv:2105.11155](https://arxiv.org/abs/2105.11155), [doi:10.1038/s41586-022-04624-1](https://doi.org/10.1038/s41586-022-04624-1).
- [9] M. Ablikim, et al., Precise Measurements of Decay Parameters and  $CP$  Asymmetry with Entangled  $\Lambda - \bar{\Lambda}$  Pairs Pairs, *Phys. Rev. Lett.* 129 (13) (2022) 131801. [doi:10.1103/PhysRevLett.129.131801](https://doi.org/10.1103/PhysRevLett.129.131801).
- [10] M. Ablikim, et al., Tests of CP symmetry in entangled  $\Xi^0\text{-}\Xi^0$  pairs, *Phys. Rev. D* 108 (3) (2023) L031106. [arXiv:2305.09218](https://arxiv.org/abs/2305.09218), [doi:10.1103/PhysRevD.108.L031106](https://doi.org/10.1103/PhysRevD.108.L031106).
- [11] A. Apostolakis, et al., A Determination of the CP violation parameter  $\eta_{+-}$  from the decay of strangeness tagged neutral kaons, *Phys. Lett. B* 458 (1999) 545–552. [doi:10.1016/S0370-2693\(99\)00596-1](https://doi.org/10.1016/S0370-2693(99)00596-1).
- [12] A. Angelopoulos, et al., A Determination of the CPT violation parameter  $\text{Re}(\delta)$  from the semileptonic decay of strangeness tagged neutral kaons, *Phys. Lett. B* 444 (1998) 52–60. [doi:10.1016/S0370-2693\(98\)01357-4](https://doi.org/10.1016/S0370-2693(98)01357-4).
- [13] I. I. Bigi, A. I. Sanda, *CP violation*, Vol. 9, Cambridge University Press, 2009. [doi:10.1017/CBO9780511581014](https://doi.org/10.1017/CBO9780511581014).
- [14] M. S. Sozzi, On the direct CP violation parameter  $\epsilon'$ , *Eur. Phys. J. C* 36 (2004) 37–42. [doi:10.1140/epjc/s2004-01868-3](https://doi.org/10.1140/epjc/s2004-01868-3).
- [15] R. L. Workman, et al., Review of Particle Physics, *PTEP* 2022 (2022) 083C01. [doi:10.1093/ptep/ptac097](https://doi.org/10.1093/ptep/ptac097).
- [16] H. Gisbert, A. Pich, Direct CP violation in  $K^0 \rightarrow \pi\pi$ : Standard Model Status, *Rept. Prog. Phys.* 81 (7) (2018) 076201. [doi:10.1088/1361-6633/aac18e](https://doi.org/10.1088/1361-6633/aac18e).
- [17] Z. Bai, et al., Standard Model Prediction for Direct CP Violation in  $K \rightarrow \pi\pi$  Decay, *Phys. Rev. Lett.* 115 (21) (2015) 212001. [doi:10.1103/PhysRevLett.115.212001](https://doi.org/10.1103/PhysRevLett.115.212001).

- [18] R. Abbott, et al., Direct CP violation and the  $\Delta I = 1/2$  rule in  $K \rightarrow \pi\pi$  decay from the standard model, Phys. Rev. D 102 (5) (2020) 054509. doi:[10.1103/PhysRevD.102.054509](https://doi.org/10.1103/PhysRevD.102.054509).
- [19] N. Salone, P. Adlarson, V. Batozskaya, A. Kupsc, S. Leupold, J. Tandean, Study of CP violation in hyperon decays at super-charm-tau factories with a polarized electron beam, Phys. Rev. D 105 (11) (2022) 116022. doi:[10.1103/PhysRevD.105.116022](https://doi.org/10.1103/PhysRevD.105.116022).
- [20] T. D. Lee, C.-N. Yang, General Partial Wave Analysis of the Decay of a Hyperon of Spin 1/2, Phys. Rev. 108 (1957) 1645–1647. doi:[10.1103/PhysRev.108.1645](https://doi.org/10.1103/PhysRev.108.1645).
- [21] E. Perotti, G. Fäldt, A. Kupsc, S. Leupold, J. J. Song, Polarization observables in  $e^+e^-$  annihilation to a baryon-antibaryon pair, Phys. Rev. D 99 (5) (2019) 056008. doi:[10.1103/PhysRevD.99.056008](https://doi.org/10.1103/PhysRevD.99.056008).
- [22] M. Tanabashi, et al., Review of Particle Physics, Phys. Rev. D 98 (3) (2018) 030001. doi:[10.1103/PhysRevD.98.030001](https://doi.org/10.1103/PhysRevD.98.030001).
- [23] M. Ablikim, et al., Investigation of the  $\Delta I=1/2$  Rule and Test of CP Symmetry through the Measurement of Decay Asymmetry Parameters in  $\Xi$ -Decays, Phys. Rev. Lett. 132 (10) (2024) 101801. arXiv:[2309.14667](https://arxiv.org/abs/2309.14667), doi:[10.1103/PhysRevLett.132.101801](https://doi.org/10.1103/PhysRevLett.132.101801).
- [24] M. Ablikim, et al., Polarization and Entanglement in Baryon-Antibaryon Pair Production in Electron-Positron Annihilation, Nature Phys. 15 (2019) 631–634. doi:[10.1038/s41567-019-0494-8](https://doi.org/10.1038/s41567-019-0494-8).
- [25] D. G. Ireland, M. Döring, D. I. Glazier, J. Haidenbauer, M. Mai, R. Murray-Smith, D. Rönchen, Kaon Photoproduction and the  $\Lambda$  Decay Parameter  $\alpha_-$ , Phys. Rev. Lett. 123 (18) (2019) 182301. arXiv:[1904.07616](https://arxiv.org/abs/1904.07616), doi:[10.1103/PhysRevLett.123.182301](https://doi.org/10.1103/PhysRevLett.123.182301).
- [26] M. Ablikim, et al.,  $\Sigma^+$  and  $\bar{\Sigma}^-$  polarization in the  $J/\psi$  and  $\psi(3686)$  decays, Phys. Rev. Lett. 125 (5) (2020) 052004. arXiv:[2004.07701](https://arxiv.org/abs/2004.07701), doi:[10.1103/PhysRevLett.125.052004](https://doi.org/10.1103/PhysRevLett.125.052004).
- [27] M. Ablikim, et al., Test of CP Symmetry in Hyperon to Neutron Decays, Phys. Rev. Lett. 131 (19) (2023) 191802. arXiv:[2304.14655](https://arxiv.org/abs/2304.14655), doi:[10.1103/PhysRevLett.131.191802](https://doi.org/10.1103/PhysRevLett.131.191802).

- [28] M. Huang, et al., New measurement of  $\Xi^- \rightarrow \Lambda\pi^-$  decay parameters, Phys. Rev. Lett. 93 (2004) 011802. [doi:10.1103/PhysRevLett.93.011802](https://doi.org/10.1103/PhysRevLett.93.011802).
- [29] M. Ablikim, et al., Model-Independent Determination of the Spin of the  $\Omega^-$  and Its Polarization Alignment in  $\psi(3686) \rightarrow \Omega^-\bar{\Omega}^+$ , Phys. Rev. Lett. 126 (9) (2021) 092002. [arXiv:2007.03679](https://arxiv.org/abs/2007.03679), [doi:10.1103/PhysRevLett.126.092002](https://doi.org/10.1103/PhysRevLett.126.092002).
- [30] O. E. Overseth, S. Pakvasa, Final-state interactions in nonleptonic hyperon decay, Phys. Rev. 184 (1969) 1663–1667. [doi:10.1103/PhysRev.184.1663](https://doi.org/10.1103/PhysRev.184.1663).
- [31] T. Holmstrom, et al., Search for CP violation in charged-Xi and Lambda hyperon decays, Phys. Rev. Lett. 93 (2004) 262001. [doi:10.1103/PhysRevLett.93.262001](https://doi.org/10.1103/PhysRevLett.93.262001).
- [32] J. F. Donoghue, S. Pakvasa, Signals of CP Nonconservation in Hyperon Decay, Phys. Rev. Lett. 55 (1985) 162. [doi:10.1103/PhysRevLett.55.162](https://doi.org/10.1103/PhysRevLett.55.162).
- [33] J. F. Donoghue, X.-G. He, S. Pakvasa, Hyperon Decays and CP Nonconservation, Phys. Rev. D 34 (1986) 833. [doi:10.1103/PhysRevD.34.833](https://doi.org/10.1103/PhysRevD.34.833).
- [34] X.-G. He, H. Murayama, S. Pakvasa, G. Valencia, CP violation in hyperon decays from supersymmetry, Phys. Rev. D 61 (2000) 071701. [doi:10.1103/PhysRevD.61.071701](https://doi.org/10.1103/PhysRevD.61.071701).
- [35] S. R. Beane, P. F. Bedaque, A. Parreno, M. J. Savage, Exploring hyperons and hypernuclei with lattice QCD, Nucl. Phys. A 747 (2005) 55–74. [doi:10.1016/j.nuclphysa.2004.09.081](https://doi.org/10.1016/j.nuclphysa.2004.09.081).
- [36] J. G. Korner, M. Kuroda,  $e^+e^-$  Annihilation Into Baryon-anti-Baryon Pairs, Phys. Rev. D 16 (1977) 2165. [doi:10.1103/PhysRevD.16.2165](https://doi.org/10.1103/PhysRevD.16.2165).
- [37] G. Fäldt, A. Kupsc, Hadronic structure functions in the  $e^+e^- \rightarrow \bar{\Lambda}\Lambda$  reaction, Phys. Lett. B772 (2017) 16–20. [doi:10.1016/j.physletb.2017.06.011](https://doi.org/10.1016/j.physletb.2017.06.011).

- [38] M. Ablikim, et al., Study of  $J/\psi$  and  $\psi(3686)$  decay to  $\Lambda\bar{\Lambda}$  and  $\Sigma^0\bar{\Sigma}^0$  final states, Phys. Rev. D 95 (5) (2017) 052003. [arXiv:1701.07191](#), [doi:10.1103/PhysRevD.95.052003](#).
- [39] M. Ablikim, et al., First measurements of J/Psi decays into Sigma+ anti-Sigma- and Xi0 anti-Xi0, Phys. Rev. D 78 (2008) 092005. [arXiv:0810.1896](#), [doi:10.1103/PhysRevD.78.092005](#).
- [40] M. Ablikim, et al., Strong and Weak CP Tests in Sequential Decays of Polarized  $\Sigma^0$  Hyperons, Phys. Rev. Lett. 133 (10) (2024) 101902. [arXiv:2406.06118](#), [doi:10.1103/PhysRevLett.133.101902](#).
- [41] M. Ablikim, et al., Study of  $J/\psi$  and  $\psi(3686) \rightarrow \Sigma(1385)^0\bar{\Sigma}(1385)^0$  and  $\Xi^0\bar{\Xi}^0$ , Phys. Lett. B 770 (2017) 217–225. [arXiv:1612.08664](#), [doi:10.1016/j.physletb.2017.04.048](#).
- [42] P. A. Zyla, et al., Review of Particle Physics, PTEP 2020 (8) (2020) 083C01. [doi:10.1093/ptep/ptaa104](#).
- [43] M. Ablikim, et al., Precision Measurement of the Decay  $\Sigma^+ \rightarrow p\gamma$  in the Process  $J/\psi \rightarrow \Sigma^+\Sigma^-$ , Phys. Rev. Lett. 130 (21) (2023) 211901. [arXiv:2302.13568](#), [doi:10.1103/PhysRevLett.130.211901](#).
- [44] M. Ablikim, et al., Measurement of the Decay  $\Xi^0 \rightarrow \Lambda\gamma$  with Entangled  $\Xi^0\bar{\Xi}^0$  Pairs (8 2024). [arXiv:2408.16654](#).
- [45] V. Batozskaya, A. Kupsc, N. Salone, J. Wiechnik, Semileptonic decays of spin-entangled baryon-antibaryon pairs, Phys. Rev. D 108 (1) (2023) 016011. [arXiv:2302.07665](#), [doi:10.1103/PhysRevD.108.016011](#).
- [46] M. Ablikim, et al., Measurement of the Absolute Branching Fraction and Decay Asymmetry of  $\Lambda \rightarrow n\gamma$ , Phys. Rev. Lett. 129 (21) (2022) 212002. [arXiv:2206.10791](#), [doi:10.1103/PhysRevLett.129.212002](#).
- [47] G. R. Farrar, Weak radiative decay of the sigma+ and lambda hyperons, Phys. Rev. D 4 (1971) 212–220. [doi:10.1103/PhysRevD.4.212](#).
- [48] J. R. Batley, et al., First observation and branching fraction and decay parameter measurements of the weak radiative decay  $\Xi^0 \rightarrow \Lambda e^+ e^-$

- e-, Phys. Lett. B 650 (2007) 1–8. [arXiv:hep-ex/0703023](#), doi:  
[10.1016/j.physletb.2007.04.066](#).
- [49] H. Park, et al., Evidence for the decay  $\Sigma^+ \rightarrow p \mu^+ \mu^-$ , Phys. Rev. Lett. 94 (2005) 021801. [arXiv:hep-ex/0501014](#), doi:[10.1103/PhysRevLett.94.021801](#).
- [50] R. Aaij, et al., Evidence for the rare decay  $\Sigma^+ \rightarrow p \mu^+ \mu^-$ , Phys. Rev. Lett. 120 (22) (2018) 221803. [arXiv:1712.08606](#), doi:[10.1103/PhysRevLett.120.221803](#).
- [51] X.-G. He, J. Tandean, G. Valencia, The Decay  $\Sigma^+ \rightarrow p l^+ l^-$  within the standard model, Phys. Rev. D 72 (2005) 074003. [arXiv:hep-ph/0506067](#), doi:[10.1103/PhysRevD.72.074003](#).
- [52] X.-G. He, J. Tandean, G. Valencia, Decay rate and asymmetries of  $\Sigma^+ \rightarrow p \mu^+ \mu^-$ , JHEP 10 (2018) 040. [arXiv:1806.08350](#), doi:[10.1007/JHEP10\(2018\)040](#).
- [53] F. Erben, V. Gülpers, M. T. Hansen, R. Hodgson, A. Portelli, Prospects for a lattice calculation of the rare decay  $\Sigma^+ \rightarrow p \ell^+ \ell^-$ , JHEP 04 (2023) 108. [arXiv:2209.15460](#), doi:[10.1007/JHEP04\(2023\)108](#).
- [54] M. Pospelov, A. Ritz, Electric dipole moments as probes of new physics, Annals Phys. 318 (2005) 119–169. [arXiv:hep-ph/0504231](#), doi:[10.1016/j.aop.2005.04.002](#).
- [55] S. S. Nair, E. Perotti, S. Leupold, Constraining P and CP violation in the main decay of the neutral Sigma hyperon, Phys. Lett. B 788 (2019) 535–541. [arXiv:1802.02801](#), doi:[10.1016/j.physletb.2018.09.065](#).
- [56] A. Kadeer, J. G. Korner, U. Moosbrugger, Helicity analysis of semileptonic hyperon decays including lepton mass effects, Eur. Phys. J. C 59 (2009) 27–47. [arXiv:hep-ph/0511019](#), doi:[10.1140/epjc/s10052-008-0801-5](#).
- [57] N. Cabibbo, E. C. Swallow, R. Winston, Semileptonic hyperon decays, Ann. Rev. Nucl. Part. Sci. 53 (2003) 39–75. [arXiv:hep-ph/0307298](#), doi:[10.1146/annurev.nucl.53.013103.155258](#).

- [58] S. Sasaki, Hyperon vector form factor from 2+1 flavor lattice QCD, Phys. Rev. D 86 (2012) 114502. [arXiv:1209.6115](#), [doi:10.1103/PhysRevD.86.114502](#).
- [59] A. N. Cooke, Lattice QCD study of octet hyperon semi-leptonic decays, Ph.D. thesis, Edinburgh U. (2014).
- [60] L. Pondrom, R. Handler, M. Sheaff, P. T. Cox, J. Dworkin, O. E. Overseth, T. Devlin, L. Schachinger, K. J. Heller, New Limit on the Electric Dipole Moment of the  $\Lambda$  Hyperon, Phys. Rev. D 23 (1981) 814–816. [doi:10.1103/PhysRevD.23.814](#).
- [61] F.-K. Guo, U.-G. Meissner, Baryon electric dipole moments from strong CP violation, JHEP 12 (2012) 097. [arXiv:1210.5887](#), [doi:10.1007/JHEP12\(2012\)097](#).
- [62] D. Atwood, A. Soni, Chiral perturbation theory constraint on the electric dipole moment of the Lambda hyperon, Phys. Lett. B 291 (1992) 293–296. [doi:10.1016/0370-2693\(92\)91048-E](#).
- [63] A. Pich, E. de Rafael, Strong CP violation in an effective chiral Lagrangian approach, Nucl. Phys. B 367 (1991) 313–333. [doi:10.1016/0550-3213\(91\)90019-T](#).
- [64] B. Borasoy, The Electric dipole moment of the neutron in chiral perturbation theory, Phys. Rev. D 61 (2000) 114017. [arXiv:hep-ph/0004011](#), [doi:10.1103/PhysRevD.61.114017](#).
- [65] X. G. He, J. P. Ma, Testing of P and CP symmetries with  $e^+e^- \rightarrow \Lambda\bar{\Lambda}$ , Phys. Lett. B 839 (2023) 137834. [arXiv:2212.08243](#), [doi:10.1016/j.physletb.2023.137834](#).
- [66] Y. Du, X.-G. He, J.-P. Ma, X.-Y. Du, Fundamental Tests of P and CP Symmetries Using Octet Baryons at the  $J/\psi$  Threshold (5 2024). [arXiv:2405.09625](#).
- [67] X.-G. He, J. P. Ma, B. McKellar, CP violation in  $J/\psi \rightarrow \Lambda\bar{\Lambda}$ , Phys. Rev. D 47 (1993) R1744–R1746. [arXiv:hep-ph/9211276](#), [doi:10.1103/PhysRevD.47.R1744](#).

- [68] X.-G. He, J. P. Ma, B. McKellar, CP violation in fermion pair decays of neutral boson particles, *Phys. Rev. D* 49 (1994) 4548–4552. [arXiv:hep-ph/9310243](#), [doi:10.1103/PhysRevD.49.4548](#).
- [69] J. Fu, H.-B. Li, J.-P. Wang, F.-S. Yu, J. Zhang, Probing hyperon electric dipole moments with a full angular analysis, *Phys. Rev. D* 108 (9) (2023) L091301. [arXiv:2307.04364](#), [doi:10.1103/PhysRevD.108.L091301](#).
- [70] A. Bondar, A. Grabovsky, A. Reznichenko, A. Rudenko, V. Vorobyev, Measurement of the weak mixing angle at a Super Charm-Tau factory with data-driven monitoring of the average electron beam polarization, *JHEP* 03 (2020) 076. [arXiv:1912.09760](#), [doi:10.1007/JHEP03\(2020\)076](#).
- [71] L. K. Li, et al., Search for CP violation and measurement of branching fractions and decay asymmetry parameters for  $\Lambda_c^+ \rightarrow \Lambda h^+$  and  $\Lambda_c^+ \rightarrow \Sigma^0 h^+$  ( $h=K, \pi$ ), *Sci. Bull.* 68 (2023) 583–592. [arXiv:2208.08695](#), [doi:10.1016/j.scib.2023.02.017](#).
- [72] J. H. Kuhn, E. Mirkes, Structure functions in tau decays, *Z. Phys. C* 56 (1992) 661–672, [Erratum: *Z.Phys.C* 67, 364 (1995)]. [doi:10.1007/BF01474741](#).
- [73] V. Cirigliano, J. Jenkins, M. Gonzalez-Alonso, Semileptonic decays of light quarks beyond the Standard Model, *Nucl. Phys. B* 830 (2010) 95–115. [arXiv:0908.1754](#), [doi:10.1016/j.nuclphysb.2009.12.020](#).
- [74] E. A. Garcés, M. Hernández Villanueva, G. López Castro, P. Roig, Effective-field theory analysis of the  $\tau^- \rightarrow \eta^{(\prime)} \pi^- \nu_\tau$  decays, *JHEP* 12 (2017) 027. [arXiv:1708.07802](#), [doi:10.1007/JHEP12\(2017\)027](#).
- [75] V. Cirigliano, A. Crivellin, M. Hoferichter, No-go theorem for non-standard explanations of the  $\tau \rightarrow K_S \pi \nu_\tau$  CP asymmetry, *Phys. Rev. Lett.* 120 (14) (2018) 141803. [arXiv:1712.06595](#), [doi:10.1103/PhysRevLett.120.141803](#).
- [76] S. Arteaga, L.-Y. Dai, A. Guevara, P. Roig, Tension between  $e^+e^- \rightarrow \eta \pi^- \pi^+$  and  $\tau^- \rightarrow \eta \pi^- \pi^0 \nu_\tau$  data and nonstandard interactions, *Phys. Rev. D* 106 (9)

- (2022) 096016. [arXiv:2209.15537](https://arxiv.org/abs/2209.15537), [doi:10.1103/PhysRevD.106.096016](https://doi.org/10.1103/PhysRevD.106.096016).
- [77] G. P. Lepage, S. J. Brodsky, Exclusive Processes in Perturbative Quantum Chromodynamics, *Phys. Rev. D* 22 (1980) 2157. [doi:10.1103/PhysRevD.22.2157](https://doi.org/10.1103/PhysRevD.22.2157).
- [78] J. Gasser, H. Leutwyler, Chiral Perturbation Theory to One Loop, *Annals Phys.* 158 (1984) 142. [doi:10.1016/0003-4916\(84\)90242-2](https://doi.org/10.1016/0003-4916(84)90242-2).
- [79] J. Gasser, H. Leutwyler, Chiral Perturbation Theory: Expansions in the Mass of the Strange Quark, *Nucl. Phys. B* 250 (1985) 465–516. [doi:10.1016/0550-3213\(85\)90492-4](https://doi.org/10.1016/0550-3213(85)90492-4).
- [80] B. Ananthanarayan, G. Colangelo, J. Gasser, H. Leutwyler, Roy equation analysis of pi pi scattering, *Phys. Rept.* 353 (2001) 207–279. [arXiv:hep-ph/0005297](https://arxiv.org/abs/hep-ph/0005297), [doi:10.1016/S0370-1573\(01\)00009-6](https://doi.org/10.1016/S0370-1573(01)00009-6).
- [81] R. Garcia-Martin, R. Kaminski, J. R. Pelaez, J. Ruiz de Elvira, F. J. Yndurain, The Pion-pion scattering amplitude. IV: Improved analysis with once subtracted Roy-like equations up to 1100 MeV, *Phys. Rev. D* 83 (2011) 074004. [arXiv:1102.2183](https://arxiv.org/abs/1102.2183), [doi:10.1103/PhysRevD.83.074004](https://doi.org/10.1103/PhysRevD.83.074004).
- [82] D. Gómez Dumm, P. Roig, Dispersive representation of the pion vector form factor in  $\tau \rightarrow \pi\pi\nu_\tau$  decays, *Eur. Phys. J. C* 73 (8) (2013) 2528. [arXiv:1301.6973](https://arxiv.org/abs/1301.6973), [doi:10.1140/epjc/s10052-013-2528-1](https://doi.org/10.1140/epjc/s10052-013-2528-1).
- [83] S. González-Solís, P. Roig, A dispersive analysis of the pion vector form factor and  $\tau^- \rightarrow K^- K_S \nu_\tau$  decay, *Eur. Phys. J. C* 79 (5) (2019) 436. [arXiv:1902.02273](https://arxiv.org/abs/1902.02273), [doi:10.1140/epjc/s10052-019-6943-9](https://doi.org/10.1140/epjc/s10052-019-6943-9).
- [84] Z. Y. Zhou, G. Y. Qin, P. Zhang, Z. Xiao, H. Q. Zheng, N. Wu, The Pole structure of the unitary, crossing symmetric low energy pi pi scattering amplitudes, *JHEP* 02 (2005) 043. [arXiv:hep-ph/0406271](https://arxiv.org/abs/hep-ph/0406271), [doi:10.1088/1126-6708/2005/02/043](https://doi.org/10.1088/1126-6708/2005/02/043).

- [85] L. Y. Dai, X. G. Wang, H. Q. Zheng, Pole Analysis on Unitarized  $SU(3) \times SU(3)$  One Loop  $\chi$ PT Amplitudes, Commun. Theor. Phys. 57 (2012) 841–848. [arXiv:1108.1451](#), [doi:10.1088/0253-6102/57/5/15](#).
- [86] Z.-H. Guo, J. A. Oller, Resonances from meson-meson scattering in U(3) CHPT, Phys. Rev. D 84 (2011) 034005. [arXiv:1104.2849](#), [doi:10.1103/PhysRevD.84.034005](#).
- [87] Z.-H. Guo, J. A. Oller, J. Ruiz de Elvira, Chiral dynamics in form factors, spectral-function sum rules, meson-meson scattering and semi-local duality, Phys. Rev. D 86 (2012) 054006. [arXiv:1206.4163](#), [doi:10.1103/PhysRevD.86.054006](#).
- [88] J. R. Pelaez, A. Rodas, J. Ruiz De Elvira, Global parameterization of  $\pi\pi$  scattering up to 2 GeV, Eur. Phys. J. C 79 (12) (2019) 1008. [arXiv:1907.13162](#), [doi:10.1140/epjc/s10052-019-7509-6](#).
- [89] D.-L. Yao, L.-Y. Dai, H.-Q. Zheng, Z.-Y. Zhou, A review on partial-wave dynamics with chiral effective field theory and dispersion relation, Rept. Prog. Phys. 84 (7) (2021) 076201. [arXiv:2009.13495](#), [doi:10.1088/1361-6633/abfa6f](#).
- [90] B. Moussallam, Analyticity constraints on the strangeness changing vector current and applications to  $\tau \rightarrow K \pi \nu(\tau)$ ,  $\tau \rightarrow K \pi \pi \nu(\tau)$ , Eur. Phys. J. C 53 (2008) 401–412. [arXiv:0710.0548](#), [doi:10.1140/epjc/s10052-007-0464-7](#).
- [91] D. R. Boito, R. Escribano, M. Jamin,  $K \pi$  vector form-factor, dispersive constraints and  $\tau \rightarrow \nu(\tau) K \pi$  decays, Eur. Phys. J. C 59 (2009) 821–829. [arXiv:0807.4883](#), [doi:10.1140/epjc/s10052-008-0834-9](#).
- [92] D. R. Boito, R. Escribano, M. Jamin,  $K \pi$  vector form factor constrained by  $\tau^- \rightarrow K \pi \nu_\tau$  and  $K_{l3}$  decays, JHEP 09 (2010) 031. [arXiv:1007.1858](#), [doi:10.1007/JHEP09\(2010\)031](#).
- [93] V. Bernard, First determination of  $f_+(0)|V_{us}|$  from a combined analysis of  $\tau \rightarrow K \pi \nu_\tau$  decay and  $\pi K$  scattering with constraints from  $K_{l3}$  decays, JHEP 06 (2014) 082. [arXiv:1311.2569](#), [doi:10.1007/JHEP06\(2014\)082](#).

- [94] R. Escribano, S. González-Solís, M. Jamin, P. Roig, Combined analysis of the decays  $\tau^- \rightarrow K_S \pi^- \nu_\tau$  and  $\tau^- \rightarrow K^- \eta \nu_\tau$ , JHEP 09 (2014) 042. [arXiv:1407.6590](#), [doi:10.1007/JHEP09\(2014\)042](#).
- [95] R. Escribano, S. Gonzalez-Solis, P. Roig,  $\tau^- \rightarrow K^- \eta^{(\prime)} \nu_\tau$  decays in Chiral Perturbation Theory with Resonances, JHEP 10 (2013) 039. [arXiv:1307.7908](#), [doi:10.1007/JHEP10\(2013\)039](#).
- [96] D. Stamen, D. Hariharan, M. Hoferichter, B. Kubis, P. Stoffer, Kaon electromagnetic form factors in dispersion theory, Eur. Phys. J. C 82 (5) (2022) 432. [arXiv:2202.11106](#), [doi:10.1140/epjc/s10052-022-10348-3](#).
- [97] C. Leroy, J. Pestieau, Tau Decay and Second Class Currents, Phys. Lett. B 72 (1978) 398–399. [doi:10.1016/0370-2693\(78\)90148-X](#).
- [98] A. Pich, 'Anomalous'  $\eta$  Production in Tau Decay, Phys. Lett. B 196 (1987) 561–565. [doi:10.1016/0370-2693\(87\)90821-5](#).
- [99] S. Descotes-Genon, B. Moussallam, Analyticity of  $\eta\pi$  isospin-violating form factors and the  $\tau \rightarrow \eta\pi\nu$  second-class decay, Eur. Phys. J. C 74 (2014) 2946. [arXiv:1404.0251](#), [doi:10.1140/epjc/s10052-014-2946-8](#).
- [100] R. Escribano, S. Gonzalez-Solis, P. Roig, Predictions on the second-class current decays  $\tau^- \rightarrow \pi^- \eta^{(\prime)} \nu_\tau$ , Phys. Rev. D 94 (3) (2016) 034008. [arXiv:1601.03989](#), [doi:10.1103/PhysRevD.94.034008](#).
- [101] Y.-J. Shi, C.-Y. Seng, F.-K. Guo, B. Kubis, U.-G. Meißner, W. Wang, Two-Meson Form Factors in Unitarized Chiral Perturbation Theory, JHEP 04 (2021) 086. [arXiv:2011.00921](#), [doi:10.1007/JHEP04\(2021\)086](#).
- [102] M. Döring, U.-G. Meißner, W. Wang, Chiral Dynamics and S-wave Contributions in Semileptonic B decays, JHEP 10 (2013) 011. [arXiv:1307.0947](#), [doi:10.1007/JHEP10\(2013\)011](#).
- [103] S. Ropertz, C. Hanhart, B. Kubis, A new parametrization for the scalar pion form factors, Eur. Phys. J. C 78 (12) (2018) 1000. [arXiv:1809.06867](#), [doi:10.1140/epjc/s10052-018-6416-6](#).

- [104] V. Bernard, N. Kaiser, U. G. Meissner,  $\pi K$  scattering in chiral perturbation theory to one loop, Nucl. Phys. B 357 (1991) 129–152. doi:10.1016/0550-3213(91)90461-6.
- [105] M. Jamin, J. A. Oller, A. Pich, S wave K pi scattering in chiral perturbation theory with resonances, Nucl. Phys. B 587 (2000) 331–362. arXiv:hep-ph/0006045, doi:10.1016/S0550-3213(00)00479-X.
- [106] H. Q. Zheng, Z. Y. Zhou, G. Y. Qin, Z. Xiao, J. J. Wang, N. Wu, The kappa resonance in s wave pi K scatterings, Nucl. Phys. A 733 (2004) 235–261. arXiv:hep-ph/0310293, doi:10.1016/j.nuclphysa.2003.12.021.
- [107] M. Jamin, J. A. Oller, A. Pich, Strangeness changing scalar form-factors, Nucl. Phys. B 622 (2002) 279–308. arXiv:hep-ph/0110193, doi:10.1016/S0550-3213(01)00605-8.
- [108] L. Von Detten, F. Noël, C. Hanhart, M. Hoferichter, B. Kubis, On the scalar  $\pi K$  form factor beyond the elastic region, Eur. Phys. J. C 81 (5) (2021) 420. arXiv:2103.01966, doi:10.1140/epjc/s10052-021-09169-7.
- [109] J. A. Miranda, P. Roig, Effective-field theory analysis of the  $\tau^- \rightarrow \pi^- \pi^0 \nu_\tau$  decays, JHEP 11 (2018) 038. arXiv:1806.09547, doi:10.1007/JHEP11(2018)038.
- [110] J. Rendón, P. Roig, G. Toledo Sánchez, Effective-field theory analysis of the  $\tau^- \rightarrow (K\pi)^- \nu_\tau$  decays, Phys. Rev. D 99 (9) (2019) 093005. arXiv:1902.08143, doi:10.1103/PhysRevD.99.093005.
- [111] S. González-Solís, A. Miranda, J. Rendón, P. Roig, Effective-field theory analysis of the  $\tau^- \rightarrow K^-(\eta^{(\prime)}, K^0) \nu_\tau$  decays, Phys. Rev. D 101 (3) (2020) 034010. arXiv:1911.08341, doi:10.1103/PhysRevD.101.034010.
- [112] G. Colangelo, M. Finkemeier, R. Urech, Tau decays and chiral perturbation theory, Phys. Rev. D 54 (1996) 4403–4418. arXiv:hep-ph/9604279, doi:10.1103/PhysRevD.54.4403.

- [113] D. Gomez Dumm, A. Pich, J. Portoles,  $\tau \rightarrow \pi \pi \pi \nu(\tau)$  decays in the resonance effective theory, Phys. Rev. D 69 (2004) 073002. [arXiv:hep-ph/0312183](#), [doi:10.1103/PhysRevD.69.073002](#).
- [114] D. G. Dumm, P. Roig, A. Pich, J. Portoles,  $\tau \rightarrow \pi \pi \pi \nu(\tau)$  decays and the  $a(1)(1260)$  off-shell width revisited, Phys. Lett. B 685 (2010) 158–164. [arXiv:0911.4436](#), [doi:10.1016/j.physletb.2010.01.059](#).
- [115] O. Shekhovtsova, T. Przedzinski, P. Roig, Z. Was, Resonance chiral Lagrangian currents and  $\tau$  decay Monte Carlo, Phys. Rev. D 86 (2012) 113008. [arXiv:1203.3955](#), [doi:10.1103/PhysRevD.86.113008](#).
- [116] I. M. Nugent, T. Przedzinski, P. Roig, O. Shekhovtsova, Z. Was, Resonance chiral Lagrangian currents and experimental data for  $\tau^- \rightarrow \pi^- \pi^- \pi^+ \nu_\tau$ , Phys. Rev. D 88 (2013) 093012. [arXiv:1310.1053](#), [doi:10.1103/PhysRevD.88.093012](#).
- [117] D. G. Dumm, P. Roig, A. Pich, J. Portoles, Hadron structure in  $\tau \rightarrow KK \pi \nu(\tau)$  decays, Phys. Rev. D 81 (2010) 034031. [arXiv:0911.2640](#), [doi:10.1103/PhysRevD.81.034031](#).
- [118] D. Gomez Dumm, P. Roig, Resonance Chiral Lagrangian analysis of  $\tau^- \rightarrow \eta^{(\prime)} \pi^- \pi^0 \nu_\tau$  decays, Phys. Rev. D 86 (2012) 076009. [arXiv:1208.1212](#), [doi:10.1103/PhysRevD.86.076009](#).
- [119] Z.-H. Guo, Study of  $\tau^- \rightarrow V P \nu(\tau)$  in the framework of resonance chiral theory, Phys. Rev. D 78 (2008) 033004. [arXiv:0806.4322](#), [doi:10.1103/PhysRevD.78.033004](#).
- [120] G. Ecker, R. Unterdorfer, Four pion production in  $e^+ e^-$  annihilation, Eur. Phys. J. C 24 (2002) 535–545. [arXiv:hep-ph/0203075](#), [doi:10.1007/s10052-002-0960-8](#).
- [121] V. Cirigliano, G. Ecker, H. Neufeld, Radiative tau decay and the magnetic moment of the muon, JHEP 08 (2002) 002. [arXiv:hep-ph/0207310](#), [doi:10.1088/1126-6708/2002/08/002](#).

- [122] Z.-H. Guo, P. Roig, One meson radiative tau decays, Phys. Rev. D 82 (2010) 113016. [arXiv:1009.2542](#), [doi:10.1103/PhysRevD.82.113016](#).
- [123] J. A. Miranda, P. Roig, New  $\tau$ -based evaluation of the hadronic contribution to the vacuum polarization piece of the muon anomalous magnetic moment, Phys. Rev. D 102 (2020) 114017. [arXiv:2007.11019](#), [doi:10.1103/PhysRevD.102.114017](#).
- [124] A. Guevara, G. L. Castro, P. Roig, Improved description of dilepton production in  $\tau \rightarrow \nu_\tau P$ - decays, Phys. Rev. D 105 (7) (2022) 076007. [arXiv:2111.09994](#), [doi:10.1103/PhysRevD.105.076007](#).
- [125] M. A. Arroyo-Ureña, G. Hernández-Tomé, G. López-Castro, P. Roig, I. Rosell, Radiative corrections to  $\tau \rightarrow \pi(K)\nu_\tau[\gamma]$ : A reliable new physics test, Phys. Rev. D 104 (9) (2021) L091502. [arXiv:2107.04603](#), [doi:10.1103/PhysRevD.104.L091502](#).
- [126] M. A. Arroyo-Ureña, G. Hernández-Tomé, G. López-Castro, P. Roig, I. Rosell, One-loop determination of  $\tau \rightarrow \pi(K)\nu_\tau[\gamma]$  branching ratios and new physics tests, JHEP 02 (2022) 173. [arXiv:2112.01859](#), [doi:10.1007/JHEP02\(2022\)173](#).
- [127] C. Chen, C.-G. Duan, Z.-H. Guo, Triple-product asymmetry in the radiative two-pion tau decay, JHEP 08 (2022) 144. [arXiv:2201.12764](#), [doi:10.1007/JHEP08\(2022\)144](#).
- [128] R. Escribano, J. A. Miranda, P. Roig, Radiative corrections to the  $\tau \rightarrow (P_1 P_2) \nu_\tau$  ( $P_{1,2} = \pi, K$ ) decays, Phys. Rev. D 109 (5) (2024) 053003. [arXiv:2303.01362](#), [doi:10.1103/PhysRevD.109.053003](#).
- [129] H. B. Meyer, Lattice QCD and the Timelike Pion Form Factor, Phys. Rev. Lett. 107 (2011) 072002. [arXiv:1105.1892](#), [doi:10.1103/PhysRevLett.107.072002](#).
- [130] X. Feng, S. Aoki, S. Hashimoto, T. Kaneko, Timelike pion form factor in lattice QCD, Phys. Rev. D 91 (5) (2015) 054504. [arXiv:1412.6319](#), [doi:10.1103/PhysRevD.91.054504](#).
- [131] C. Andersen, J. Bulava, B. Hörz, C. Morningstar, The  $I = 1$  pion-pion scattering amplitude and timelike pion form factor from  $N_f = 2 + 1$  lattice

- QCD, Nucl. Phys. B 939 (2019) 145–173. [arXiv:1808.05007](#), [doi:10.1016/j.nuclphysb.2018.12.018](#).
- [132] A. Baroni, R. A. Briceño, M. T. Hansen, F. G. Ortega-Gama, Form factors of two-hadron states from a covariant finite-volume formalism, Phys. Rev. D 100 (3) (2019) 034511. [arXiv:1812.10504](#), [doi:10.1103/PhysRevD.100.034511](#).
- [133] J. H. Kuhn, E. Mirkes, CP violation in semileptonic tau decays with unpolarized beams, Phys. Lett. B 398 (1997) 407–414. [arXiv:hep-ph/9609502](#), [doi:10.1016/S0370-2693\(97\)00233-5](#).
- [134] S. Y. Choi, K. Hagiwara, M. Tanabashi, CP violation in  $\tau \rightarrow 3 \pi$  tau-neutrino, Phys. Rev. D 52 (1995) 1614–1626. [arXiv:hep-ph/9412203](#), [doi:10.1103/PhysRevD.52.1614](#).
- [135] S. Y. Choi, J. Lee, J. Song, CP violation in the Cabibbo suppressed decay  $\tau \rightarrow K \pi$  tau-neutrino with polarized tau leptons, Phys. Lett. B 437 (1998) 191–200. [arXiv:hep-ph/9804268](#), [doi:10.1016/S0370-2693\(98\)00872-7](#).
- [136] I. I. Bigi, A. I. Sanda, A 'Known' CP asymmetry in tau decays, Phys. Lett. B 625 (2005) 47–52. [arXiv:hep-ph/0506037](#), [doi:10.1016/j.physletb.2005.08.033](#).
- [137] I. I. Bigi, CP Violation in  $\tau$  Decays at SuperB & Super-Belle II Experiments - like Finding Signs of Dark Matter, Nucl. Phys. B Proc. Suppl. 253-255 (2014) 91–94. [arXiv:1210.2968](#), [doi:10.1016/j.nuclphysbps.2014.09.022](#).
- [138] D. Delepine, G. Lopez Castro, L. T. Lopez Lozano, CP violation in semileptonic tau lepton decays, Phys. Rev. D 72 (2005) 033009. [arXiv:hep-ph/0503090](#), [doi:10.1103/PhysRevD.72.033009](#).
- [139] D. Delepine, G. Faisel, C. A. Ramirez, Exploring new physics contributions to  $CP$  violation in  $\tau^- \rightarrow K^- \pi^0 \nu_\tau$ , Eur. Phys. J. C 81 (4) (2021) 368. [arXiv:1806.05090](#), [doi:10.1140/epjc/s10052-021-09150-4](#).

- [140] A. Datta, K. Kiers, D. London, P. J. O’Donnell, A. Szykman, CP Violation in Hadronic tau Decays, Phys. Rev. D 75 (2007) 074007, [Erratum: Phys.Rev.D 76, 079902 (2007)]. [arXiv:hep-ph/0610162](#), [doi:10.1103/PhysRevD.76.079902](#).
- [141] K. Kiers, K. Little, A. Datta, D. London, M. Nagashima, A. Szykman, CP violation in tau  $\rightarrow$  K pi pi nu(tau), Phys. Rev. D 78 (2008) 113008. [arXiv:0808.1707](#), [doi:10.1103/PhysRevD.78.113008](#).
- [142] T. Huang, J.-M. Yang, B.-L. Young, X.-M. Zhang, Effective CP violating operators of the tau lepton and some of their phenomenologies, Phys. Rev. D 58 (1998) 073007. [arXiv:hep-ph/9803334](#), [doi:10.1103/PhysRevD.58.073007](#).
- [143] T. Huang, W. Lu, Z.-j. Tao, Search for nonstandard model CP/T violation at tau charm factory, Phys. Rev. D 55 (1997) 1643–1652. [arXiv:hep-ph/9609220](#), [doi:10.1103/PhysRevD.55.1643](#).
- [144] U. Kilian, J. G. Korner, K. Schilcher, Y. L. Wu, Lepton hadron angular correlations in semileptonic tau decays, Z. Phys. C 62 (1994) 413–419. [doi:10.1007/BF01555900](#).
- [145] G. Lopez Castro, L. Lopez-Lozano, A. Rosado, Violation of CP and T in semileptonic decays due to scalar interactions, Phys. Rev. D 80 (2009) 096004. [arXiv:0911.1148](#), [doi:10.1103/PhysRevD.80.096004](#).
- [146] Y. S. Tsai, Production of polarized tau pairs and tests of CP violation using polarized e+e- colliders near threshold, Phys. Rev. D 51 (1995) 3172–3181. [arXiv:hep-ph/9410265](#), [doi:10.1103/PhysRevD.51.3172](#).
- [147] Y.-s. Tsai, The Investigation of CP violation through the decay of polarized tau leptons, Phys. Lett. B 378 (1996) 272–278. [doi:10.1016/0370-2693\(96\)00403-0](#).
- [148] C. Wang, X.-H. Guo, Y. Liu, R.-C. Li, Direct CP violation in  $\tau^\pm \rightarrow K^\pm \rho^0(\omega) \nu_\tau \rightarrow K^\pm \pi^+ \pi^- \nu_\tau$ , Eur. Phys. J. C 74 (11) (2014) 3140. [arXiv:1408.0086](#), [doi:10.1140/epjc/s10052-014-3140-8](#).
- [149] N. Mileo, K. Kiers, A. Szykman, Probing sensitivity to charged scalars through partial differential widths:  $\tau \rightarrow K \pi \pi \nu_\tau$  decays, Phys. Rev.

- D 91 (7) (2015) 073006. [arXiv:1410.1909](#), [doi:10.1103/PhysRevD.91.073006](#).
- [150] I. I. Bigi, Probing CP Violation in  $\tau^- \rightarrow \nu(K\pi/K2\pi/3K/K3\pi)^-$  Decays (4 2012). [arXiv:1204.5817](#).
- [151] X.-D. Shi, X.-W. Kang, I. Bigi, W.-P. Wang, H.-P. Peng, Prospects for CP and P violation in  $\Lambda_c^+$  decays at Super Tau Charm Facility, Phys. Rev. D 100 (11) (2019) 113002. [arXiv:1904.12415](#), [doi:10.1103/PhysRevD.100.113002](#).
- [152] D. Kimura, K. Y. Lee, T. Morozumi, The Form factors of  $\tau \rightarrow K\pi(\eta)\nu$  and the predictions for CP violation beyond the standard model, PTEP 2013 (2013) 053B03, [Erratum: PTEP 2013, 099201 (2013), Erratum: PTEP 2014, 089202 (2014)]. [arXiv:1201.1794](#), [doi:10.1093/ptep/ptt013](#).
- [153] L. Zhang, X.-W. Kang, X.-H. Guo, L.-Y. Dai, T. Luo, C. Wang, A comprehensive study on the semileptonic decay of heavy flavor mesons, JHEP 02 (2021) 179. [arXiv:2012.04417](#), [doi:10.1007/JHEP02\(2021\)179](#).
- [154] R. N. Faustov, V. O. Galkin, X.-W. Kang, Semileptonic decays of  $D$  and  $D_s$  mesons in the relativistic quark model, Phys. Rev. D 101 (1) (2020) 013004. [arXiv:1911.08209](#), [doi:10.1103/PhysRevD.101.013004](#).
- [155] R. N. Faustov, V. O. Galkin, X.-W. Kang, Relativistic description of the semileptonic decays of bottom mesons, Phys. Rev. D 106 (1) (2022) 013004. [arXiv:2206.10277](#), [doi:10.1103/PhysRevD.106.013004](#).
- [156] G. Calderon, D. Delepine, G. L. Castro, Is there a paradox in CP asymmetries of  $\tau^{+-} \rightarrow K(L,S)\pi^{+-} \nu$  decays?, Phys. Rev. D 75 (2007) 076001. [arXiv:hep-ph/0702282](#), [doi:10.1103/PhysRevD.75.076001](#).
- [157] J. P. Lees, et al., Search for CP Violation in the Decay  $\tau^- \rightarrow \pi^- K_S^0 (>= 0\pi^0)\nu_{\tau}$ , Phys. Rev. D 85 (2012) 031102, [Erratum: Phys.Rev.D 85, 099904 (2012)]. [arXiv:1109.1527](#), [doi:10.1103/PhysRevD.85.031102](#).

- [158] Y. Grossman, Y. Nir, CP Violation in  $\tau^\pm \rightarrow \pi^\pm K_S \nu$  and  $D^\pm \rightarrow \pi^\pm K_S$ : The Importance of  $K_S - K_L$  Interference, JHEP 04 (2012) 002. [arXiv:1110.3790](#), [doi:10.1007/JHEP04\(2012\)002](#).
- [159] H. Z. Devi, L. Dhargyal, N. Sinha, Can the observed CP asymmetry in  $\tau \rightarrow K \pi \nu_\tau$  be due to nonstandard tensor interactions?, Phys. Rev. D 90 (1) (2014) 013016. [arXiv:1308.4383](#), [doi:10.1103/PhysRevD.90.013016](#).
- [160] K. M. Watson, Some general relations between the photoproduction and scattering of pi mesons, Phys. Rev. 95 (1954) 228–236. [doi:10.1103/PhysRev.95.228](#).
- [161] F.-Z. Chen, X.-Q. Li, Y.-D. Yang, X. Zhang, CP asymmetry in  $\tau \rightarrow K_S \pi \nu_\tau$  decays within the Standard Model and beyond, Phys. Rev. D 100 (11) (2019) 113006. [arXiv:1909.05543](#), [doi:10.1103/PhysRevD.100.113006](#).
- [162] F.-Z. Chen, X.-Q. Li, S.-C. Peng, Y.-D. Yang, H.-H. Zhang, CP asymmetry in the angular distributions of  $\tau \rightarrow K_S \pi \nu_\tau$  decays. Part II. General effective field theory analysis, JHEP 01 (2022) 108. [arXiv:2107.12310](#), [doi:10.1007/JHEP01\(2022\)108](#).
- [163] D. A. L. Aguilar, J. Rendón, P. Roig, CP violation in two-meson Tau decays induced by heavy new physics (9 2024). [arXiv:2409.05588](#).
- [164] A. Dighe, S. Ghosh, G. Kumar, T. S. Roy, Tensors for tending to tensions in  $\tau$  decays (2 2019). [arXiv:1902.09561](#).
- [165] H. Sang, X. Shi, X. Zhou, X. Kang, J. Liu, Feasibility study of CP violation in  $\tau \rightarrow K_S \pi \nu_\tau$  decays at the Super Tau Charm Facility, Chin. Phys. C 45 (5) (2021) 053003. [arXiv:2012.06241](#), [doi:10.1088/1674-1137/abeb07](#).
- [166] M. Bischofberger, et al., Search for CP violation in  $\tau \rightarrow K_S^0 \pi \nu_\tau$  decays at Belle, Phys. Rev. Lett. 107 (2011) 131801. [arXiv:1101.0349](#), [doi:10.1103/PhysRevLett.107.131801](#).
- [167] G. Bonvicini, et al., Search for CP violation in tau  $\rightarrow$  K pi tau-neutrino decays, Phys. Rev. Lett. 88 (2002) 111803. [arXiv:hep-ex/0111095](#), [doi:10.1103/PhysRevLett.88.111803](#).

- [168] R. L. Workman, Others, Review of Particle Physics, PTEP 2022 (2022) 083C01. [doi:10.1093/ptep/ptac097](https://doi.org/10.1093/ptep/ptac097).
- [169] J. Abdallah, et al., Study of tau-pair production in photon-photon collisions at LEP and limits on the anomalous electromagnetic moments of the tau lepton, Eur. Phys. J. C 35 (2004) 159–170. [arXiv:hep-ex/0406010](https://arxiv.org/abs/hep-ex/0406010), [doi:10.1140/epjc/s2004-01852-y](https://doi.org/10.1140/epjc/s2004-01852-y).
- [170] F. Cornet, J. I. Illana, Tau pair production via photon-photon collisions at LEP, Phys. Rev. D 53 (1996) 1181–1184. [arXiv:hep-ph/9503466](https://arxiv.org/abs/hep-ph/9503466), [doi:10.1103/PhysRevD.53.1181](https://doi.org/10.1103/PhysRevD.53.1181).
- [171] P. Achard, et al., Muon pair and tau pair production in two photon collisions at LEP, Phys. Lett. B 585 (2004) 53–62. [arXiv:hep-ex/0402037](https://arxiv.org/abs/hep-ex/0402037), [doi:10.1016/j.physletb.2004.02.012](https://doi.org/10.1016/j.physletb.2004.02.012).
- [172] W. Lohmann, Electromagnetic and weak moments of the tau-lepton, Nucl. Phys. B Proc. Suppl. 144 (2005) 122–127. [arXiv:hep-ex/0501065](https://arxiv.org/abs/hep-ex/0501065), [doi:10.1016/j.nuclphysbps.2005.02.017](https://doi.org/10.1016/j.nuclphysbps.2005.02.017).
- [173] K. Inami, et al., Search for the electric dipole moment of the tau lepton, Phys. Lett. B 551 (2003) 16–26. [arXiv:hep-ex/0210066](https://arxiv.org/abs/hep-ex/0210066), [doi:10.1016/S0370-2693\(02\)02984-2](https://doi.org/10.1016/S0370-2693(02)02984-2).
- [174] J. Biebel, T. Riemann, Predictions for anomalous tau+ tau- gamma production at LEP-1, Z. Phys. C 76 (1997) 53–58. [arXiv:hep-ph/9610437](https://arxiv.org/abs/hep-ph/9610437), [doi:10.1007/s002880050526](https://doi.org/10.1007/s002880050526).
- [175] S. S. Gau, T. C. Paul, J. Swain, L. Taylor, Radiative tau lepton pair production as a probe of anomalous electromagnetic couplings of the tau, Nucl. Phys. B 523 (1998) 439–449. [arXiv:hep-ph/9712360](https://arxiv.org/abs/hep-ph/9712360), [doi:10.1016/S0550-3213\(98\)00121-7](https://doi.org/10.1016/S0550-3213(98)00121-7).
- [176] M. Acciarri, et al., Measurement of the anomalous magnetic and electric dipole moments of the tau lepton, Phys. Lett. B 434 (1998) 169–179. [doi:10.1016/S0370-2693\(98\)00736-9](https://doi.org/10.1016/S0370-2693(98)00736-9).
- [177] W. Bernreuther, O. Nachtmann, P. Overmann, The CP violating electric and weak dipole moments of the tau lepton from threshold to 500-GeV, Phys. Rev. D 48 (1993) 78–88. [doi:10.1103/PhysRevD.48.78](https://doi.org/10.1103/PhysRevD.48.78).

- [178] X. Chen, Y. Wu, Search for the Electric Dipole Moment and anomalous magnetic moment of the tau lepton at tau factories, JHEP 10 (2019) 089. [arXiv:1803.00501](#), [doi:10.1007/JHEP10\(2019\)089](#).
- [179] W. Bernreuther, L. Chen, O. Nachtmann, Electric dipole moment of the tau lepton revisited, Phys. Rev. D 103 (9) (2021) 096011. [arXiv:2101.08071](#), [doi:10.1103/PhysRevD.103.096011](#).
- [180] M. Acciarri, et al., Measurement of the weak dipole moments of the tau lepton, Phys. Lett. B 426 (1998) 207–216. [doi:10.1016/S0370-2693\(98\)00290-1](#).
- [181] A. Heister, et al., Search for anomalous weak dipole moments of the tau lepton, Eur. Phys. J. C 30 (2003) 291–304. [arXiv:hep-ex/0209066](#), [doi:10.1140/epjc/s2003-01286-1](#).
- [182] M. J. Booth, The Electric dipole moment of the W and electron in the Standard Model (1 1993). [arXiv:hep-ph/9301293](#).
- [183] M. Köksal, A. A. Billur, A. Gutiérrez-Rodríguez, M. A. Hernández-Ruíz, Model-independent sensitivity estimates for the electromagnetic dipole moments of the  $\tau$ -lepton at the CLIC, Phys. Rev. D 98 (1) (2018) 015017. [arXiv:1804.02373](#), [doi:10.1103/PhysRevD.98.015017](#).
- [184] M. Köksal, Model-independent study on the anomalous  $\tau\tau^-\gamma$  couplings at the ILC, Nucl. Phys. B 971 (2021) 115520. [arXiv:2104.01003](#), [doi:10.1016/j.nuclphysb.2021.115520](#).
- [185] A. Gutiérrez-Rodríguez, C. Pérez-Mayorga, A. González-Sánchez, Sensitivity Estimates on the Electromagnetic Dipole Moments of the  $\tau$ -Lepton at Future  $e^+e^-$  Linear Colliders, Int. J. Theor. Phys. 61 (5) (2022) 132. [doi:10.1007/s10773-022-05119-5](#).
- [186] X. Sun, et al., Search for the electric dipole moment of the tau lepton at the Super Tau-Charm Facility (2024). [arXiv:2411.19469](#).
- [187] X.-D. Shi, X.-R. Zhou, X.-S. Qin, H.-P. Peng, A fast simulation package for STCF detector, JINST 16 (03) (2021) P03029. [arXiv:2011.01654](#), [doi:10.1088/1748-0221/16/03/P03029](#).

- [188] S. Jadach, B. F. L. Ward, Z. Was, The Precision Monte Carlo event generator KK for two fermion final states in  $e^+e^-$  collisions, *Comput. Phys. Commun.* 130 (2000) 260–325. [arXiv:hep-ph/9912214](#), [doi:10.1016/S0010-4655\(00\)00048-5](#).
- [189] Z. Was, TAUOLA the library for tau lepton decay, and KKMC / KORALB / KORALZ /... status report, *Nucl. Phys. B Proc. Suppl.* 98 (2001) 96–102. [arXiv:hep-ph/0011305](#), [doi:10.1016/S0920-5632\(01\)01200-2](#).
- [190] D. Epifanov, et al., Study of  $\tau^- \rightarrow K(S) \pi^- \nu(\tau)$  decay at Belle, *Phys. Lett. B* 654 (2007) 65–73. [arXiv:0706.2231](#), [doi:10.1016/j.physletb.2007.08.045](#).
- [191] R. Barlow, Systematic errors: Facts and fictions, in: *Conference on Advanced Statistical Techniques in Particle Physics, 2002*, pp. 134–144. [arXiv:hep-ex/0207026](#).
- [192] B. R. Ko, E. Won, B. Golob, P. Pakhlov, Effect of nuclear interactions of neutral kaons on CP asymmetry measurements, *Phys. Rev. D* 84 (2011) 111501. [arXiv:1006.1938](#), [doi:10.1103/PhysRevD.84.111501](#).
- [193] Z.-Z. Xing, An overview of  $D^0$  anti- $D^0$  mixing and CP violation, *Chin. Phys. C* 32 (2008) 483–487. [doi:10.1088/1674-1137/32/6/015](#).
- [194] R. Aaij, et al., Observation of CP Violation in Charm Decays, *Phys. Rev. Lett.* 122 (21) (2019) 211803. [arXiv:1903.08726](#), [doi:10.1103/PhysRevLett.122.211803](#).
- [195] R. Aaij, et al., Measurement of the Time-Integrated CP Asymmetry in  $D^0 \rightarrow K^- K^+$  Decays, *Phys. Rev. Lett.* 131 (9) (2023) 091802. [arXiv:2209.03179](#), [doi:10.1103/PhysRevLett.131.091802](#).
- [196] S. Iguro, U. Nierste, E. Overduin, M. Schüßler,  $SU(3)_F$  sum rules for CP asymmetry of  $D_{(s)}$  decays (8 2024). [arXiv:2408.03227](#).
- [197] Z.-z. Xing, A U-spin prediction for the CP-forbidden transition  $e^+e^- \rightarrow D^0 \bar{D}^0 \rightarrow (K^+ K^-)_D (\pi^+ \pi^-)_D$ , *Mod. Phys. Lett. A* 34 (29) (2019) 1950238. [arXiv:1903.09566](#), [doi:10.1142/S0217732319502389](#).

- [198] H.-Y. Cheng, C.-W. Chiang, Direct CP violation in two-body hadronic charmed meson decays, Phys. Rev. D 85 (2012) 034036, [Erratum: Phys.Rev.D 85, 079903 (2012)]. [arXiv:1201.0785](#), [doi:10.1103/PhysRevD.85.034036](#).
- [199] H.-Y. Cheng, C.-W. Chiang, SU(3) symmetry breaking and CP violation in  $D \rightarrow PP$  decays, Phys. Rev. D 86 (2012) 014014. [arXiv:1205.0580](#), [doi:10.1103/PhysRevD.86.014014](#).
- [200] H.-n. Li, C.-D. Lu, F.-S. Yu, Branching ratios and direct CP asymmetries in  $D \rightarrow PP$  decays, Phys. Rev. D 86 (2012) 036012. [arXiv:1203.3120](#), [doi:10.1103/PhysRevD.86.036012](#).
- [201] M. Saur, F.-S. Yu, Charm  $CPV$ : observation and prospects, Sci. Bull. 65 (2020) 1428–1431. [arXiv:2002.12088](#), [doi:10.1016/j.scib.2020.04.020](#).
- [202] L.-L. Chau, H.-Y. Cheng, CP Violation in the Partial Decay Rates of Charm and Beauty Mesons, Phys. Rev. Lett. 53 (1984) 1037. [doi:10.1103/PhysRevLett.53.1037](#).
- [203] F. Buccella, M. Lusignoli, G. Mangano, G. Miele, A. Pugliese, P. Santorelli, CP Violating asymmetries in charged D meson decays, Phys. Lett. B 302 (1993) 319–325. [arXiv:hep-ph/9212253](#), [doi:10.1016/0370-2693\(93\)90402-4](#).
- [204] F. Buccella, M. Lusignoli, G. Miele, A. Pugliese, P. Santorelli, Nonleptonic weak decays of charmed mesons, Phys. Rev. D 51 (1995) 3478–3486. [arXiv:hep-ph/9411286](#), [doi:10.1103/PhysRevD.51.3478](#).
- [205] Q. Qin, H.-n. Li, C.-D. Lü, F.-S. Yu, Branching ratios and direct CP asymmetries in  $D \rightarrow PV$  decays, Phys. Rev. D 89 (5) (2014) 054006. [arXiv:1305.7021](#), [doi:10.1103/PhysRevD.89.054006](#).
- [206] H.-N. Li, C.-D. Lü, F.-S. Yu, Implications on the first observation of charm CPV at LHCb, [arXiv:1903.10638](#).
- [207] H.-Y. Cheng, C.-W. Chiang, Revisiting CP violation in  $D \rightarrow PP$  and  $VP$  decays, Phys. Rev. D 100 (9) (2019) 093002. [arXiv:1909.03063](#), [doi:10.1103/PhysRevD.100.093002](#).

- [208] H.-Y. Cheng, C.-W. Chiang, CP violation in quasi-two-body  $D \rightarrow VP$  decays and three-body D decays mediated by vector resonances, Phys. Rev. D 104 (7) (2021) 073003. [arXiv:2104.13548](#), [doi:10.1103/PhysRevD.104.073003](#).
- [209] C.-P. Jia, H.-Y. Jiang, J.-P. Wang, F.-S. Yu, Final-state rescattering mechanism of charmed baryon decays, JHEP 11 (2024) 072. [arXiv:2408.14959](#), [doi:10.1007/JHEP11\(2024\)072](#).
- [210] C.-Q. Geng, X.-G. He, X.-N. Jin, C.-W. Liu, C. Yang, Complete determination of SU(3)<sub>F</sub> amplitudes and strong phase in  $\Lambda_c^+ \rightarrow \Xi^0 K^+$ , Phys. Rev. D 109 (7) (2024) L071302. [arXiv:2310.05491](#), [doi:10.1103/PhysRevD.109.L071302](#).
- [211] H. Zhong, F. Xu, H.-Y. Cheng, Topological Diagrams and Hadronic Weak Decays of Charmed Baryons (1 2024). [arXiv:2401.15926](#).
- [212] H. Zhong, F. Xu, H.-Y. Cheng, Analysis of hadronic weak decays of charmed baryons in the topological diagrammatic approach, Phys. Rev. D 109 (11) (2024) 114027. [arXiv:2404.01350](#), [doi:10.1103/PhysRevD.109.114027](#).
- [213] X.-G. He, C.-W. Liu, Large CP violation in charmed baryon decays (4 2024). [arXiv:2404.19166](#).
- [214] J. M. Link, et al., Study of the decay asymmetry parameter and CP violation parameter in the  $\Lambda_b^0 \rightarrow \Lambda_b^- \pi^+$  decay, Phys. Lett. B 634 (2006) 165–172. [arXiv:hep-ex/0509042](#), [doi:10.1016/j.physletb.2006.01.017](#).
- [215] Y. B. Li, et al., Measurements of the branching fractions of the semileptonic decays  $\Xi_c^0 \rightarrow \Xi^- \ell^+ \nu_\ell$  and the asymmetry parameter of  $\Xi_c^0 \rightarrow \Xi^- \pi^+$ , Phys. Rev. Lett. 127 (12) (2021) 121803. [arXiv:2103.06496](#), [doi:10.1103/PhysRevLett.127.121803](#).
- [216] R. Aaij, et al., A measurement of the  $CP$  asymmetry difference in  $\Lambda_c^+ \rightarrow p K^- K^+$  and  $p \pi^- \pi^+$  decays, JHEP 03 (2018) 182. [arXiv:1712.07051](#), [doi:10.1007/JHEP03\(2018\)182](#).
- [217] I. I. Bigi, Probing CP Asymmetries in Charm Baryons Decays (6 2012). [arXiv:1206.4554](#).

- [218] R. Aaij, et al., Search for  $CP$  violation in  $\Xi_c^+ \rightarrow pK^-\pi^+$  decays using model-independent techniques, *Eur. Phys. J. C* 80 (10) (2020) 986. [arXiv:2006.03145](#), [doi:10.1140/epjc/s10052-020-8365-0](#).
- [219] J.-P. Wang, Q. Qin, F.-S. Yu,  $CP$  violation observables in baryon decays, [arXiv:2411.18323](#).
- [220] M. Ablikim, et al., Precision measurement of the  $e^+e^- \rightarrow \Lambda_c^+\bar{\Lambda}_c^-$  cross section near threshold, *Phys. Rev. Lett.* 120 (13) (2018) 132001. [arXiv:1710.00150](#), [doi:10.1103/PhysRevLett.120.132001](#).
- [221] M. Ablikim, et al., Measurement of the Energy-Dependent Electromagnetic Form Factors of a Charmed Baryon (7 2023). [arXiv:2307.07316](#).
- [222] M. Ablikim, et al., Measurements of absolute hadronic branching fractions of  $\Lambda_c^+$  baryon, *Phys. Rev. Lett.* 116 (5) (2016) 052001. [arXiv:1511.08380](#), [doi:10.1103/PhysRevLett.116.052001](#).
- [223] R. Aaij, et al., Amplitude analysis of the  $\Lambda_c^+ \rightarrow pK^-\pi^+$  decay and  $\Lambda_c^+$  baryon polarization measurement in semileptonic beauty hadron decays, *Phys. Rev. D* 108 (1) (2023) 012023. [arXiv:2208.03262](#), [doi:10.1103/PhysRevD.108.012023](#).
- [224] W. Detmold, C. Lehner, S. Meinel,  $\Lambda_b \rightarrow p\ell^-\bar{\nu}_\ell$  and  $\Lambda_b \rightarrow \Lambda_c\ell^-\bar{\nu}_\ell$  form factors from lattice QCD with relativistic heavy quarks, *Phys. Rev. D* 92 (3) (2015) 034503. [arXiv:1503.01421](#), [doi:10.1103/PhysRevD.92.034503](#).
- [225] D. Wang, P.-F. Guo, W.-H. Long, F.-S. Yu,  $K_S^0 - K_L^0$  asymmetries and  $CP$  violation in charmed baryon decays into neutral kaons, *JHEP* 03 (2018) 066. [arXiv:1709.09873](#), [doi:10.1007/JHEP03\(2018\)066](#).
- [226] L. B. Okun, B. M. Pontecorvo, V. I. Zakharov, On the Possible Violation of  $CP$ -Invariance in the Decays of Charmed Particles, *Lett. Nuovo Cim.* 13 (1975) 218. [doi:10.1007/BF02742679](#).
- [227] A. Pais, S. B. Treiman,  $CP$  Violation in Charmed Particle Decays, *Phys. Rev. D* 12 (1975) 2744–2750, [Erratum: *Phys.Rev.D* 16, 2390 (1977)]. [doi:10.1103/PhysRevD.12.2744](#).

- [228] J. J. Aubert, et al., Experimental Observation of a Heavy Particle  $J$ , Phys. Rev. Lett. 33 (1974) 1404–1406. [doi:10.1103/PhysRevLett.33.1404](https://doi.org/10.1103/PhysRevLett.33.1404).
- [229] J. E. Augustin, et al., Discovery of a Narrow Resonance in  $e^+e^-$  Annihilation, Phys. Rev. Lett. 33 (1974) 1406–1408. [doi:10.1103/PhysRevLett.33.1406](https://doi.org/10.1103/PhysRevLett.33.1406).
- [230] H. Georgi,  $D$  - anti- $D$  mixing in heavy quark effective field theory, Phys. Lett. B 297 (1992) 353–357. [arXiv:hep-ph/9209291](https://arxiv.org/abs/hep-ph/9209291), [doi:10.1016/0370-2693\(92\)91274-D](https://doi.org/10.1016/0370-2693(92)91274-D).
- [231] T. Ohl, G. Ricciardi, E. H. Simmons,  $D$  - anti- $D$  mixing in heavy quark effective field theory: The Sequel, Nucl. Phys. B 403 (1993) 605–632. [arXiv:hep-ph/9301212](https://arxiv.org/abs/hep-ph/9301212), [doi:10.1016/0550-3213\(93\)90364-U](https://doi.org/10.1016/0550-3213(93)90364-U).
- [232] I. I. Y. Bigi, N. G. Uraltsev,  $D^0$  - anti- $D^0$  oscillations as a probe of quark hadron duality, Nucl. Phys. B 592 (2001) 92–106. [arXiv:hep-ph/0005089](https://arxiv.org/abs/hep-ph/0005089), [doi:10.1016/S0550-3213\(00\)00604-0](https://doi.org/10.1016/S0550-3213(00)00604-0).
- [233] A. F. Falk, Y. Grossman, Z. Ligeti, A. A. Petrov,  $SU(3)$  breaking and  $D^0$  - anti- $D^0$  mixing, Phys. Rev. D 65 (2002) 054034. [arXiv:hep-ph/0110317](https://arxiv.org/abs/hep-ph/0110317), [doi:10.1103/PhysRevD.65.054034](https://doi.org/10.1103/PhysRevD.65.054034).
- [234] A. F. Falk, Y. Grossman, Z. Ligeti, Y. Nir, A. A. Petrov, The  $D^0$  - anti- $D^0$  mass difference from a dispersion relation, Phys. Rev. D 69 (2004) 114021. [arXiv:hep-ph/0402204](https://arxiv.org/abs/hep-ph/0402204), [doi:10.1103/PhysRevD.69.114021](https://doi.org/10.1103/PhysRevD.69.114021).
- [235] Y. Amhis, et al., Averages of  $b$ -hadron,  $c$ -hadron, and  $\tau$ -lepton properties as of 2021, Phys. Rev. D 107 (2023) 052008. [arXiv:2206.07501](https://arxiv.org/abs/2206.07501), [doi:10.1103/PhysRevD.107.052008](https://doi.org/10.1103/PhysRevD.107.052008).
- [236] E. Golowich, J. Hewett, S. Pakvasa, A. A. Petrov, Implications of  $D^0$  -  $\bar{D}^0$  Mixing for New Physics, Phys. Rev. D 76 (2007) 095009. [arXiv:0705.3650](https://arxiv.org/abs/0705.3650), [doi:10.1103/PhysRevD.76.095009](https://doi.org/10.1103/PhysRevD.76.095009).
- [237] K. Blum, Y. Grossman, Y. Nir, G. Perez, Combining  $K^0$  - anti- $K^0$  mixing and  $D^0$  - anti- $D^0$  mixing to constrain the flavor structure of new physics,

- Phys. Rev. Lett. 102 (2009) 211802. [arXiv:0903.2118](#), [doi:10.1103/PhysRevLett.102.211802](#).
- [238] S. Pakvasa, D0 - anti-D0 mixing and new physics, *Pramana* 72 (2009) 205–215. [doi:10.1007/s12043-009-0017-8](#).
- [239] Z.-z. Xing, D0 - anti-D0 mixing and CP violation in neutral D meson decays, *Phys. Rev. D* 55 (1997) 196–218. [arXiv:hep-ph/9606422](#), [doi:10.1103/PhysRevD.55.196](#).
- [240] I. I. Y. Bigi, D0 Anti-d0 Mixing and CP Violation in *D* Decays: Can There Be High Impact Physics in Charm Decays?, *Conf. Proc. C* 890523 (1989) 169–195.
- [241] J. R. Fry, T. Ruf, Prospects of studying CP violation and mixing in D decays at a tau charm factory, *Conf. Proc. C* 930601 (1993) 387–405.
- [242] G. Blaylock, A. Seiden, Y. Nir, The Role of CP violation in D0 anti-D0 mixing, *Phys. Lett. B* 355 (1995) 555–560. [arXiv:hep-ph/9504306](#), [doi:10.1016/0370-2693\(95\)00787-L](#).
- [243] Z.-z. Xing, S. Zhou, D0 - anti- $\bar{D}^0$  Mixing and CP Violation in D0 vs anti-D0  $\rightarrow$   $K^{*+} K^-$  Decays, *Phys. Rev. D* 75 (2007) 114006. [arXiv:0704.0971](#), [doi:10.1103/PhysRevD.75.114006](#).
- [244] Y. Grossman, A. L. Kagan, Y. Nir, New physics and CP violation in singly Cabibbo suppressed D decays, *Phys. Rev. D* 75 (2007) 036008. [arXiv:hep-ph/0609178](#), [doi:10.1103/PhysRevD.75.036008](#).
- [245] Z.-z. Xing, Measuring CP violation and testing factorization in  $B(d) \rightarrow D^{*+} D^-$  and  $B(s) \rightarrow D^{*(s)+} D(s)^-$  decays, *Phys. Lett. B* 443 (1998) 365–372. [arXiv:hep-ph/9809496](#), [doi:10.1016/S0370-2693\(98\)01285-4](#).
- [246] K. Abe, et al., Observation of the decay  $B^0 \rightarrow D^+ D^{*-}$ , *Phys. Rev. Lett.* 89 (2002) 122001. [arXiv:hep-ex/0206014](#), [doi:10.1103/PhysRevLett.89.122001](#).
- [247] B. Aubert, et al., Measurement of time-dependent CP asymmetries in  $B^0 \rightarrow D^{(*)\pm} D^\mp$  decays, *Phys. Rev. Lett.* 95 (2005) 131802. [arXiv:hep-ex/0505092](#), [doi:10.1103/PhysRevLett.95.131802](#).

- [248] I. I. Y. Bigi, A. I. Sanda, On  $D^0$  - anti- $D^0$  Mixing and CP Violation, Phys. Lett. B 171 (1986) 320–324. doi:[10.1016/0370-2693\(86\)91557-1](https://doi.org/10.1016/0370-2693(86)91557-1).
- [249] D.-s. Du, Searching for Possible Large CP Violation Effects in Neutral Charm Meson Decays, Phys. Rev. D 34 (1986) 3428. doi:[10.1103/PhysRevD.34.3428](https://doi.org/10.1103/PhysRevD.34.3428).
- [250] D. M. Asner, W. M. Sun, Time-independent measurements of  $D^0$  - anti- $D^0$  mixing and relative strong phases using quantum correlations, Phys. Rev. D 73 (2006) 034024, [Erratum: Phys.Rev.D 77, 019901 (2008)]. arXiv:[hep-ph/0507238](https://arxiv.org/abs/hep-ph/0507238), doi:[10.1103/PhysRevD.73.034024](https://doi.org/10.1103/PhysRevD.73.034024).
- [251] D.-s. Du, CP violation for neutral charmed meson decays to CP eigenstates, Eur. Phys. J. C 50 (2007) 579–584. arXiv:[hep-ph/0608313](https://arxiv.org/abs/hep-ph/0608313), doi:[10.1140/epjc/s10052-007-0242-6](https://doi.org/10.1140/epjc/s10052-007-0242-6).
- [252] I. I. Bigi, Matter-antimatter oscillations and CP violation as manifested through quantum mysteries, Rept. Prog. Phys. 70 (2007) 1869–1936. doi:[10.1088/0034-4885/70/11/R03](https://doi.org/10.1088/0034-4885/70/11/R03).
- [253] Z.-Z. Xing, Effect of  $K^0$  - anti- $K^0$  mixing on CP asymmetries in weak decays of D and B mesons, Phys. Lett. B 353 (1995) 313–318, [Erratum: Phys.Lett.B 363, 266 (1995)]. arXiv:[hep-ph/9505272](https://arxiv.org/abs/hep-ph/9505272), doi:[10.1016/0370-2693\(95\)92845-D](https://doi.org/10.1016/0370-2693(95)92845-D).
- [254] I. I. Y. Bigi, H. Yamamoto, Interference between Cabibbo allowed and doubly forbidden transitions in  $D \rightarrow K(S), K(L) + \pi$ 's decays, Phys. Lett. B 349 (1995) 363–366. arXiv:[hep-ph/9502238](https://arxiv.org/abs/hep-ph/9502238), doi:[10.1016/0370-2693\(95\)00285-S](https://doi.org/10.1016/0370-2693(95)00285-S).
- [255] H. J. Lipkin, Z.-z. Xing, Flavor symmetry,  $K^0$  - anti- $K^0$  mixing and new physics effects on CP violation in  $D^{*+}$  and  $D^{*+}(s)$  decays, Phys. Lett. B 450 (1999) 405–411. arXiv:[hep-ph/9901329](https://arxiv.org/abs/hep-ph/9901329), doi:[10.1016/S0370-2693\(99\)00170-7](https://doi.org/10.1016/S0370-2693(99)00170-7).
- [256] F.-S. Yu, D. Wang, H.-n. Li, CP asymmetries in charm decays into neutral kaons, Phys. Rev. Lett. 119 (18) (2017) 181802. arXiv:[1707.09297](https://arxiv.org/abs/1707.09297), doi:[10.1103/PhysRevLett.119.181802](https://doi.org/10.1103/PhysRevLett.119.181802).

- [257] Y.-F. Shen, W.-J. Song, Q. Qin, CP violation induced by neutral meson mixing interference, *Phys. Rev. D* 110 (3) (2024) L031301. [arXiv:2301.05848](#), [doi:10.1103/PhysRevD.110.L031301](#).
- [258] W.-J. Song, Y.-F. Shen, Q. Qin, Double-mixing CP violation in  $B$  decays, *Eur. Phys. J. C* 84 (2024) 1030. [arXiv:2403.01904](#), [doi:10.1140/epjc/s10052-024-13350-z](#).
- [259] D. Cronin-Hennessy, et al., Measurement of Charm Production Cross Sections in  $e+e-$  Annihilation at Energies between 3.97 and 4.26-GeV, *Phys. Rev. D* 80 (2009) 072001. [arXiv:0801.3418](#), [doi:10.1103/PhysRevD.80.072001](#).
- [260] M. Ablikim, et al., Measurement of the  $D \rightarrow K^- \pi^+ \pi^+ \pi^-$  and  $D \rightarrow K^- \pi^+ \pi^0$  coherence factors and average strong-phase differences in quantum-correlated  $D\bar{D}$  decays, *JHEP* 05 (2021) 164. [arXiv:2103.05988](#), [doi:10.1007/JHEP05\(2021\)164](#).
- [261] M. Ablikim, et al., Model-independent determination of the relative strong-phase difference between  $D^0$  and  $\bar{D}^0 \rightarrow K_{S,L}^0 \pi^+ \pi^-$  and its impact on the measurement of the CKM angle  $\gamma/\phi_3$ , *Phys. Rev. D* 101 (11) (2020) 112002. [arXiv:2003.00091](#), [doi:10.1103/PhysRevD.101.112002](#).
- [262] R. Aaij, et al., Observation of the Mass Difference Between Neutral Charm-Meson Eigenstates, *Phys. Rev. Lett.* 127 (11) (2021) 111801. [arXiv:2106.03744](#), [doi:10.1103/PhysRevLett.127.111801](#).
- [263] J. S. Schwinger, The Theory of quantized fields. 1., *Phys. Rev.* 82 (1951) 914–927. [doi:10.1103/PhysRev.82.914](#).
- [264] S. Chekanov, et al., Search for contact interactions, large extra dimensions and finite quark radius in  $e p$  collisions at HERA, *Phys. Lett. B* 591 (2004) 23–41. [arXiv:hep-ex/0401009](#), [doi:10.1016/j.physletb.2004.03.081](#).
- [265] H. A. Bethe, The Electromagnetic shift of energy levels, *Phys. Rev.* 72 (1947) 339–341. [doi:10.1103/PhysRev.72.339](#).

- [266] F. J. Dyson, The Radiation theories of Tomonaga, Schwinger, and Feynman, *Phys. Rev.* 75 (1949) 486–502. [doi:10.1103/PhysRev.75.486](https://doi.org/10.1103/PhysRev.75.486).
- [267] K. G. Wilson, J. B. Kogut, The Renormalization group and the epsilon expansion, *Phys. Rept.* 12 (1974) 75–199. [doi:10.1016/0370-1573\(74\)90023-4](https://doi.org/10.1016/0370-1573(74)90023-4).
- [268] S. Weinberg, E. Witten, Limits on Massless Particles, *Phys. Lett. B* 96 (1980) 59–62. [doi:10.1016/0370-2693\(80\)90212-9](https://doi.org/10.1016/0370-2693(80)90212-9).
- [269] P. A. Zyla, et al., Review of Particle Physics, *PTEP* 2020 (8) (2020) 083C01. [doi:10.1093/ptep/ptaa104](https://doi.org/10.1093/ptep/ptaa104).
- [270] K. R. Schubert, T Violation and CPT Tests in Neutral-Meson Systems, *Prog. Part. Nucl. Phys.* 81 (2015) 1–38. [arXiv:1409.5998](https://arxiv.org/abs/1409.5998), [doi:10.1016/j.pnpnp.2014.12.001](https://doi.org/10.1016/j.pnpnp.2014.12.001).
- [271] J. R. Batley, et al., A Precision measurement of direct CP violation in the decay of neutral kaons into two pions, *Phys. Lett. B* 544 (2002) 97–112. [arXiv:hep-ex/0208009](https://arxiv.org/abs/hep-ex/0208009), [doi:10.1016/S0370-2693\(02\)02476-0](https://doi.org/10.1016/S0370-2693(02)02476-0).
- [272] E. Abouzaid, et al., Precise Measurements of Direct CP Violation, CPT Symmetry, and Other Parameters in the Neutral Kaon System, *Phys. Rev. D* 83 (2011) 092001. [arXiv:1011.0127](https://arxiv.org/abs/1011.0127), [doi:10.1103/PhysRevD.83.092001](https://doi.org/10.1103/PhysRevD.83.092001).
- [273] G. Colangelo, J. Gasser, H. Leutwyler,  $\pi\pi$  scattering, *Nucl. Phys. B* 603 (2001) 125–179. [arXiv:hep-ph/0103088](https://arxiv.org/abs/hep-ph/0103088), [doi:10.1016/S0550-3213\(01\)00147-X](https://doi.org/10.1016/S0550-3213(01)00147-X).
- [274] J. S. Bell, J. Steinberger, Weak Interactions of Kaons, in: *Proceedings of the Oxford Int. Conf. on Elementary Particles, 1965*, pp. 195–222.
- [275] G. D’Ambrosio, G. Isidori, Determination of CP and CPT violation parameters in the neutral kaon system using the Bell-Steinberger relation and data from the KLOE experiment, *JHEP* 12 (2006) 011. [arXiv:hep-ex/0610034](https://arxiv.org/abs/hep-ex/0610034), [doi:10.1088/1126-6708/2006/12/011](https://doi.org/10.1088/1126-6708/2006/12/011).

- [276] M. Antonelli, G. D’Ambrosio, M. Sozzi, CPT Invariance Testa in Neutral Kaon Decay (PDG review article), PTEP 2022 (2022) 871. doi:[10.1093/ptep/ptac097](https://doi.org/10.1093/ptep/ptac097).
- [277] H.-Y. Cheng, Radiative kaon decays  $K^\pm \rightarrow \pi^\pm \pi^0 \gamma$  and direct CP violation, Phys. Rev. D 49 (1994) 3771–3774. arXiv:[hep-ph/9308204](https://arxiv.org/abs/hep-ph/9308204), doi:[10.1103/PhysRevD.49.3771](https://doi.org/10.1103/PhysRevD.49.3771).
- [278] G. D’Ambrosio, G. Isidori, CP violation in kaon decays, Int. J. Mod. Phys. A 13 (1998) 1–94. arXiv:[hep-ph/9611284](https://arxiv.org/abs/hep-ph/9611284), doi:[10.1142/S0217751X98000020](https://doi.org/10.1142/S0217751X98000020).
- [279] Y. Zou, et al., New measurement of the amplitude of the CP conserving decay  $K_S^0 \rightarrow \pi^+ \pi^- \pi^0$ , Phys. Lett. B 369 (1996) 362–366. doi:[10.1016/0370-2693\(96\)00040-8](https://doi.org/10.1016/0370-2693(96)00040-8).
- [280] R. Adler, et al., CPLEAR results on the CP parameters of neutral kaons decaying to  $\pi^+ \pi^- \pi^0$ , Phys. Lett. B 407 (1997) 193–200. doi:[10.1016/S0370-2693\(97\)00757-0](https://doi.org/10.1016/S0370-2693(97)00757-0).
- [281] D. Babusci, et al., A new limit on the CP violating decay  $K_S \rightarrow 3\pi^0$  with the KLOE experiment, Phys. Lett. B 723 (2013) 54–60. arXiv:[1301.7623](https://arxiv.org/abs/1301.7623), doi:[10.1016/j.physletb.2013.05.008](https://doi.org/10.1016/j.physletb.2013.05.008).
- [282] A. Alavi-Harati, et al., A Measurement of the  $K_L$  Charge Asymmetry, Phys. Rev. Lett. 88 (2002) 181601. arXiv:[hep-ex/0202016](https://arxiv.org/abs/hep-ex/0202016), doi:[10.1103/PhysRevLett.88.181601](https://doi.org/10.1103/PhysRevLett.88.181601).
- [283] A. Anastasi, et al., Measurement of the charge asymmetry for the  $K_S \rightarrow \pi e \nu$  decay and test of CPT symmetry with the KLOE detector, JHEP 09 (2018) 021. arXiv:[1806.08654](https://arxiv.org/abs/1806.08654), doi:[10.1007/JHEP09\(2018\)021](https://doi.org/10.1007/JHEP09(2018)021).
- [284] B. Schwingerheuer, et al., CPT tests in the neutral kaon system, Phys. Rev. Lett. 74 (1995) 4376–4379. doi:[10.1103/PhysRevLett.74.4376](https://doi.org/10.1103/PhysRevLett.74.4376).
- [285] R. A. Briere, B. Winstein, Determining the phase of a strong scattering amplitude from its momentum dependence to better than 1-degree: The Example of Kaon regeneration, Phys. Rev. Lett. 75 (1995) 402–405, [Erratum: Phys.Rev.Lett. 75, 2070 (1995)]. doi:[10.1103/PhysRevLett.75.402](https://doi.org/10.1103/PhysRevLett.75.402).